Advanced lateral flow assays for point of care diagnostics

Dissertation

der Mathematisch-Naturwissenschaftlichen Fakultät
der Eberhard Karls Universität Tübingen
zur Erlangung des Grades eines
Doktors der Naturwissenschaften
(Dr. rer. nat.)

vorgelegt von
Dipl. Chem. Christoph Ruppert
aus Saarlouis

Tübingen
2021

Gedruckt mit Genehmigung der Mathematisch-Naturwissenschaftlichen Fakultät der Eberhard Karls Universität Tübingen.

Tag der mündlichen Qualifikation:	18.05.2021
Dekan:	Prof. Dr. Thilo Stehle
1. Berichterstatter:	Prof. Dr. Stefan Laufer
2. Berichterstatter:	Prof. Dr. René Csuk

Acknowledgements

I would like to express my gratitude to everybody in my life that contributed with their support in the generation of this thesis.

First I want to thank Prof. Dr. Hans-Peter Deigner for the supervision of this thesis and the opportunity to work in his research group. He encouraged me to pursue my ideas and provided me with support and scientific expertise throughout the last years of research. I am very grateful to Prof. Deigner for being my mentor and making this work possible.

Further I would like to thank Prof. Dr. Stefan Laufer for his guidance and support. I am grateful for the advice and effort he contributed to this thesis and included publications that enabled me to present this work.

I also want to thank my former work colleague Mostafa Mahmoud for the productive scientific discussions, joyful teamwork and his friendship over the last years. Further I want to thank my other work colleagues as well, especially Helga Weinschrott, Marina Taichrib, Prof. Dr. Matthias Kohl, Lars Kaiser and Simone Rentschler for being a great Team that made me feel at home.

Finally, I want to thank my family, friends and my girlfriend Jasmin Gehring for their love and support.

Abbreviations

3D	3 dimensional
AuNP	gold nanoparticles, gold nanospheres
CCD	charged-coupled device (sensor in digital camera)
CM	capture molecule
CMOS	Complementary metal–oxide–semiconductor (sensor in digital camera)
COVI-19	Coronavirus disease 2019
CRP	C-reactive protein
DNA	deoxyribonucleic acid
EDC	*N*-Ethyl-*N*'-(3-dimethylaminopropyl)-carbodiimid, EDAC
FRET	förster resonance energy transfer
h	hour
hCG	human chorionic gonadotropin
IL-6	interleukin-6
kDa	kilodalton
L	liter
LED	light emitting diode
LFA	lateral flow assay
LOB	limit of blank
LOD	limit of detection
LOQ	limit of quantification
NP	nanoparticle
NALFIA	nucleic acid lateral flow immune assay
NALFT	nucleic acid lateral flow teststrip
nm	nanometer
nmol	nanomole
POC	point of care
QD	quantum dot
RNA	ribonucleic acid
RGB	red/green/blue color space
SIRS	systemic inflammatory response syndrome
sulfo-NHS	hydroxy-2,5-dioxopyrrolidin

SELEX	systematic evolution of ligands by exponential enrichment
TBA	thrombin binding aptamer
TDM	therapeutic drug monitoring
UV	ultra-violet

Table of Contents

I. Summary

Lateral flow assays (LFAs) for medical applications are an important tool allowing patients and/or medical professionals to perform rapid and reliable diagnostics directly onsite. Because LFAs provide usable information with a time to result of ≤ 30 min or even as little as 5 min, this diagnostic tool is well suited for applications in precision medicine and point of care (POC) diagnostics, in which rapid results or cost effective drug monitoring are needed. If accurate quantitative results are required, readout hardware is mandatory. Readers should be portable, and ideally inexpensive and easily available. In this regard, smartphones, with their increasing photography capability and computational power, are an excellent choice as readers. Images acquired by smartphones can provide results of similar quality to those of professional laboratory equipment in certain settings. Beyond the imaging hardware, the label, such as commonly used gold nanoparticles (AuNPs), is an essential component in LFAs, determining their sensitivity and multiplexing capabilities.

In total, we researched three LFA assays for use in drug monitoring of digoxin or screening of the blood inflammation and coagulation biomarkers C-reactive protein (CRP), interleukin-6 (IL-6) and thrombin and published the results. Progress was achieved in smartphone imaging and optical multiplexing, using green and red quantum dots (QDs) as labels.

In the first part, a low-tech smartphone readout system for drug monitoring of cardiac glycoside digoxin was built. Images acquired with an iPhone 5S and a simple darkbox made from black cardboard were processed with a customized Shiny app. The quantitative results were compared with data acquired with a professional laboratory imager, and only minor differences were observed in key assay measures (19.8–16.9 nmol/L limit of detection). The assay is suitable for detecting the clinically relevant range and thus could be used for close interval home monitoring of this potentially toxic drug with a narrow therapeutic window. For the digoxin LFAs, we used spherical AuNPs with 50 nm diameter in a competitive setup. The colorimetric assay is compatible with most commercially available, professional lateral flow readers, because the chosen AuNP dye poses the common standard. The setup demonstrated excellent performance and is suitable for cost effective drug monitoring at patient´s homes or in resource poor areas. However, the use of AuNP dyes without post-processing steps has limited sensitivity and lacks multiplexing capability.

For the second part, we chose red and green fluorescent QDs as labels to achieve a rapid optical duplex LFA for quantitative detection of the inflammation biomarkers IL-6 and CRP. The assay was designed as a sandwich immunoassay for simultaneous readout of red (IL-6) and green (CRP) emitting QD labeled antibodies against the target analytes. We achieved a highly sensitive and rapid POC assay that could aid in distinguishing between sepsis and other inflammatory events. Along with the assay, we created the MultiFlow Shiny app, which was used to process and manage data from our assay but could also be used for easy and rapid data handling of all strip- or line-based assays. The software includes tools for image processing and advanced background correction, and it can generate calibration profiles for assays, including key measures such as the limit of detection, limit of quantification and limit of blank for fitted linear models. Readout was performed with a professional laboratory imager equipped with suitable emission color filters that were matched to the used QD labels. Although the assay performed well, the specialized and bulky readout system limited the potential for POC applications, because of its lack of portability.

In the third part, we used QD labels to develop a duplex LFA for the inflammation and coagulation biomarkers IL-6 and thrombin. Green QD antibody conjugates were used for detection of IL-6. For detection of thrombin, however, we used conjugates of thrombin binding aptamers and red QDs for detection of thrombin. The hybrid assay combined two different classes of capture molecules in a rapid single-step assay while achieving optical duplexing for the readout of both target proteins simultaneously. For imaging, a 3D-printed LFA imager with an inbuilt LED UV light source in combination with a Huawei P30 Pro smartphone was used. Images were processed by separation of RGB channels. The generated green and red channel images could then be directly used for quantification of both analytes, IL-6, and thrombin. Although the limit of detection for IL-6 did not attain the achieved sensitivity of the sepsis assay in Publication 2, the optical duplexing from a single smartphone image is a major achievement for enhancing the multiplexing capabilities of LFAs with affordable and easily available readout hardware, such as our open source 3D-printed smartphone imager. In particular, the combination with aptamers as capture molecules enables new possibilities. In the future, the assay could be combined with the MultiFlow Shiny app from Publication 2 by adding an RGB separator module to the toolkit. Therefore, this assay holds promise for further applications in rapid and affordable diagnostic tool based multiplex LFAs for smartphone readout, even in homes or areas with limited

resources and infrastructure.

II. Zusammenfassung

Lateral Flow Assays (LFAs) für den Einsatz in medizinischen Anwendungen sind ein wichtiges Werkzeug für die schnelle und zuverlässige Diagnose vor Ort, durch den Patienten selbst und/oder medizinisches Fachpersonal. LFAs bieten verwertbare Informationen in einer Analysezeit von ≤ 30 min, wobei besonders schnelle Tests auch in weniger als 5 min Ergebnisse liefern können. Diese Diagnoseinstrumente sind deshalb perfekt geeignet für Anwendungen in den Bereichen Präzisionsmedizin und der patientennahen Diagnostik vor Ort, wenn sofort verfügbare Informationen oder kosteneffiziente Tests zur Überwachung von Medikamentenspiegeln benötigt werden. Wenn präzise quantitative Ergebnisse gebraucht werden, ist der Einsatz technischer Messgeräte unverzichtbar. Diese müssen tragbar und nach Möglichkeit günstig, sowie leicht verfügbar sein. Aus diesem Grund sind moderne Smartphones mit hochwertigen Kamerasystemen und starker Rechenleistung eine hervorragende Wahl. Aufgenommene Fotos können dabei unter den richtigen Rahmenbedingungen ähnlich gute Ergebnisse liefern wie professionelle Laborgeräte. Zusätzlich zum gewählten Messgerät ist das verwendete Label, bzw. Farbstoff, eine bestimmende Größe für die Leistungsfähigkeit, insbesondere für die Sensitivität und multiplex Eignung, eines LFA. Hier kommen meist Gold-Nanopartikel (AuNPs) zur Anwendung.

Insgesamt wurden 3 LFA Tests für den Einsatz zum Monitoring von Digoxin und zur Analyse der Entzündungs- und Koagulationsbiomarker C-reaktives Protein (CRP), Interleukin-6 (IL-6) und Thrombin in Blutproben erforscht und die Ergebnisse publiziert. Gute Resultate wurden dabei in den Themenbieten Smartphone Bildgebung, sowie optisches Multiplexing, durch den Einsatz von grünen und roten, sog. Quantenpunkten (QDs) als Label, erzielt.

Im ersten Teil wurde ein Low-Tech Smartphone-Auswertungssystem für die Blutspiegelanalyse des Herzglykosids Digoxin erstellt. Dazu wurden Fotos von einem iPone 5S, unter Verwendung einer einfachen Dunkelkammer aus schwarzem Karton, aufgenommen und mit einer individuell programmierten Shiny app ausgewertet. Die quantitativen Ergebnisse wurden mit den Messdaten eines professionellen Labor Imager verglichen, wodurch wir zeigen konnten, dass es nur geringe Unterschiede in den erreichten Assay Kennzahlen gibt (19.8 bzw. 16.9 nmol/L Detektionslimit). Der

Digoxin LFA deckt den therapeutisch relevanten Bereich ab, so dass er für das Monitoring dieses potentiell toxischen Medikaments, mit einem schmalen therapeutischen Fenster, in kurzen Intervallen geeignet ist. Es wurden Gold-Nanopartikel mit 50nm Durchmesser in einem kompetitiven Format verwendet. Der kolorimetrische Assay ist mit den meisten kommerziell erhältlichen, professionellen Messgeräten auswertbar, weil die verwendeten AuNP Farbstoffe dem meistverwendeten Typ entsprechen und daher kompatibel sind. Der Test bewies exzellente Leistung und ist geeignet für kosteneffiziente Anwendungen im Monitoring von Therapeutika, zu Haus, oder in ressourcenarmen Umgebungen. Die Verwendung von Gold Nanopartikel Farbstoffen ohne Nachbearbeitungsschritte hat jedoch Beschränkungen in der Sensitivität und der Eignung zum optischen Multiplexing.

Im zweiten Teil wurden rote und grüne, fluoreszierende Quantenpunkten (QD) als Label für einen schnellen optischen duplex LFA zur quantitativen Analyse der Entzündungsbiomarker Interleukin-6 (IL-6) und C-reaktives-Protein (CRP) verwendet. Der Assay ist designed als Sandwich Immunoassay für die gleichzeitige Auswertung von rot (IL-6) und grün (CRP) emittierenden, QD gelabelten Antikörpern gegen die Ziel-Analyten. Wir erreichten damit einen sehr sensitiven Assay, der dabei helfen kann Sepsis und andere inflammatorische Ereignisse zu unterscheiden. Zusammen mit dem Assay erstellten wir die MultiFlow Shiny App und verwendeten diese für die Bearbeitung und das Management der erhaltenen Datensätze. Die App kann für die Auswertung aller Streifen- oder Linien Assays verwendet werden. Sie verfügt über Werkzeuge zur Bildverarbeitung, fortgeschrittene Hintergrundkorrektur und kann Kalibrierungsprofile für eingeschleuste Assays erstellen, welche Kennzahlen wie Limit of Detection (LOD), Limit of Quantification (LOQ) und Limit of Blank (LOB) aus angepassten linearen Modellen berechnen. Die Bildgebung erfolgte dabei durch einen professionellen Labor Imager, welcher mit passenden optischen Emissionsfiltern zur farblichen Trennung der verwendeten Quantenpunkte bestückt war. Der Assay bewies eine hohe Leistungsfähigkeit, aber das komplexe und sperrige Auswertungssystem reduziert das Potential für Point of Care Anwendungen, weil es nicht tragbar ist.

Im dritten Teil wurden Quantenpunkte als Label benutzt um einen LFA für die Entzündungs- und Gerinnungsbiomarker IL-6 und Thrombin durchzuführen. Grüne QD Antikörper Konjugate wurden zur Messung von IL-6 benutzt. Zur Detektion von Thrombin wurde jedoch ein Konjugat aus roten QDs und Thrombin bindenden Aptameren (TBA) benutzt. Der Hybrid-Assay kombiniert 2 verschiedene Klassen von

Fängermolekülen in einem schnellen Einstufigen LFA, wobei wir über optische duplex Auswertung beide Proteine gleichzeitig bestimmen konnten. Zur Bildgebung wurde ein 3D-gedruckter LFA Imager mit eingebauter UV-LED-Lichtquelle in Kombination mit einem Huawei P30 Pro Smartphone benutzt. Beim Auswerten der Fotos wurden die RGB-Farbkanäle getrennt. Danach konnten die erzeugten Bilder des grünen und roten Kanals direkt zur Quantifizierung von beiden Analyten, IL-6 und Thrombin, genutzt werden. Auch wenn der LOD von IL-6 nicht die gleiche Sensitivität erreichte wie der Sepsis Assay aus Publikation 2, so ist die optische duplex-Auswertung von Smartphone Fotos, insbesondere in Kombination mit unserem 3D-gedrukten, günstigen, und leicht verfügbaren Open-Source Imager ein großer Erfolg um die multiplex Eignung von LFAs zu erhöhen. Die Kombination von Aptameren als Fängermolekülen erschließt zusätzlich neue Möglichkeiten. Der Assay könnte weiterführend mit der Multiflow Shiny App aus Publikation 2 gekoppelt werden, indem zum Werkzeugkasten der App ein RGB-Separator-Modul hinzugefügt wird. Der erforschte Assay erfüllt daher alle Voraussetzungen, um als Muster für künftige, schnelle und günstige multiplex LFAs mit Smartphone Auswertung zu dienen. Das Setup ist dabei besonders geeignet zum Einsatz beim Home-Monitoring oder in Infrastruktur-Schwachen Gebieten.

III. List of scientific publications / contribution of authors

Publication 1: (published)

Ruppert C, Phogat N, Laufer S, Kohl M and Deigner HP. A smartphone readout system for gold nanoparticle-based lateral flow assays: application to monitoring of digoxigenin. *Microchim Acta* **186,** 119 (2019). https://doi.org/10.1007/s00604-018-3195-6

Contributions to Publication 1

Christoph Ruppert:	General idea generation, experimental work and data generation, primary writing of the manuscript, data processing and interpretation, proofreading and editing of the manuscript
Navneet Phogat:	Data processing and interpretation, partial writing of the data processing chapter, programming of software tools
Stefan Laufer:	proofreading and editing of the manuscript
Matthias Kohl:	Partial writing of the data processing chapter, proofreading and editing of the manuscript, project financing, corresponding author
Hans-Peter Deigner:	Partial writing, proofreading, editing and final approval of the manuscript, project financing, corresponding author

Publication 2: (published)

Ruppert C, Kaiser L, Jacob LJ, Laufer S, Kohl M and Deigner HP. Duplex Shiny app quantification of the sepsis biomarkers C-reactive protein and interleukin-6 in a fast quantum dot labeled lateral low assay. J Nanobiotechnol 18, 130 (2020) https://doi.org/10.1186/s12951-020-00688-1

Contributions to Publication 2

Christoph Ruppert:	General idea generation, experimental work and data generation, primary writing of the manuscript, data processing and interpretation, proofreading and editing of the manuscript
Lars Kaiser:	Partial writing, support in nanoparticle-antibody conjugate characterization, proofreading and editing of the manuscript
Lisa Johanna Jacob:	Partial experimental work (pre experiments), involvement in idea generation
Stefan Laufer:	Proofreading and editing of the manuscript
Matthias Kohl:	Partial writing of the data processing chapter, data processing and interpretation, programming of software tools, proofreading and editing of the manuscript, project financing, corresponding author
Hans-Peter Deigner:	Partial writing, proofreading, editing and final approval of the manuscript, project financing, corresponding author

Publication 3: (published)

Mahmoud M, Ruppert C, Rentschler S, Laufer S and Deigner HP. Combining aptamers and antibodies: lateral flow quantification for thrombin and interleukin-6 with smartphone readout. Sensors and Actuators B: Chemical 333, 129246 (2020) https://doi.org/10.1016/j.snb.2020.129246

Contributions to Publication 3

Mostafa Mahmoud:	idea generation, experimental work and data generation, writing of the manuscript, data processing and interpretation, proofreading and editing
Christoph Ruppert:	Idea generation, experimental work and data generation, writing of the manuscript, data processing and interpretation, proofreading and editing
Simone Rentschler:	Partial writing, proofreading, experimentation and editing of the manuscript
Stefan Laufer:	Proofreading and editing of the manuscript
Hans-Peter Deigner:	Partial writing, proofreading, editing and final approval of the manuscript, project financing, corresponding author

1. Introduction

1.1 Lateral flow assays

Lateral flow assays (LFAs) are a commonly used, popular platform technology for onsite analysis of biomolecules. Application areas include agriculture, food analysis, biomarker detection in body fluids, pathogen detection and drug monitoring. LFAs are easy to use and portable, provide rapid results and are very cost effective. Therefore, they are a preferable choice for point of care (POC) diagnostics that can be used by medical professionals or untrained individuals such as patients, in home testing [1–3]. Most LFAs such as the well-known home pregnancy test (the first commercially available LFA, Unipath Clearview, launched in 1988) for human chorionic gonadotropin are qualitative or semi-quantitative and are interpreted by the operator on the basis of a visual cutoff. For generation of accurate, quantitative results, the use of professional readout hardware based on laser scanners or camera systems is mandatory. In recent developments smartphones are gaining in importance because their modern inbuilt cameras with high resolution are well-suited for strip readout, thus allowing them to potentially serve as POC devices. For common single color LFAs, e.g., based on gold-nanoparticle labeled antibodies, the number of targeted biomarkers is limited to approximately 5 test lines for analytes, owing to microfluidic limitations. To further

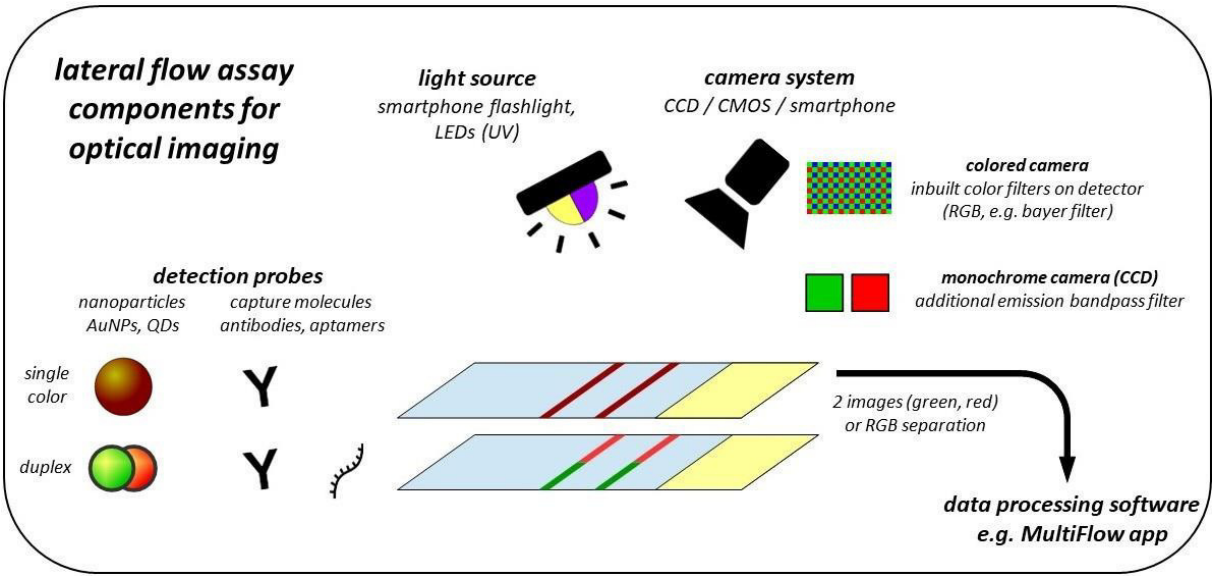

Figure 1: *lateral flow assay components for optical imaging*
Assay components: detection probes (nanoparticle conjugates), membrane (printed test and control line, antibodies, streptavidin and haptens); optical components (LED-light source, camera system (CCD, CMOS), optional color filters and data processing software (e.g. MultiFlow Shiny app).

increase the number of diagnostic targets optical multiplexing can be achieved through the use of special labels, such as quantum dot (QD) semiconductor nanocrystals, which are suitable for optical separation of (fluorescence) signals [4]. Depending on the application and desired target molecules, LFAs can be designed in different formats. Large biomolecules such as proteins (e.g., interleukin-6, IL-6 or C-reactive-protein, CRP) or peptides that are sufficiently large enough to present several antibody binding sites, can be detected in a sandwich Immunoassay format (e.g. Publication 2&3). For small molecules, as often required for drug monitoring approaches or toxin detection a, competitive design is often necessary (e.g., Publication 1) [3, 5].

1.1.1 Nanoparticle dyes for lateral flow assays

Colored Nanoparticles

The most commonly used colored labels used in lateral flow (immuno-) assays are gold nanoparticles (AuNPs), commonly 10-60 nm in size [4,6]. AuNPs and other colored labels based on e.g. precious metals, such as silver and platinum or carbon nanoparticles/nanotubes provide the benefit of colored lines that can be seen with the naked eye and thereby allow for visual interpretation in qualitative and semi-quantitative LFAs. AuNPs exhibit a red color owing to their main absorption peak typically in the blue-green range (520-540 nm) of the visible light spectrum. This main absorption peak (surface plasmon resonance peak) is caused by collective oscillation of free conduction electrons [7]. Approaches for signal enhancement in AuNP based LFAs exist, such as silver enhancement, wherein silver ions under reducing conditions are deposited as elemental silver on the surfaces of bound AuNPs; double labeling with a secondary dye (e.g., smaller AuNPs); or coupling to a secondary detection enzyme, such as horse radish peroxidase or alkaline phosphatase. However, these signal enhancement techniques commonly need a second post-processing step which decreases their suitability for rapid POC assays [8–11]. For the use of AuNP labels without a post-processing step, the signal strength and consequently the assay sensitivities are lower than those with fluorescent labels such as QDs.

Fluorescent Nanoparticles

Fluorescent labels for LFAs, such as quantum dots (QDs), lanthanide-based nanoparticles or polymer microspheres containing organic fluorescent dyes are gaining in popularity as labels for LFAs due to their favorable optical properties. They can be used to enhance sensitivity, because QDs in particular provide high fluorescent quantum yields and large absorption coefficients, and are highly resistant towards photo-bleaching and degradation, thus making them very effective labels for the development of high sensitivity LFAs [4]. Fluorescent probes also allow for experimental setups based on Förster resonance energy transfer in combination with a secondary acceptor fluorescent dye or quencher [12].

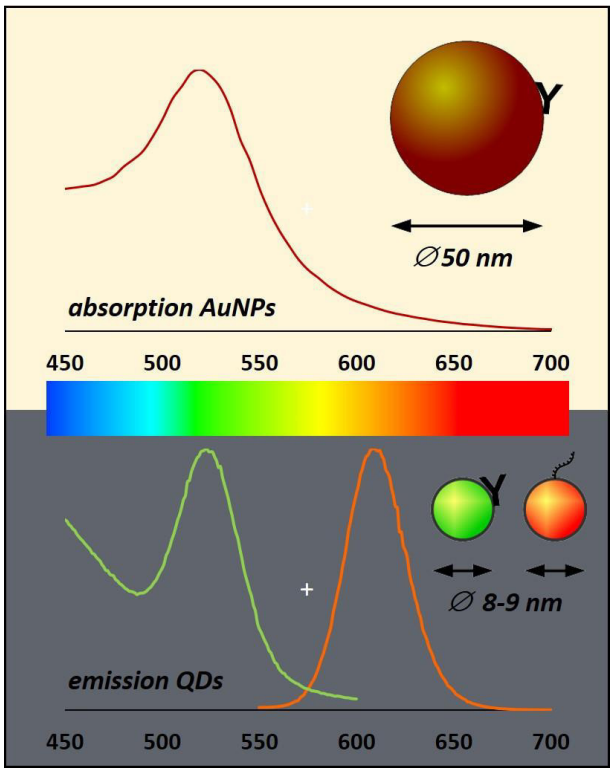

Figure 2: *top: absorption spectrum of ∅ 50 nm λ_{max}=520 nm; illustration of AuNP with bound antibody on the surface*
bottom: emission spectrum of green (λ_{max}=525 nm) and red (λ_{max}=605 nm) QDs; illustration of QDs bound to antibody or aptamer strand.

QDs are excellent labels for optical multiplex approaches, as performed in Publications 2 & 3 for our duplex LFAs, because of the provided sharp emission peaks that can be tuned to a distinct center wavelength depending on the size of the QD semiconductor nanocrystals used. The excitation is performed simultaneously for all QDs with a single UV-light source (commonly λ_{max} = 365 nm) outside the range of interest.

1.1.2 Capture molecules and conjugate synthesis

Antibodies as capture molecules

Antibodies for distinct target analytes or as secondary antibodies on the control line are the most common type of capture molecules used in LFAs. If antibodies are used as a biorecognition element, LFAs can also be called lateral flow Immunoassays (LFIA) [3]. Antibody based detection in LFAs is mainly dependent on the characteristics of the antibodies used, such as their binding constants and specificity, and the capabilities of the (nanoparticle-) labels used. Furthermore, the influence of sample buffers and the wicking speed of used LFA membranes are parameters that can influence the assay performance.
Publication 1 & 2 provide examples of this experimental setup. Publication 3 uses a mixed system with antibody-based detection of IL-6 and aptamer-based detection for the second target, thrombin.

Nucleic acids as capture molecules

Beyond antibodies, which are well-established capture molecules in LFAs, other approaches use oligonucleotides, DNA or RNA as recognition elements. Assays containing antibodies, e.g., those against tags for recognition of hybridized DNA strands on the test line or to capture unbound (labeled) strands on the control line are also called `nucleic acid lateral flow Immunoassay´ (NALFIA) or `nucleic acid lateral flow test strip´ (NALFT) if no antibodies are contained in the system [1,2]. There are approaches for sensing bacterial RNA via isothermal amplification by using AuNPs for labeling and several approaches for detection of complementary DNA strands [13–15]. Another approach is the use of aptamers as capture molecules, such as that in the system used in Publication 3 for the quantification of thrombin [16]. Aptamers are artificial, short, single stranded oligonucleotides that specifically bind target molecules by adsorption, and function similarly to detection via antibodies [17]. They are generated through in vitro selection, by a technique called `systematic evolution of ligands by exponential enrichment´ (SELEX), in which large DNA or RNA libraries are screened for binding/adsorption to an introduced target molecule. Once selected, aptamers can be produced synthetically or through modified bacteria in a large scale, at low cost, without the batch variations often seen with antibodies [18]. The drawbacks

are that just few reliable aptamer constructs with suitable sensitivity and specificity have been well characterized (one example is the used thrombin binding aptamer, TBA) and that ideal buffer conditions are crucial, particularly if quantitative results are desired. Aptamer-based approaches exist for LFAs with applications for foodborne toxins, microRNAs, or blood components, such as thrombin in project 3 [16,19,20].

Conjugation chemistry

For conjugation of capture molecules, such as antibodies and aptamers, to nanoparticle dyes, different approaches can be chosen. Unmodified AuNPs can adsorb proteins, such as antibodies, owing to ionic interaction leading to the formation of protein AuNP complexes under pH values near the isoelectric point of the bound protein. The formed conjugates, however, have low stability, are highly sensitive to pH and salt concentration and differ in their behavior depending on the capture molecule to nanoparticle ratio [21,22]. A more predictable approach exploiting passive adsorption is biotin/streptavidin modified capture molecules and nanoparticles [23]. However, if a biotin/streptavidin system is necessary to link other assay components, as in Publication 3, this approach is not usable. Therefore, in all three publications included in this thesis, covalent synthesis of modified AuNP and QD nanoparticles to antibodies and DNA-aptamers was chosen. This strategy resulted in reproducible and stable high performance nanoparticle conjugates as functional biosensors for target detection in LFAs [21].

For introduction of surface groups, e.g., carboxyl groups, to AuNPs, such as the particles used in Publication 1, common thiol containing reagents like lipoic acid or 11-mercaptoundecanoic acid, are used. This reagents, through the strong affinity of sulfur to gold surfaces, forms strong covalent bonds [24,25]. Another approach is the encapsulation of nanoparticles with polymer coatings, such as the QDs in Publications 2 & 3, which included the desired surface groups, such as carboxyl- or amine groups [26]. Carboxylated nanoparticles can then be conjugated to the desired capture molecules containing amine groups via carbodiimide linker chemistry (Figure 3).

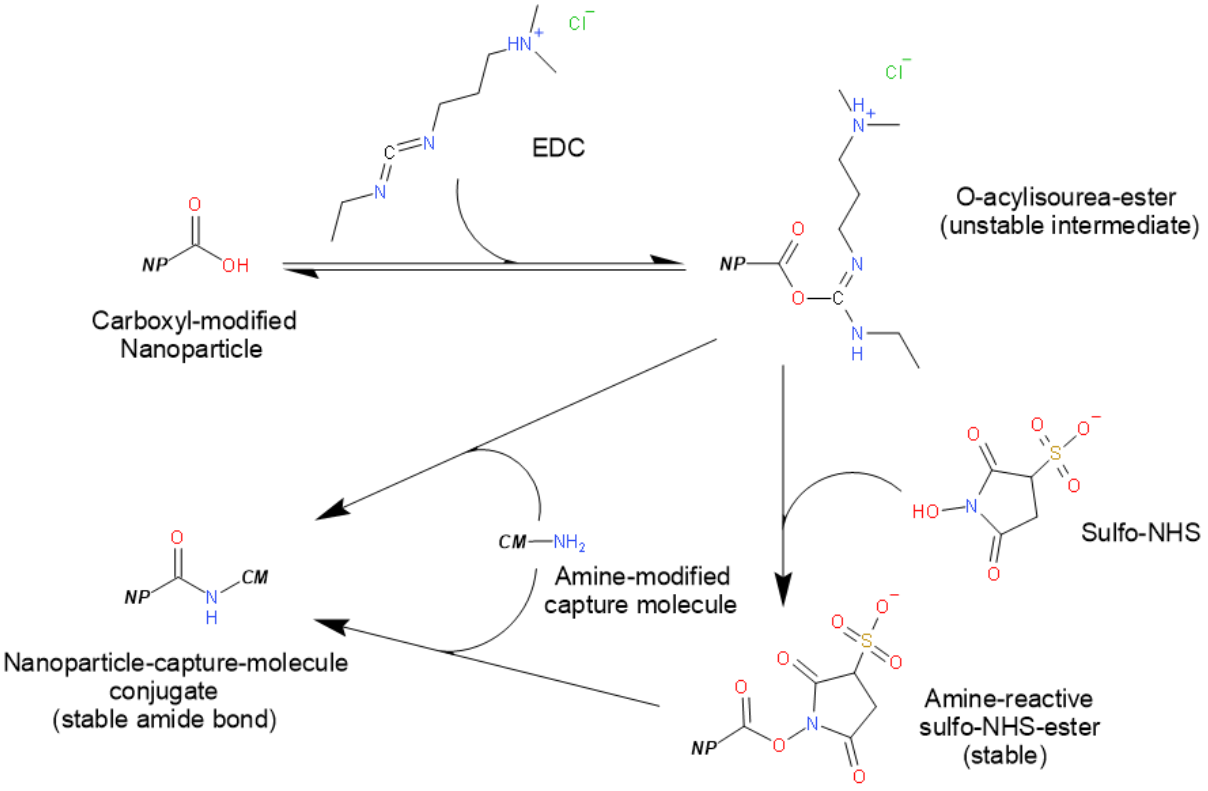

Figure 3: Covalent conjugation of carboxylated nanoparticles (NP) to amine containing/modified capture molecules (CM) by use of EDC/sulfo-NHS as zero length linker

1.1.3 LFA signal detection and readout hardware

For qualitative, and to some extent semi-quantitative, analysis, LFAs can be interpreted by visual inspection if sufficiently high amounts of target analyte is present, such as in home pregnancy tests, and if colored labels, such as AuNPs are used [27]. Numerous products for qualitative analysis of a target analyte threshold by visual cutoff are available in fields, such as diagnostics and food-/agriculture quality control [28]. For the acquisition of quantitative results, as is needed in most medical applications, the use of a suitable readout hardware is mandatory. Approaches for magnetic or electric detection of corresponding labels are available for use in LFAs, but the most used readout method is optical detection. For optical readout of LFAs methods include different camera systems (CCD-, CMOS- or smartphone cameras) and laser scanners in combination with corresponding light sources [27–30].

The improved performance of modern smartphones, owing to their increased computational power and high resolution camera systems, has resulted in particular interest in using these ubiquitously available devices for the design of POC diagnostic assays, such as LFA´s [31]. There are many approaches using smartphones as readout devices. These systems work with or without additional hardware parts, depending on the intended use and complexity of the designed LFA´s [31]. Particularly interesting is the deployment of 3D-printed accessories,

which have been successfully used in diagnostic or food safety quality control applications [32–35]. Designed 3D-patterns can be shared without logistic limitations worldwide, even in remote areas. These designs can also be customized easily to meet the needs of users in various settings, especially in research poor areas [34].

1.2 Diagnostic approaches

1.2.1 Therapeutic drug monitoring

Therapeutic drug monitoring (TDM) is the measurement of the concentrations of administered drugs. It is used to control and adjust the dosing of medications that have narrow therapeutic windows and strong adverse effects, or to achieve personalized dosing depending on patients response [36]. Substances are detected in commonly assayed in body fluids, such as blood or urine. In clinical practice, TDM is applied for monitoring tricyclic antidepressants, antiepileptic drugs, immunosuppressive drugs, and other potentially harmful substances. Analytical techniques include chromatographic methods, mass-spectroscopy and Immunoassays [37–39].

In Publication 1, a functional LFA for monitoring the cardiac glycoside digoxin, by using the hapten digoxigenin as the target, was composed. Digoxin is a cardiac glycoside used primarily in the treatment of systolic heart failure and atrial fibrillation. It has a narrow therapeutic range between 0.5 and 2 nmol/L serum concentrations with severe toxic adverse effects starting at 2.5 nmol/L. The elimination half-life for digoxin renal excretion in healthy people varies between 26 and 45 hours. In patients with impaired kidney function, elimination time can be prolonged, so that digoxin therapy without proper TDM poses a substantial risk of drug accumulation and exceeding the toxicity threshold [40–43]. Figure 4 illustrates the serum concentration of this drug for appropriate therapy through oral and intravenous administration.

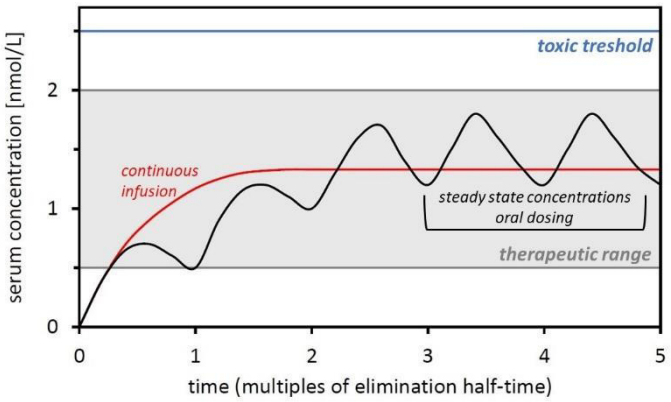

Figure 4: *Serum concentration of dixogin for oral dosing and continuous infusion.*

1.2.2 Inflammation and coagulation markers

C-reactive protein (CRP), interleukin-6 (IL-6) and thrombin are clinically relevant biomarkers associated with infectious deceases, (chronic) inflammation and blood coagulation. Analysis of these targets can aid in diagnosing certain dangerous medical conditions, such as sepsis, systemic inflammatory response syndrome (SIRS) and cytokine storm syndrome (which has received increased interest in the ongoing COVID-19 pandemic) [44,45]. Sepsis is a life-threatening condition caused by an excessive inflammatory immune response due to bacterial infection. It frequently leads to organ failure and poses major public health concerns, owing to very high mortality rates [46,47]. Along with sepsis, inflammation immune syndromes, such as SIRS and cytokine storm, have similar symptoms but different causes, so that adjustments in treatment are important to achieve optimal outcomes [46]. The administration of antibiotics, for instance, is beneficial for patients suffering with sepsis but poses an additional burden if the cause of inflammation is viral (e.g., COVID-19 associated cytokine storm), necrosis, autoimmune associated or even toxin related [46]. In clinical practice diagnosis of sepsis according to the most recent definition, sepsis-3, is performed on the basis of clinical parameters, such as respiratory rate, blood pressure and lactate levels, which can be assessed quickly but are not very specific [45]. For modern diagnostic approaches, analysis of biomarkers is recommended, thus making the development of rapid POC devices mandatory, owing to the short timeframe (less than 30 min to start of treatment) required to achieve good success rates [48].

CRP is one of the most important acute phase proteins and a well-established biomarker for infection and inflammation in clinical practice [49]. The 120 kDa pentamer rapidly shows elevated levels in response to noxious events and is also used to monitor the progress of infection treatment with e.g., antibiotics [44,49]. Further analysis of IL-6, an early proinflammatory biomarker that is produced by B- and T-cells in response to bacterial pathogens, but is less sensitive to viral infections, was chosen for this work to compose both our duplex QD assays [50]. Il-6 also triggers coagulation cascades in response to SARS-CoV-2 induced inflammation, particularly in severe COVID-19 cases. To complete the diagnostic setup, we chose thrombin as analytic target, because it shows variating levels in bacterial and viral infections. Elevated thrombin levels are indicative of high risk for thrombosis, such as COVID-19 induced micro-thrombosis events [51,52].

2. Objective

The objective of this work was to research improvements and increase the scope and applicability of lateral flow assays as platform technology for complex diagnostic issues in the context of point of care diagnostics and precision medicine. This aim requires rapid, easy to operate and cost effective LFA strips suitable for robust quantification of diagnostic targets and a corresponding readout and data processing solution. To meet these requirements and enable use of the LFA platform for multi-parameter diagnostics, we focused on the use of smartphones, as ubiquitously available readout devices, while doubling the potential target amount on a single test strip by introducing optical duplex detection of two differently colored QD dyes conjugated to either antibodies or aptamers as biosensors.

Project 1 (Publication 1) was intended to provide a proof of concept for quantitative smartphone detection, in therapeutic drug monitoring (TDM) for a toxic medication, the cardiac glycoside digoxin. This drug has a narrow therapeutic window (0.5-2.0 nmol/L serum concentration) and severe toxic adverse effects with overdose. The developed system should ideally work with no or very little additional (hardware-) components, e.g., external light sources, and should be based on a cost effective and reliable biosensor composed from anti-digoxigenin antibodies bound to a common AuNP dye.

Project 2 (publication 2) was intended to achieve an optical duplex assay to simultaneously detect the concentration of two selected inflammation biomarkers, IL-6 and CRP, on a single test line. The capabilities of red and green QDs as labels for a composed rapid, yet sensitive Immunoassay should be investigated, and reproducible protocols for synthesis of QD-antibody conjugates should be developed. Beyond the multiplexing potential of QD dyes, the high signal intensity and additional beneficial optical benchmarks of QDs enabled the system to be suitable for high sensitivity quantification, particularly for IL-6, owing to the low blood concentrations of this analyte in medical samples.

Project 3 (Publication 3) was intended to combine the benefits of project 1 & 2 by composition of an optical duplex assay, which is compatible with a developed, mostly 3D-printed imager accessory. Furthermore, the introduction of an aptamer-based biosensor composed of QDs and thrombin binding aptamer (TBA) should further enhance variability of the LFA platform technology.

3. Results and discussion

3.1 Publication 1: A smartphone readout system for gold nanoparticle-based lateral flow assays: application to monitoring digoxigenin

Ruppert C, Phogat N, Laufer S, Kohl M and Deigner HP.

Microchimica Acta **186,** 119 (2019).

https://doi.org/10.1007/s00604-018-3195-6

Status: published ***Manuscript pages:*** ***26-34***

Microchimica Acta (2019) 186: 119
https://doi.org/10.1007/s00604-018-3195-6

ORIGINAL PAPER

A smartphone readout system for gold nanoparticle-based lateral flow assays: application to monitoring of digoxigenin

Christoph Ruppert[1,2,3] · Navneet Phogat[1,2,3] · Stefan Laufer[3] · Matthias Kohl[1,2] · Hans-Peter Deigner[1,2,4]

Received: 14 September 2018 / Accepted: 20 December 2018 / Published online: 19 January 2019

Abstract

For modern approaches in precision medicine, fast and easy-to-use point-of-care diagnostics (POCs) are essential. Digoxin was chosen as an example of a drug requiring close monitoring. Digoxin is a cardiac glycoside used for the treatment of tachycardia with a narrow therapeutic window of 0.5–2.0 ng·mL^{-1}, and toxic effects are common for concentrations above 2.5 ng·mL^{-1}. For monitoring of blood concentration levels and treatment of intoxication, highly selective antibodies for digoxin and its hapten, digoxigenin, are available. A smartphone readout system is described for measuring digoxigenin in human serum using a common gold nanoparticle lateral flow assay (LFA). The R-package GNSplex, which also includes a Shiny app for quantitative test interpretation based on linear models, is used for image analysis. Images of lateral flow strips were taken with an iPhone camera and a simple darkbox made from black cardboard. Sensitivity and accuracy of the quantitative smartphone system as well as analytical parameters such as limit of detection (LOD) were determined and compared to data obtained with a high resolution BioImager. The data show that the smartphone based digoxin assay yields reliable quantitative results within the clinically relevant concentration range.

Keywords Lateral flow assay · Point-of-care diagnostics · Smartphone imaging · Nanoparticles · Image processing, R-package · Shiny app

Introduction

An important aspect of precision medicine is the measurement of drug, metabolite and biomarker concentrations at high frequencies, e.g., from blood or plasma, for diagnosis and control of therapeutic dosages. This measurement can be critical for matching the therapeutic window concentrations and for decreasing physical stress for the treated patient, especially for potentially toxic drugs with severe adverse effects. For example, organ transplant patients with immunosuppressive medications or HIV-infected people on anti-retroviral treatments are groups that benefit from high frequency therapeutic drug monitoring (TDM) [1, 2]. Fast and easy-to-use point-of-care devices and diagnostics (POCs) that can be performed by the patient are required to address this need. These self-monitoring tests must be cost-effective and would preferably not require additional hardware for measurement and data processing.

Here, a gold nanoparticle lateral flow assay (LFA) for digoxigenin was used to establish a smartphone-based readout system for home monitoring of cardiac glycoside digoxin. Digoxin is a cardiac glycoside used for treatment of tachycardia with a narrow therapeutic window of 0.5–2.0 ng·mL^{-1}; at serum concentrations above 2.5 ng·mL^{-1}, intoxication is likely. Digoxin is frequently administered in combination with beta-blockers, and control of blood concentrations is important [3, 4]. Monitoring of digoxin levels in patients is common practice and is usually performed through quantitative ELISA.

The binding epitope of most highly selective antibodies used in digoxin assays is digoxigenin, which is a

Electronic supplementary material The online version of this article (https://doi.org/10.1007/s00604-018-3195-6) contains supplementary material, which is available to authorized users.

✉ Matthias Kohl
kohl@hs-furtwangen.de

✉ Hans-Peter Deigner
dei@hs-furtwangen.de

[1] Medical and Life Sciences Faculty, Furtwangen University, Jakob-Kienzle Str. 17, 78054 Villingen-Schwenningen, Germany

[2] Institute of Precision Medicine, Furtwangen University, Jakob-Kienzle Str. 17, 78054 Villingen-Schwenningen, Germany

[3] Department of Pharmaceutical Chemistry, Pharmaceutical Institute, University of Tuebingen, Auf der Morgenstelle 8, 72076 Tuebingen, Germany

[4] EXIM Department, Fraunhofer Institute IZI, 10057 Rostock, Germany

deglycosylated derivative (Fig. 1). Digoxigenin is widely used as a hapten or binding tag for immunoassays, allowing transfer of our system to further diagnostic targets.

Lateral flow immunoassays are currently used for qualitative, semiquantitative and, to some extent, quantitative applications, including a widespread distribution in nonlab environments [5]. Imaging and readout hardware is available but far from being affordable for home use. The first smartphone approaches for point-of-care diagnostics usually involved additional attachment parts or special post-treatment of the used LFAs. Zangheri et al. described a chemiluminescence-based lateral flow method for cortisol sensing in saliva. The method employs a 3D-printed ABS plastic accessory with an incorporated lens and can reach detection limits as low as 0.3 ng·mL^{-1} [6]. Mudanyali and colleagues reported on a smartphone-based platform with a 3D-printed accessory including incorporated LEDs for illumination to obtain qualitative lateral flow assay results [7]. Several more approaches, such as a study by You et al., use smartphone readers for detection of thyroid-stimulating hormone, and work by Lee et al. used this method for detection of Aflatoxin B1. However, these approaches all use customized add-ons [8, 9]. For readout of our lateral flow assays, we use an iPhone 5S in combination with a simple darkbox made from black cardboard (Fig. 2).

To increase the scope and statistical power of the collected quantitative data, we developed an algorithm in the statistical software R including the colorimetric readout of test strips and tools for background- and baseline correction. We found that this setup affords viable quantitative data, similar to results acquired by a high performance BioImager System as a reference. To further increase the usability of our approach, we generated the R-package GNSplex including the algorithm for data processing; to simplify access to our algorithm, we added a Shiny app to ouR-package.

Experimental

Reagents and materials

Digoxigenin, BSA (bovine serum albumin), human serum, Tween-20, EDC (*N*-(3-Dimethylaminopropyl)-*N*′-ethylcarbodiimide hydrochloride), Sulfo-NHS (sulfosuccinimidyl 4,4′-azipentanoate), BIS-TRIS hydrochloride (2,2-Bis(hydroxymethyl)-2,2′,2″-nitrilotriethanol), sodium chloride, Triton X-100, HEPES (4-(2-hydroxyethyl)-1-piperazineethanesulfonic acid) and Pur-A-Lyzer-Midi (6000-8000MWCO) were purchased from Sigma Aldrich (https://www.sigmaaldrich.com). PBS (Phosphate buffered saline 10×) was purchased from AppliChem (https://www.itwreagents.com). α-digoxigenin-monoclonal-antibodies were purchased from Roche (https://lifescience.roche.com). Spherical gold nanoparticles, 50 nm Lipoic Acid NanoXact Gold, were purchased from nanoComposix (https://nanocomposix.eu/). Lateral-Flow-Assay strips for the LFA were provided by R-Biopharm (https://r-biopharm.com/de). The test line (tl) consists of a digoxigenin-BSA-conjugate. The control line (cl) consists of anti-mouse-polyclonal antibody. Test and control lines are 5 mm apart. The membrane material is nitrocellulose with 0.5 μm pore size. Buffers and reagents were prepared in milli-Q water (18.2 MΩ·cm).

Immunoprobe composition and synthesis

Synthesis of spherical gold bioprobes

A 1 μL quantity of a freshly prepared EDC/sulfo-NHS solution (c = 5.5 mmol·L^{-1} in milliQ water, 100.000-fold molar excess) was added to 1 ml of 50 nm Lipoic Acid NanoXact Gold particles (c = 56.5 pmol) and incubated at 250 rpm, 7 °C for 30 min in the dark. A dialysis tube (MWCO 6000-8000 kDa) was used to remove excess of EDC/sulfo-NHS. The mixture was dialyzed against 800 ml HEPES-buffer

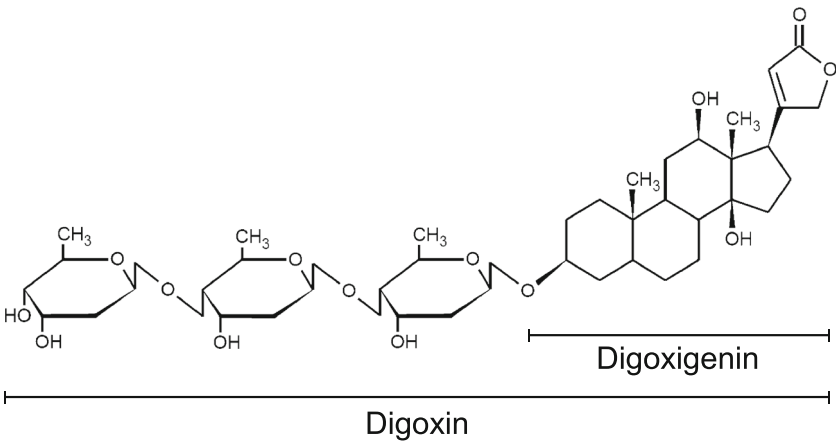

Fig. 1 Structure of target drug digoxin and its derivative digoxigenin (hapten for antibody coupling)

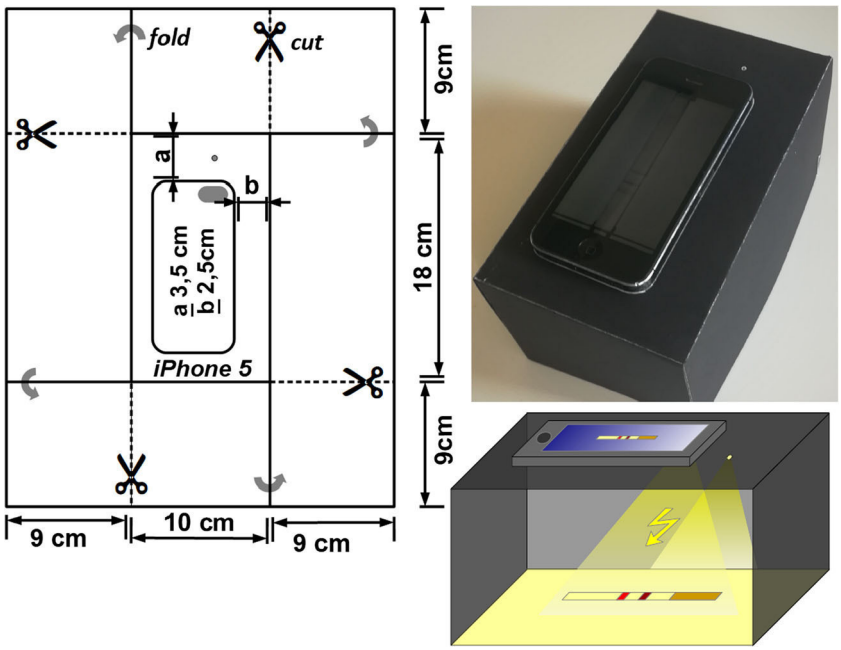

Fig. 2 Cutting pattern for the darkbox from black cardboard with dimensions; picture of darkbox for smartphone (iPhone 5 s) imaging; illustration of darkbox for smartphone imaging. Pictures were taken in standard settings with a flashlight. For adjustment of the built-in autofocus, a 1 mm hole allowing little external light is also included in the topside of the darkbox

(20 mM 0.1% Tween 20 pH 7.2) for 90 min, at room temperature (RT), in the dark. Then, a 120-fold excess of Digoxigenin-antibody (1 μL c = 6.6 μmol·L^{-1}) was added. The reaction mix was incubated for 2 h, 250 rpm, 7 °C in the dark. Then, 10% BSA-solution in HEPES was added to a final content of 1%. The volume of AuNP-conjugate solution was adjusted to a final volume of 1.5 mL with 1% BSA in HEPES. Conjugates obtained can be stored at 4 °C in the dark for several weeks.

LFA assay procedure, samples and reagents

Digoxigenin stock solutions for calibration with concentrations of 0,1,20,40,60,80,100 nmol·L^{-1} were prepared in PBS (pH 7.4, 0.01 M; 0.001 M EDTA). Every calibration solution was measured in five repetitions. Digoxigenin samples in human serum were prepared at concentrations of 0, 1, 5, 10, 15, 20, 25, 30, 40, 60, 80, 100 nmol·L^{-1} (three repetitions). The running buffer (RB) contained 0.05 M BIS-TRIS, 8% Triton X-100, 0.3% BSA.

A 10 μL sample (digoxigenin calibration solution or serum sample), 45 μL of running buffer, and 15 μL of conjugate solution were mixed in a 2 mL flat bottom reaction vessel; 30 s after mixing, the components the Digoxigenin LFA-strip were placed in the sample mix. The runtime for the 70 μL sample mix was 5 min. The test-strips were then placed on a flat surface and allowed to dry for 10 min. LFA-strips then were then ready for readout through the iPhone 5S or BioImager (ChemStudio Plus, Analytic Jena).

LFA assay principle and format

A direct competitive digoxigenin-LFA assay based on colorimetric bioprobes (gold nanoparticle-antibody-conjugates) was used in the detection method. Digoxigenin calibration solutions or spiked samples in human serum and antibody conjugates were mixed and applied on the LFA-membranes. Bioprobes without bound digoxigenin were bound to the test line. Otherwise, if digoxigenin was bound to the conjugated antibodies on the nanoparticle surface, the probes migrated further to the control line, where anti-mouse secondary antibodies bound to the mouse primary antibodies from the bioprobes. The colored bands on the test/control lines are photographed (in our case, using a CMOS smartphone camera from the iPhone 5S and a cardboard darkbox or BioImager (ChemStudio Plus with a 16MP CCD camera).

The colorimetric signal on the test-line is inversely related to the digoxigenin concentration in the samples. With the control-line as a calibration standard, signals can be normalized and calibrated for different readout devices using the same statistical methods (see: Data acquisition and processing) (Fig. 3).

GNSplex: an R-package for analysis of the data of gold nanoparticle-based bioassay

GNSplex is an open-source package completely developed in the statistical software R [10]. It is mainly based on the bioconductor package *EBImage* as well as R-packages *ggplot2 and ggpmisc* [10–13]. *GNSplex* utilizes the

implemented functionalities of *EBImage* to process jpeg images from lateral flow strips cut to a specific size. Images must include the test and control line to obtain an appropriate signal. We provide templates of the jpeg files in the folder *exData* of our package *GNSplex*. *GNSplex* uses the R-packages *ggplot2* and *ggpmisc* to generate plots of the fitted linear models [10, 13]. The sources of *GNSplex* are available for download from https://github.com/NPhogat/GNSplex and can be installed in R using the package *devtools* [14, 15]. The package also includes an in-built *Shiny app* and a standalone graphical user interface (GUI) to make the analysis of the image data more user-friendly. In addition, the *Shiny app* can be used to generate an analysis report of the results via the R-package *rmarkdown* [16, 17]. BioImager and iPhone images of samples at different concentrations of digoxigenin calibration standards and spiked human serum samples were taken. The intensities of the test line (tl) and control line (cl) were extracted, the background was corrected and the normalized intensities (cl/tl) were computed. Linear models based on the normalized intensities (cl/tl) and the concentrations (nM) were used. To increase the functionality of our package, it is possible to fit simple linear models based on the standardized intensities (tl/cl) and the concentrations (nM). The package furthermore includes functions also incorporated into the GUI to compute the standard deviation (SD) within replicates of the raw intensities of the control and test line, as well as of normalized and standardized intensities, confidence intervals of normalized and standardized intensities and the Pearson correlation of the normalized and standardized intensities with respect to their predicted values. Further, the package can be used to compute the limit of detection (LOD) and limit of quantification (LOQ) statistically, based on two different methods. The first method to compute the LOD and LOQ is based on the following formulas:

$$\text{LOD} = \text{Mean of blank data} + 3^{*}(\text{standard deviation of blank data})$$
$$\text{LOQ} = \text{Mean of blank data} + 10^{*}(\text{standard deviation of blank data})$$

The formulas for the second method to compute the limit of blank (LOB), LOD and LOQ read:

$$\text{LOB} = \text{Mean of the blank data} + 1.645^{*}(\text{standard deviation of blank data})$$
$$\text{LOD} = \text{LOB} + 1.645^{*}(\text{standard deviation of 1nM sample data})$$
$$\text{LOQ} = \text{Mean of blank data} + 10^{*}(\text{standard deviation of blank data})$$

The respective results for standardized intensities are shown in the supplementary information.

Results and discussion

Data acquisition via smartphone and BioImager

For each analyte (digoxigenin) concentration, a data set of five test strips was prepared and pictures were taken either with a high class BioImager (ChemStudioPlus, 16MP CCD-camera, Analytik Jena) or with an iPhone 5S in standard settings, applying flashlight in the previously described cardboard-darkbox. The Test-line (tl) is comprised of digoxigenin-hapten, while the Control-line (cl) is comprised of the secondary

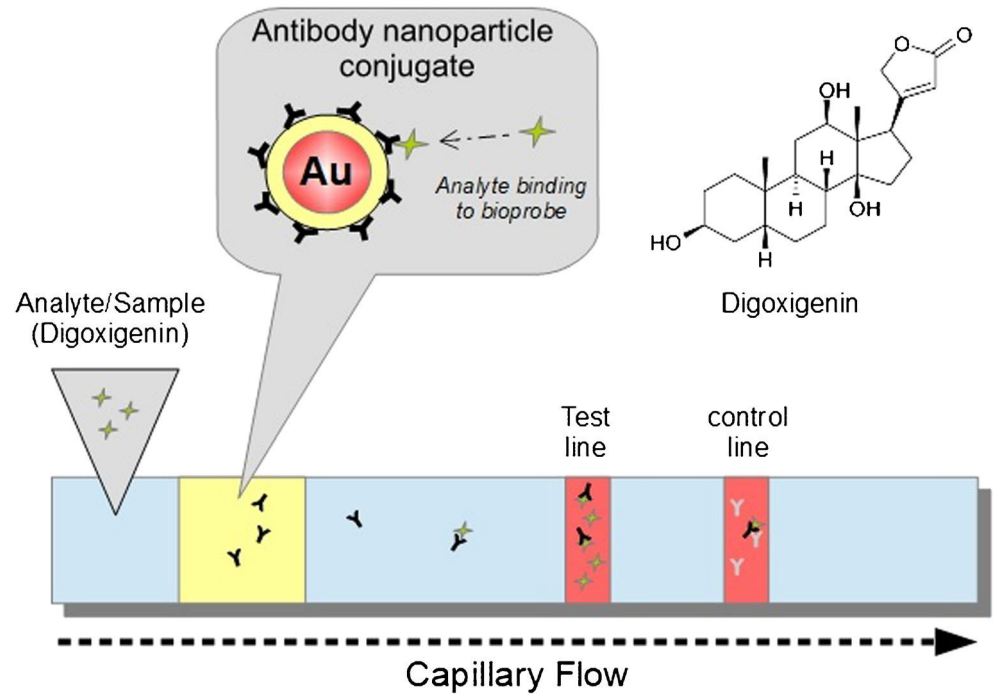

Fig. 3 Illustration of competitive lateral flow immunoassay for detection of digoxigenin. Test line/control line consist of digoxigenin-BSA-conjugate/anti mouse secondary antibodies. Sample consist of digoxigenin sample/running buffer/AuNP-anti digoxigenin-Ab–conjugates

antibody for mouse Fc-fragments. The assay format is competitive, so a high digoxigenin content in the samples corresponds to strongly colored (dark) test-lines and light-colored control lines (inverse test-line signal).

As seen in the unprocessed pictures (Fig. 4), the high-resolution pictures produced by the BioImager are sharper and denser, which may be advantageous if a visual control by naked eye is intended. In particular, very low and very high concentrations are difficult to see in the smartphone pictures.

Data processing

The main goal was to develop a user-friendly method, utilizing a smartphone, to compute digoxigenin concentrations from normalized intensities for potential use as a POC-device at home. Due to the narrow therapeutic range of digoxigenin, and based on the results of our experiments, simple linear models were used.

Analysis of the lateral flow data of digoxigenin

A common laboratory standard for colorimetric readout is the software *ImageJ*. We compare the normalized intensities and respective simple linear models computed for pure digoxigenin samples: one set of results was generated via *ImageJ* and a second set by the R-package *GNSplex*. The highest R^2 of 0.98 (Fig. 5a) was obtained for the BioImager data processed through the *ImageJ* software, followed by an R^2 of 0.96 (Fig. 5c) for the BioImager data processed with our R-package *GNSplex*. As depicted in Fig. 5b and d, the R-package, *GNSplex* works better for the iPhone data. The clearly weaker result for *ImageJ*, however, is mainly caused by the variable results measured for 100 nM. As expected, the results for the BioImager data are superior, while our R-package *GNSplex* works well; the results for the iPhone data are only slightly different from results for the BioImager data. Error bars in Fig. 5a, b, c and d represent the standard deviation of the normalized intensities within the replicates. The respective LOB (limit of blank), LOD (limit of detection) and LOQ (limit of quantification) calculated for the normalized intensities are given in Table 1. The standard deviation of the normalized intensities and the Pearson correlations between the normalized intensities and the predicted values are included in the supplementary information.

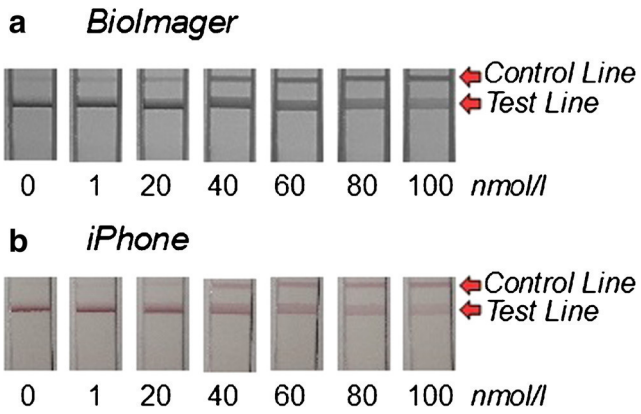

Fig. 4 Data sets of pictures taken with **a** BioImager (ChemStudio PLUS, 16 MP CCD), **b** iPhone 5S (standard settings with flashlight); Data shows first set of Calibration standard tests-trips

Analysis of the lateral flow data of digoxigenin with serum sample

This section compares the fitted simple linear regression models of the digoxigenin lateral flow assay with serum samples, where the images were processed via *ImageJ* and our R-package *GNSplex*. Figure 6 shows that the standard deviations within the replicates are smaller for ImageJ than those for *GNSplex*. However, there are high to very high R^2 values in all cases. The results indicate that our smartphone-based system has the potential to achieve accuracies similar to those of a high-end imager system. The LOB, LOD and LOQ, computed by two different approaches, are shown in Table 2. The Pearson correlations between the normalized intensities and the predicted values are included into supplementary information (Fig. 7).

Image processing through shiny app

Our *Shiny app* includes an option to generate an HTML report of the analysis by clicking the "Download" button. The report is saved in the folder "GNSplex.gui" of our R-package. One can then move the report to a new folder and keep it as a record of the analysis. The report includes the final results as well as all relevant information, such as the data, date, applied GUI settings and package dependencies to allow reproduction. Caveat: The report generation is a dynamic procedure, where a new report automatically overrides an existing previous report.

The reports for data processing through our Shiny app are attached as supplementary information (ESM). The attached document includes the full datasets: S1_ImageJ_Calibration, S2_iPhone_ImageJ_Calibration, S3_Imager_GNSplex_calibration, S4_IPhone_GNSplex_Calibration, S5_Imager_ImageJ_Serum, S6_IPhone_ImageJ_Serum, S7_Imager_GNSplex_Serum, and S8_IPhone_GNSplex_Serum and can be downloaded.

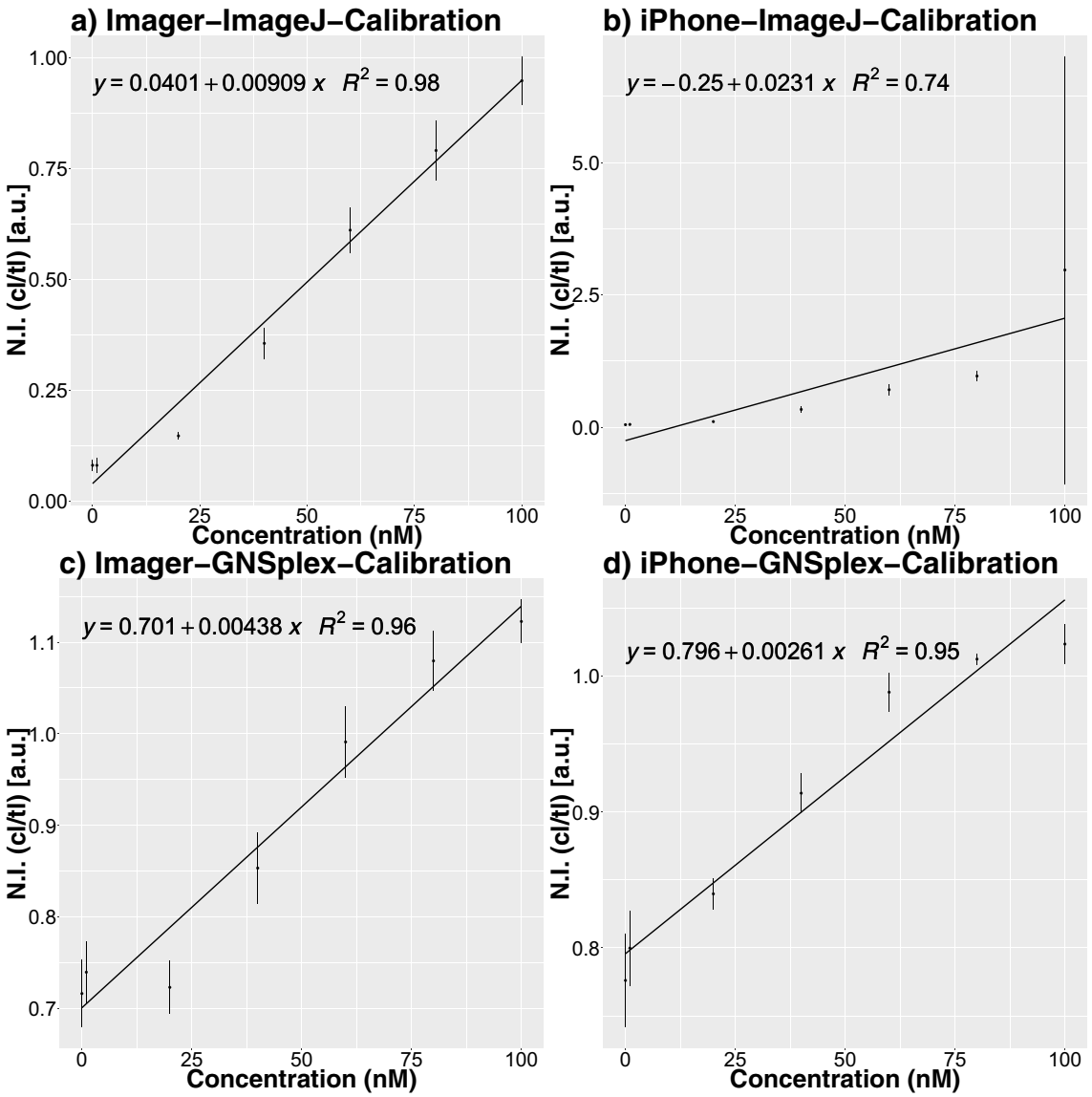

Fig. 5 Concentration vs. normalized intensities (calibration standard digoxigenin) for readout trough ImageJ and GNSplex based on Imager and iPhone data, respectively; error bars represent the standard deviation of the normalized intensities within replicates

Table 1 LOD, LOQ and LOB for ImageJ and GNSplex readout based on Imager and iPhone data (calibration standard digoxigenin), respectively

ImageJ/GNSplex data processing normalized DIG calibration [nmol·L^{-1}]	ImageJ 1st method		ImageJ 2nd method		GNSplex 1st method		GNSplex 2nd method	
	Imager	iPhone	Imager	iPhone	Imager	iPhone	Imager	iPhone
Limit of detection (LOD)	8.5	14.8	9.5	14.4	28.5	31.8	29.7	31.3
Limit of quantification (LOQ)	17.8	19.1	17.8	19.1	86.8	31.8	86.8	123.7
Limit of blank (LOB)	–	–	8.5	14.0	–	–	17.2	13.1

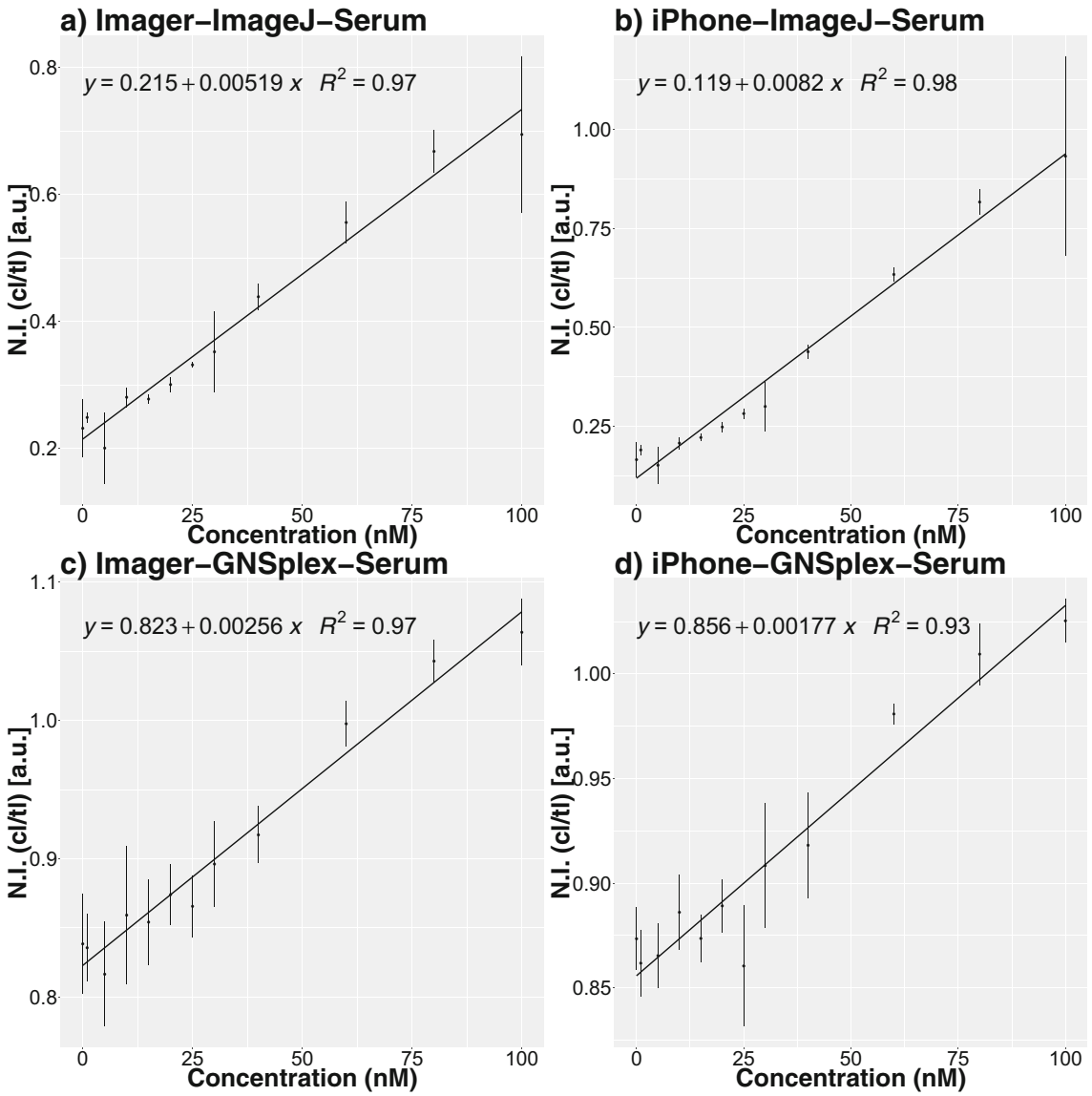

Fig. 6 Concentration vs. normalized intensities (spiked serum digoxigenin) for readout through ImageJ and GNSplex with Imager or iPhone for readout based on Imager and iPhone data, respectively. The error bars given in the figures represent the standard deviation of the normalized intensities within replicates

Table 2 LOD, LOQ and LOB for ImageJ and GNSplex readout based on Imager and iPhone data (spiked serum digoxigenin), respectively

ImageJ/GNSplex data processing normalized DIG Serum [nmol·L^{-1}]	ImageJ 1st method		ImageJ 2nd method		GNSplex 1st method		GNSplex 2nd method	
	Imager	iPhone	Imager	iPhone	Imager	iPhone	Imager	iPhone
Limit of detection (LOD)	29.1	21.9	19.8	16.9	48.3	37.0	44.7	39.4
Limit of quantification (LOQ)	89.5	59.5	89.5	59.5	146.7	77.2	146.7	77.2
Limit of blank (LOB)	–	–	17.4	14.6	–	–	29.2	29.2

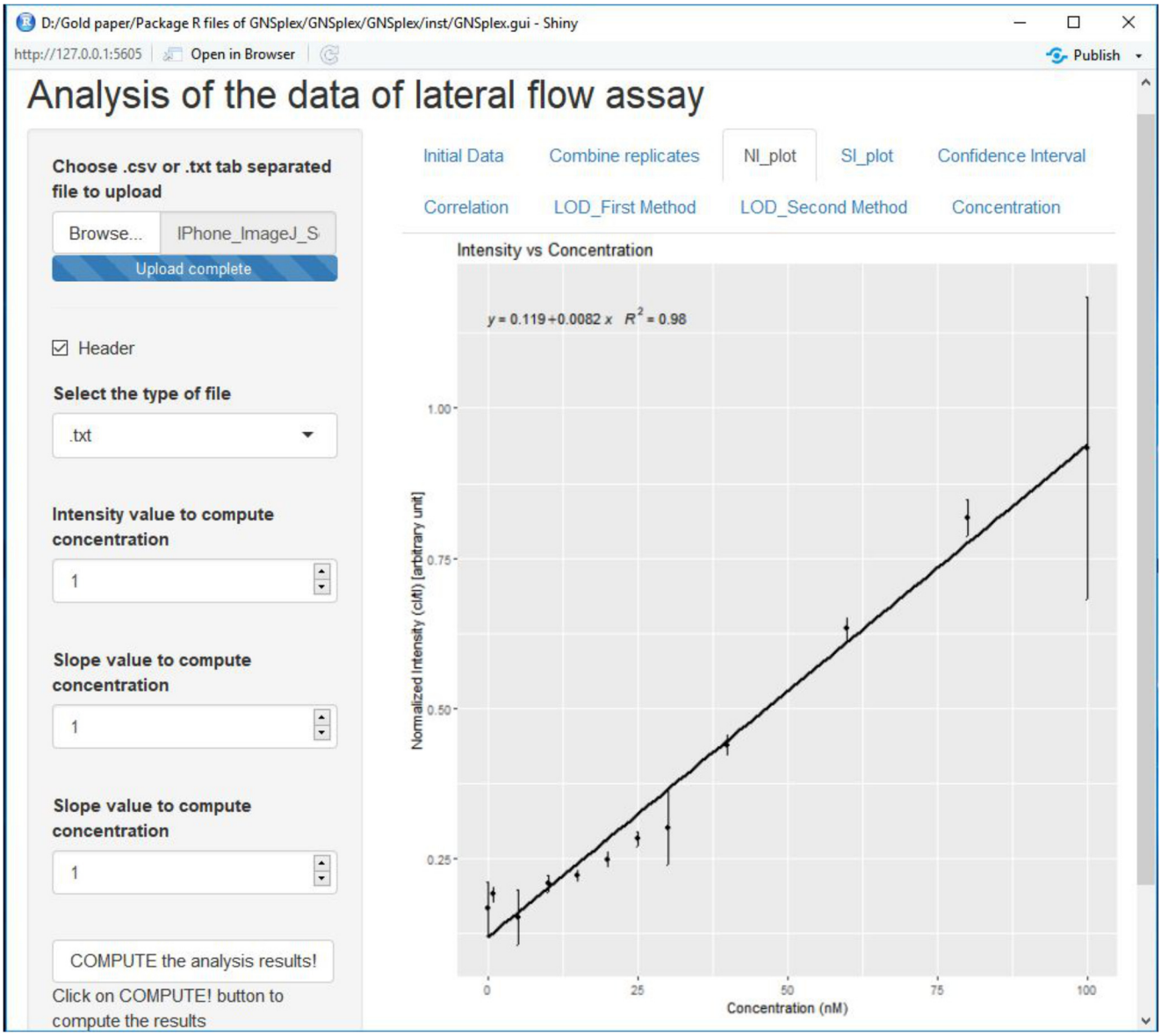

Fig. 7 Screenshot of Shiny app for automatic data processing of lateral flow assays

Conclusions

A smartphone (iPhone 5S)-based solution to compute digoxigenin concentrations from normalized intensities has been described. Either the *ImageJ* software or our open-source R-package *GNSplex* can be used for image processing. *GNSplex* can also be used to fit simple linear models to the data and by means of the fitted model, compute concentrations from normalized or standardized intensities.

A built-in Shiny app greatly increases the user-friendliness of our package and allows for extension to a web-based app that may run on a smartphone. Calibration of the lateral flow reader showed good results for reliable quantification of digoxin-spiked human serum samples. The simple cardboard darkbox can be composed in any environment with ease.

Since the quality of the acquired quantification data is comparable to readout obtained through the sophisticated laboratory hardware used as a reference, the *GNSplex* R-package and the corresponding *Shiny app* provide very attractive tools for POCTs or other lateral flow applications.

Acknowledgements Support by Bundesministerium für Bildung und Forschung (MultiFlow project, 03FH046PX4) is gratefully acknowledged.

Compliance with ethical standards Experiments and analyses performed are compliant with ethical standards.

References

1. Kowalski R, Post D, Schneider MC, Britz J, Thomas J, Deierhoi M, Lobashevsky A, Redfield R, Schweitzer E, Heredia A, Reardon E, Davis C, Bentlejewski C, Fung J, Shapiro R, Zeevi A (2003) Immune cell function testing: an adjunct to therapeutic drug monitoring in transplant patient management. Clin Transpl 17:77–88. https://doi.org/10.1034/j.1399-0012.2003.00013.x
2. Aarnoutse RE, Schapiro JM, Boucher CAB, Hekster YA (2003) Therapeutic drug monitoring. Drugs 63(8):741–753. https://doi.org/10.2165/00003495-200363080-00002
3. Smith TW, Haber E (1970) Digoxin intoxication: the relationship of clinical presentation to serum digoxin concentration. J Clin Invest 49(12):2377–2386. https://doi.org/10.1172/JCI106457
4. Bauman JL, DiDomenico RJ, Galanter WL (2006) Mechanisms, manifestations, and management of digoxin toxicity in the modern era. Am J Cardiovasc Drugs 6(2):77–86. https://doi.org/10.2165/00129784-200606020-00002
5. Posthuma-Trumpie AG, Korf J, van Amerongen A (2009) Lateral flow (immuno)assay: its strengths, weaknesses, opportunities and threats. A literature survey A. Anal Bioanal Chem 393(2):569–582. https://doi.org/10.1007/s00216-008-2287-2
6. Zangheri M, Cevenini L, Anfossi L, Baggiani C, Simoni P, Di Nardo F, Roda A (2015) A simple and compact smartphone accessory for quantitative chemiluminescence-based lateral flow immunoassay for salivary cortisol detection. Biosens Bioelectron 64:63–68. https://doi.org/10.1016/j.bios.2014.08.048
7. Mudanyali O, Dimitrov S, Sikora U, Padmanabhan S, Njavruz I, Ozcan A (2012) Integrated rapid-diagnostic-test reader platform on a cellphone. Lab Chip 12:2678–2686. https://doi.org/10.1039/C2LC40235A
8. You DJ, Park S, Yoon JY (2012) Cell-phone-based measurement of TSH using Mie scatter optimized lateral flow assays. Biosens Bioelectron 40:180–185. https://doi.org/10.1016/j.bios.2012.07.014
9. Lee S, Kim G, Moon J (2013) Performance improvement of the one-dot lateral flow immunoassay for aflatoxin B1 by using a smartphone-based Reading system. Sensors 13:5109–5116. https://doi.org/10.3390/s130405109
10. R Core Team (2017) R: a language and environment for statistical computing. R Foundation for Statistic al Computing, Vienna
11. Aphalo PJ (2017) Learn R ...as you learnt your mother tongue. learnpub, Helsinki, Git. hash: 1bf3003
12. Pau G, Fuchs F, Skylar O, Boutros M, Huber W (2010) EBImage—an R package for image processing with applications to cellular phenotypes. Bioinformatics 26:979–981. https://doi.org/10.1093/bioinformatics/btq046
13. Wickham H (2009) ggplot2: elegant graphics for data analysis. Springer-Verlag, New York. https://doi.org/10.1007/978-3-319-24277-4
14. Gentleman RC, Carey VJ, Bates DM, Balstad B, Dettling M, Dudoit S, Ellis B, Gautier L, Ge Y, Gentry J, Hornik K, Hothorn T, Huber W, Lacus S, Irizarry R, Leisch F, Li C, Maechler M, Rossini AJ, Sawitzki G, Smith C, Smyth G, Tierney L, Yang JYH, Zhang J (2004) Bioconductor: open software development for computational biology and bioinformatics. Genome Biol 5:R80. https://doi.org/10.1186/gb-2004-5-10-r80
15. Wickham H, Hester J, Chang W (2018) devtools: Tools to make developing R packages easier. R package version 20.1. https://CRAN.R-project.org/package=devtools. Accessed 29 Nov 2018
16. Chang W, Cheng J, Allaire JJ, Xie Y, McPherson J (2017) shiny: web application framework for R. https://cran.r-project.org/package=shiny. Accessed 29 Nov 2018
17. Allaire JJ, Xie Y, McPherson J, Luraschi J, Ushey K, Atkins A, Wickham H, Cheng J, Chang W (2018) rmarkdown: Dynamic Documents for R. R package version 1.9. https://CRAN.R-project.org/package=rmarkdown. Accessed 29 Nov 2018

3.2 Publication 2: Duplex Shiny app quantification of the sepsis biomarkers C-reactive protein and interleukin-6 in a fast quantum dot labeled lateral flow assay

Ruppert C, Kaiser L, Jacob LJ, Laufer S, Kohl M and Deigner HP

Journal of Nanobiotechnology 18, 130 (2020)

https://doi.org/10.1186/s12951-020-00688-1

Status: published ***Manuscript pages:*** ***36-46***

Journal of Nanobiotechnology

METHODOLOGY Open Access

Duplex Shiny app quantification of the sepsis biomarkers C-reactive protein and interleukin-6 in a fast quantum dot labeled lateral flow assay

Christoph Ruppert[1,2,3], Lars Kaiser[1,2,4], Lisa Johanna Jacob[1,2], Stefan Laufer[3], Matthias Kohl[1,2*] and Hans-Peter Deigner[1,2,5,6*]

Abstract

Fast point-of-care (POC) diagnostics represent an unmet medical need and include applications such as lateral flow assays (LFAs) for the diagnosis of sepsis and consequences of cytokine storms and for the treatment of COVID-19 and other systemic, inflammatory events not caused by infection. Because of the complex pathophysiology of sepsis, multiple biomarkers must be analyzed to compensate for the low sensitivity and specificity of single biomarker targets. Conventional LFAs, such as gold nanoparticle dyed assays, are limited to approximately five targets—the maximum number of test lines on an assay. To increase the information obtainable from each test line, we combined green and red emitting quantum dots (QDs) as labels for C-reactive protein (CRP) and interleukin-6 (IL-6) antibodies in an optical duplex immunoassay. CdSe-QDs with sharp and tunable emission bands were used to simultaneously quantify CRP and IL-6 in a single test line, by using a single UV-light source and two suitable emission filters for readout through a widely available BioImager device. For image and data processing, a customized software tool, the MultiFlow-Shiny app was used to accelerate and simplify the readout process. The app software provides advanced tools for image processing, including assisted extraction of line intensities, advanced background correction and an easy workflow for creation and handling of experimental data in quantitative LFAs. The results generated with our MultiFlow-Shiny app were superior to those generated with the popular software ImageJ and resulted in lower detection limits. Our assay is applicable for detecting clinically relevant ranges of both target proteins and therefore may serve as a powerful tool for POC diagnosis of inflammation and infectious events.

Keywords: Duplex lateral flow assay, Point-of-care diagnostics, Nanoparticles, Quantum dots, Image processing, R-package, Shiny app, Sandwich immunoassay, Multiplexing, Conjugation chemistry

Introduction

Sepsis, a life-threatening syndrome following a dysregulated host response to infection, frequently leads to organ dysfunction; it is a major public health concern because of its high mortality rates [1]. Because unspecific pathologies pose difficulties in diagnosis, the definition of sepsis has developed over time. The most recent international consensus on the definition of sepsis and septic shock, sepsis-3, was published in 2016 and defines diagnostic guidelines including hypotension, a decreased respiratory rate and a decrease in lactate levels. The *Quick Sequential Organ Failure Assessment* (qSOFA) score was further introduced for fast identification in patients at high

*Correspondence: kohl@hs-furtwangen.de; dei@hs-furtwangen.de
[1] Medical and Life Sciences Faculty, Furtwangen University, Jakob-Kienzle Str. 17, 78054 Villingen-Schwenningen, Germany
Full list of author information is available at the end of the article

risk [2]. Distinguishing sepsis from systemic inflammatory response syndrome (SIRS), which is not caused by a microbial insult, remains difficult, but this distinction is essential to determine proper treatment. For example, if a non-microbial event, such as trauma or necrosis, is the cause of inflammation, administration of antibiotics may cause unnecessary stress and increased mortality [3]. Sepsis leading to organ failure frequently involves the so-called cytokine storm, which also leads to complications in patients with COVID-19 [4]. Therefore, to achieve efficient therapeutic approaches, there is a major clinical need for biomarker assays with a fast turnaround time of $\leq$30 min to diagnose sepsis and guide therapy. Currently, no single biomarker can be used for the diagnosis of sepsis. However, evidence suggests that combined determination of multiple biomarkers might compensate for the low sensitivity and specificity of single marker molecules [5].

C-reactive protein (CRP), the clinically most important acute-phase protein, and interleukin-6 (IL-6) are both early biomarkers that can provide valuable information for distinguishing non-microbial SIRS from sepsis [6, 7]. The 120 kDa pentamer of CRP binds polysaccharides in pathogens and subsequently activates the complement pathway [3, 5, 6]. Under normal conditions, CRP levels are approximately 0.8 mg/L (38 nM) and do not exceed 10 mg/L (477 nM). Elevated CRP levels are indicative of an inflammatory process [6]; these levels can rise to up to 500 mg/L (24,000 nM) in severe cases. The proinflammatory cytokine IL-6 was chosen as the second target, because it is observed very early after noxious events and is produced almost instantly by B and T cells in response to bacterial pathogens. IL-6 weighs approximately 20 kDa, and normal levels are lower than 10 ng/L (0.5 pM). In noxious events, the IL-6 levels can rise as high as 1 µg/L (48 pM) [8]. Indeed, CRP and IL-6 levels both substantially differ between non-septic and septic patients, as well as between septic patients and patients with SIRS, thereby allowing for no sepsis, sepsis and SIRS to be differentiated [9, 10]. Furthermore, accurate quantification of CRP and IL-6 in sepsis and COVID-19 may be crucial for predicting outcomes, thus potentially enabling early therapeutic interventions and therapy control, e.g., in response to mechanical ventilation or Tocilizumab treatment [11–13]. Indeed, several other molecules, such as procalcitonin, are frequently described as potential biomarkers for sepsis [7, 14] and therefore may be included in further development of lateral flow assays, to increase the specificity of such point of care (POC) devices. A combination of CRP and IL-6 in POC devices would have numerous potential areas of application. For example, combined quantification of CRP and IL-6 might be useful for the detection of periprosthetic hip infections [15]. Furthermore, different concentration ranges

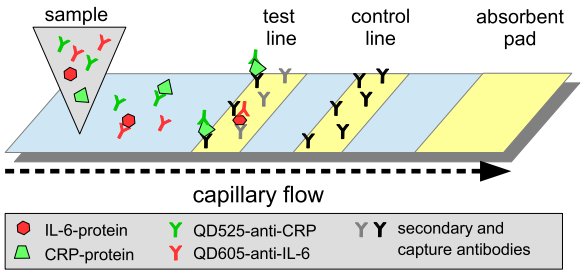

Fig. 1 Illustration of a lateral flow sandwich immunoassay. Antibodies to CRP/IL-6 bound to the test line, and the control line with secondary antibody (anti-mouse/-goat)

for CRP, as well as for IL-6, have been shown to serve as risk indicators for coronary artery disease [16–18]. The relevant detection range of both CRP and IL-6 is, however, highly dependent on the intended application.

Lateral flow immunoassays (LFIAs) are simple, rapid, robust and cost-effective devices with demonstrated potential to simplify and accelerate diagnostics in laboratory settings as well as in resource-poor environments; therefore, LFIAs are a preferable choice for POC diagnostics. Furthermore, the desired concentration ranges can easily be adjusted by varying the applied sample volumes or adding competing unlabeled antibodies, thus rendering LFIAs highly flexible. In addition, different design approaches can be used in lateral flow assays, such as sandwich assays (Fig. 1) or a competitive design to enable detection of small molecules [19, 20].

In competitive design, if antigen is present in the sample, bioprobes consisting of an antibody conjugated to a dye particle will be saturated and unable to bind the test line (see Fig. 2a). If no or little analyte is present in the sample, the bioprobe binds at the test line (see Fig. 2b). Saturated probes are captured at the control line by secondary antibodies, thus indicating that the test is valid [19, 20]. A positive assay shows one test line. The information obtained from each test line can be multiplied by using bioprobes tagged with distinct colors; accordingly, more distinct parameters can be investigated in one lateral flow assay (LFA). To date, mixing different colors at one test line has been achieved only with chromogenic bioprobes [21–23]. A mixture of fluorescent bioprobes has been used only with readout on separate test lines [24].

For detection, antibodies to CRP and IL-6 were conjugated to green and red emitting semiconductor nanocrystals, so-called quantum dots (QDs). QDs can be excited simultaneously by a single UV-light source, emit narrow, sharp peaks of a distinct color, are very resistant to photodegradation and have high fluorescence intensities, which makes QDs a very favorable and effective label for duplex or multiplex approaches in bioassays like LFAs [25, 26].

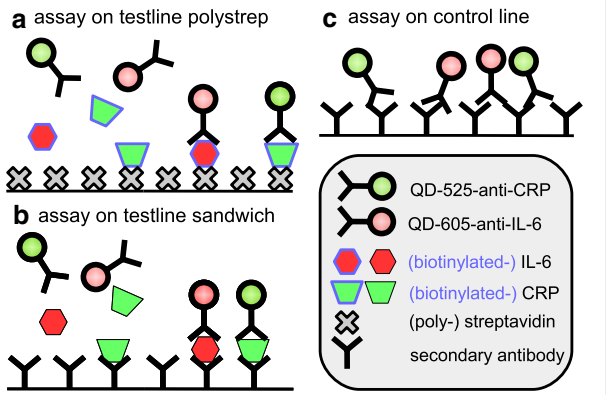

Fig. 2 Binding reaction on the lateral flow strip. **a** Model system: CRP/IL-6-Biotin conjugates bind streptavidin bound to the test line. **b** Sandwich immunoassay: antibodies to CRP/IL-6 bound to the test line. **c** Control line reaction with secondary antibody (anti-mouse)

Materials and methods

Reagents

For synthesis of QD labeled antibody conjugates, we used amine modified CANdot SeriesA QDs (em. max. 530 and em. max. 610) purchased from CAN (Hamburg, Germany) and carboxyl modified QDs (Qdot 525 ITK, Qdot 605 ITK) from Thermo Fischer Scientific (Waltham, USA). Two anti-human IL-6 antibodies (polyclonal host: goat; monoclonal host: mouse), two anti-human-C-reactive protein antibodies (polyclonal host: rabbit; monoclonal host: mouse) and recombinant human IL-6 were obtained from Peprotech (Hamburg, Germany). Secondary anti-mouse (polyclonal host: goat; anti-heavy and light chain IgG, IgA and IgM) antibodies for generation of the control lines were purchased from Sigma Aldrich (St. Louis, USA). Buffers and reagents were purchased from Sigma Aldrich. Human CRP was purchased from Life Diagnostics (West Chester, USA). Biotinylated IL-6 and CRP were provided by R-Biopharm (Darmstadt, Germany). All buffers and reagents were prepared with milliQ water (≥ 18 MΩ). Pur-A-Lyzer Midi (10 kDa MWCO) dialysis tubes and Vivaspin 500 (15 kDa MWCO) columns were purchased from Sigma Aldrich (St. Louis, USA). Lateral flow test strips with a streptavidin test line and anti-mouse-antibody control line were provided by R-Biopharm. CN 95 and CN150 lateral flow membranes were obtained from Sartorius (Goettingen, Germany).

Synthesis of QD labeled antibodies

Amine QD (CANdot-530-anti-CRP and CANdot-610-anti-IL-6) antibody conjugates were prepared with the following protocol.

For activation of QDs (CANdots Series A, amine) 1 µL stock solution (5 µM) was diluted in 184 µL 1× PBS (1 mM EDTA, pH 8.5), and 10 µL of SMCC (125 µM in milliQ water) was added. The mixture was incubated on a horizontal shaker at 22 °C for 1 h. The solution was then dialyzed (10 kDa MWCO) against 1× PBS (1 mM EDTA, pH 7) for 45 min to remove excess SMCC linker. After dialysis, the volume was adjusted to 250 µL with 1× PBS (1 mM EDTA, pH 8.5).

For antibody activation, 1 µL of antibody (anti IL-6 or CRP; 2.25 mg/L in milliQ water) was dissolved in 359 µL 1× PBS (1 mM EDTA, pH 7). Then 10 µL of Traut's reagent (2-Iminothiolan, 16.5 µM, tenfold excess) was added to a final volume of 370 µL. The mixture was incubated for 1 h at 500 rpm and 22 °C. Excess Traut's reagent was removed with a centrifugal concentrator (Vivaspin 500, 15 kDa MWCO), and the antibodies were washed twice with 500 µL PBS (1 mM EDTA, pH 7). Antibodies were then re-dispersed in 370 µL 1× PBS (1 mM EDTA) and combined with the activated QD-solution. The reaction mix was incubated for 30 min at 500 rpm and 22 °C. Then 50 µL 1% BSA in milliQ water was added to the solution to a final volume of 620 µL, and the conjugates were stored at 4 °C overnight.

Carboxyl QDs (Qdot-525-anti-CRP-conjugate and Qdot-605-anti-IL-6-conjugate) antibody conjugates were prepared with the following protocol.

A total of 5 µL of Qdot ITK stock solution (8 µM) was dissolved in 50 µL MES Buffer (50 mM, pH 6.4). Then 5 µL EDC (10 mg/mL in milliQ water) and 5 µL sulfo-NHS (10 mg/L in milliQ water) were added; the mixture was incubated for 30 min at 500 rpm and 22 °C. Then 135 µL of MES buffer (pH 6.4) and 80 µL of antibody solution (0.5 µg/mL in PBS, pH 7.4) were added to a final volume of 200 µL; the mixture was incubated for 90 min at 500 rpm and 22 °C. Then 150 µL HEPES buffer (50 mM, 0.1% Tween 20 and 10% BSA, pH 7.4) was added to a final volume of 350 µL, and the conjugates were stored at 4 °C overnight.

QD (carboxylated) conjugates were characterized by fluorescence emission spectra, agarose gel electrophoresis and dynamic light scattering to verify successful conjugation (Additional file 1: Section S1.1). Fluorescence spectra measurements were collected with a TECAN infinite 200Pro plate reader from Tecan Group Ltd. (Männedorf, Switzerland). Briefly, the prepared conjugates were diluted in ddH_2O to 100 µL. Afterward, QDs were excited at 365 nm, and the fluorescence emission between 450 and 600 nm for QD525, or 550 and 700 nm for QD605, was recorded. Emission peaks were normalized to the peak maximum by dividing the emission values by the maximum emission value. Agarose gel electrophoresis of QDs before and after conjugation to the

corresponding antibodies was performed with 0.5% (w/v) agarose gel electrophoresis in 1× Tris-acetate-EDTA buffer. Electrophoresis was performed at 10 V/cm for 20 min, and pictures were taken with a Gel iX20 Imager device (Intas, Göttingen, Germany). Dynamic light scattering measurements were performed with a Zetasizer Nano instrument (Malvern, Worcestershire UK).

Test strip production and LFA assay procedure

Three different systems were used in the development of the duplex LFA for detection of CRP and IL-6 through optical duplex detection:

1. Streptavidin assay strip production
   Streptavidin assays were performed on lateral flow strips with polystreptavidin on the test line and anti-mouse secondary antibodies on the control line (provided by R-Biopharm). Biotin labeled CRP and IL-6 proteins were used as analytes. For detection of bound biotinylated proteins, QD labeled (CAN dots Series A, 530/610 em. max.) antibody conjugates, CANdot-530-anti-CRP and CANdot-610-anti-IL-6 were applied.
2. Sandwich assay (0–20 nM) and clinical range assay strip production
   The sandwich assay LFA-strips were produced by printing anti-CRP and anti-IL-6-antibodies (0.5 mg/mL anti-CRP polyclonal rabbit; 0.5 mg/mL anti-IL-6 polyclonal rabbit) on the test line and secondary antibodies (1 mg/mL anti-mouse polyclonal goat) on the control line, at a density of 4.85 µL/cm for each line, by using a lateral flow reagent dispenser (Claremont BioSolutions, USA). For the sandwich assay, Sartorius CN95 fast wicking lateral flow membrane was used. For the clinical range assay, Sartorius CN150 high sensitivity lateral flow membrane was used. After printing, the lateral flow membranes were dried overnight in a desiccator at room temperature. The membranes were then affixed to absorbent filters (Whatman) with adhesive tape and cut into 5 mm-wide LFA-strips.
3. Assay procedure
   For all lateral flow tests, running buffer (Bis-Tris 50 mM, 8% Triton X-100 and 0.3% BSA, pH 6.4) was used. Sample proteins were dissolved in 1× PBS with a content of 0% (streptavidin assay), 1% (sandwich assay) or 10% (clinical range assay) human serum. For the streptavidin assay, biotin-labeled target proteins were used. The volume for one lateral flow test sample preparation was 100 µL or 120 µL, consisting of 5–10 µL QD-conjugates of each color, 10 µL or 50 µL target protein solution, and 55 or 70 µL running buffer. The sample mixture was prepared in 2 mL flat bottomed reaction vessels and incubated for 1 min. Then test strips were placed upright in the prepared vessels for either 10 or 20 min to allow the sample mixture to flow through the membranes. After the run, the test strips were placed on a benchtop to dry for 10 min and then imaged. Sample preparations for different assays are summarized in Table 1.

Imaging procedure

Images of test strips were acquired with a BioImager (ChemStudio PLUS, Analytik Jena) equipped with the following bandpass emission filters: filter 1, green channel, 513–557 nm (used with CANdot-530-anti-CRP and Qdot-525-anti-CRP); filter 2, red channel, 565–625 nm (used with CANdot-610-anti-IL-6 and Qdot-605-anti-IL6). Illumination/excitation of fluorescent QD-conjugates was performed with an inbuilt UV-light (top light, $\lambda = 365$ nm). Two pictures were taken with each emission filter at 16 MP resolution (highest resolution, for

Table 1 Sample preparation and processing of LFAs

	Streptavidin assay	Sandwich assay 0–20 nM	Clinical range assay
QD-antibody conjugate	10 µL CANdot-530-anti-CRP; 10 µL CANdot-610-anti-IL-6, both undiluted	10 µL Qdot-525-anti-CRP; 10 µL Qdot-605-anti-IL-6, both undiluted	10 µL Qdot-525-anti-CRP, diluted 1:1 with 0.3 µg/mL anti-CRP (mouse); 5 µL Qdot-605-anti-IL-6, undiluted
LFA-test strips	Test line, polystreptavidin; control line, anti-mouse secondary antibody	Test line, anti CRP (rabbit)/anti IL-6 (goat); control line, anti-mouse- secondary antibody; membrane CN95	Test line, anti CRP (rabbit)/anti IL-6 (goat); control line, anti-mouse- secondary antibody; membrane CN150
Sample composition	20 µL QD-conjugate 10 µL CRP/IL-6 (biotinylated), 0–20 nM in 1× PBS (pH 7.4) 70 µL running buffer	20 µL QD conjugate 10 µL CRP/IL-6, 0–20 nM in 1× PBS (1% serum, pH 7.4) 70 µL running buffer	15 µL QD conjugate 50 µL CRP (0–1000 nM)/IL-6, (0–60 pM) in 1× PBS (10% serum, pH 7.4) 55 µL running buffer
Assay time	1 min incubation of sample mix 10 min run time 10 min drying Imaging ≤ 2 min	1 min incubation of sample mix 10 min run time 10 min drying Imaging ≤ 2 min	1 min incubation of sample mix 20 min run time 10 min drying Imaging ≤ 2 min

streptavidin and sandwich assays) or 2×2 binning (for clinical range assays). Depending on the experimental setup, as well as the analyzed QD, illumination times between 1 and 20 s were chosen to achieve images with clearly visible test and control lines but no oversaturation of the lines, which has been demonstrated to have a negative influence on the readout of AUC values in ImageJ or the developed MultiFlow-Shiny app, thus leading to flat readout peaks (oversaturated peaks). Illumination times were kept constant for each experimental setup and the corresponding QD conjugates used. A detailed list of the imager settings used is shown in Additional file 1: Section S1.2.

MultiFlow-Shiny app

For image processing and data collection, we programmed readout software based on several packages of R statistical software for analysis of bioassay data, which was implemented in our MultiFlow-Shiny app [27–30]. We processed all acquired image datasets with our app and with the ImageJ (V1.50i) gel analyzer tool and compared the acquired key measures such as limit of blank (LOB), limit of detection (LOD) and limit of quantification (LOQ) [31, 32].

Our data processing MultiFlow-Shiny app can be used to process colorimetric data lists from AUC values acquired with other software, such as ImageJ, or can be used as an all-in-one solution for image readout with automated generation of a results sheet. The software allows for cropping, segmentation and background correction of the images to generate the background corrected intensity values for the bands. It combines the intensity data with experimental data, can average technical replicates and computes linear calibration curves. Furthermore, an .html report is generated, including full details about the calibration analysis. The development version of our R packages including the MultiFlow-Shiny app can be downloaded from https://github.com/stamats/MultiFlow. Further details on the MultiFlow app and an illustrated users guide for the use is available from https://stamats.github.io/MultiFlow/MultiFlow.html; a video tutorial is available from https://www.youtube.com/playlist?list=PLRgOZXM8LZ0gv2OJts1c62n0gsXO9VrAN. In the app, imported image files of LFA-strips were first cropped and segmented to select the area of interest and to include a visual control with the test and control lines being properly positioned to enable subsequent background subtraction through Otus's method and readout of line intensity values [33]. The acquired values were merged with the experimental information and exported as a .csv file, which was used to calculate concentration values derived from the duplex CRP/IL-6 LFA. The app allowed us to create custom calibration profiles for strip based bioassays and generate .html reports with the results of the calibration analysis as well as the key measures LOB, LOD and LOQ.

Results and discussion

Streptavidin assay

The objective of the experiments was to evaluate whether two analytical targets could be quantitatively detected at the same test line by using two different fluorescent labels. Therefore, biotinylated analytes (biotinylated CRP and biotinylated IL-6) in combination with two different QD-antibody conjugates (CANdot-530-anti-CRP and CANdot-610-anti-IL-6) were used. After binding of biotinylated targets to the corresponding antibody-QD-conjugates, the complex was bound on the streptavidin test line (Fig. 2a). Conjugates without target did not bind the test line but were captured on the control line containing secondary antibodies.

We first intended to use the system as a competitive immunoassay, in which the added target proteins, CRP/IL-6 without a biotin label, would compete for antibody binding, thus decreasing the fluorescence signal intensity on the test line with increasing target concentration. However, the competitive assay did not show a quantitative correlation after evaluation of the data obtained via ImageJ (Additional file 1: S2.1). We assume that this result was due to high amounts of target competing for the antibody as well as biotin/streptavidin binding sites. Indeed, evaluation with our own data processing MultiFlow-Shiny app revealed a concentration dependent decrease in test line signal intensity (Additional file 1: S2.1). However, the variability and linearity remained poor, as indicated by the low coefficient of determination. Therefore, we switched to a sandwich immunoassay approach, decreasing the number of required components.

Sandwich LFA

After demonstrating that the system generated quantitative data in the streptavidin assay, whereas the competitive assay format was unsuccessful, we designed a new LFA setup based on a sandwich immunoassay format. The test line was composed of anti-CRP and anti-IL-6 antibodies, and QD-525-anti-CRP and QD-605-anti-IL-6 antibodies were used with unlabeled CRP and IL-6 proteins as targets. Initially, we decided to use similar concentration ranges for both analytes to evaluate the linearity at comparable intensities. Because the relevant concentration ranges for both analytes differed by several orders of magnitude, we initially decided to use concentrations between 0 and 20 nM for both analytes. Indeed, when we used the data obtained from ImageJ as well as from our MultiFlow-Shiny app, the

sandwich immunoassay format clearly showed a concentration dependent signal increase for both analytes in the range of 0–20 nM. Nevertheless, the variability in the intensities obtained from ImageJ analysis still remained poor. Additional analysis with our MultiFlow-Shiny app, however, showed significantly lower variability and enhanced the limit of detection and of quantification (Fig. 3 and Table 2). This result was probably due to the automated intensity measurement in combination with background correction in the MultiFlow-Shiny app; in contrast, in classical ImageJ analysis, these parameters are defined by the user.

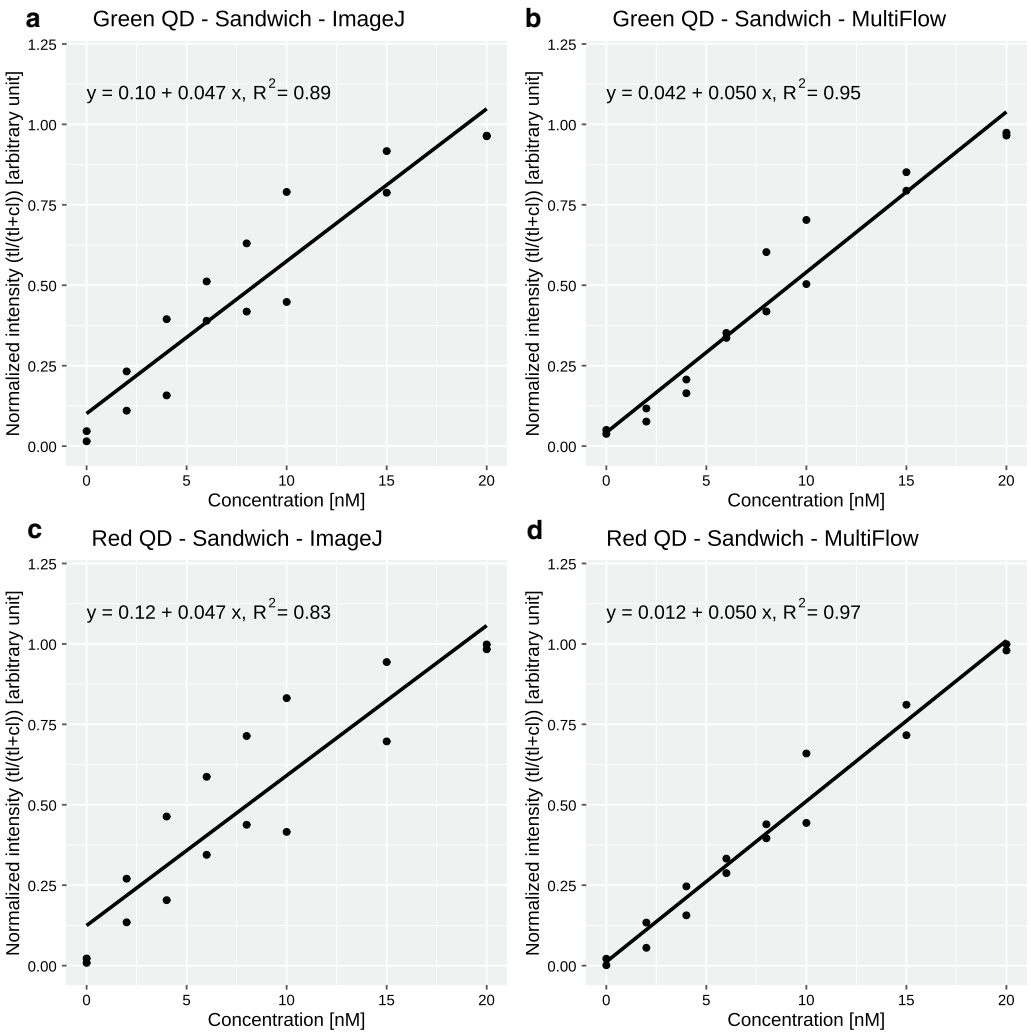

Fig. 3 Calibration curves of the LFA sandwich assay (0–20 nM)

Table 2 Key measures for the sandwich LFA

Sandwich assay 0–20 nM	Green channel QD-525-anti-CRP		Red channel QD-605-anti-IL-6	
Image processing software	**ImageJ**	**MultiFlow app**	**ImageJ**	**MultiFlow app**
LOB	Negative	0.33	Negative	0.46
LOD	2.28	1.27	1.38	2.28
LOQ	11.12	5.52	9.49	7.33
R^2 of linear fit	0.89	0.95	0.83	0.97

Figure 3 shows the calibration curves for the range of 0–20 nmol/L for CRP and IL-6. The R^2-values were clearly better for data acquired with the MultiFlow-Shiny app (0.95 and 0.97) than with *ImageJ* (0.89 and 0.83). Overall, data processing through the MultiFlow-Shiny app provides a benefit over *ImageJ*, a popular, widely used standard tool for quantification of laboratory data. The MultiFlow-Shiny app is a user-friendly solution for readout and data processing of functional LFAs that can be used not only for QD labeled antibodies but also for any kind of LFA, in principle containing an arbitrary number of bands with one or more color labeled antibodies.

Clinical range assay

As described in "Introduction", the relevant clinical range of CRP is between 38 and 24000 nM, whereas the clinical range of IL-6 is much lower, between 0.5 and 48 pM. Because our initial sandwich immunoassay was developed by using a range between 0 and 20 nM, the assay needed to be adjusted to better reflect the relevant concentration ranges observed during inflammatory events such as sepsis or bacterial/viral infections. Therefore, the detection limit of IL-6 was decreased to below 48 pM through increasing the sample amount used per LFA from 10 to 50 µL; using a slow wicking, high sensitivity lateral flow membrane; and decreasing the amount of Qdot-605-anti-IL-6-conjugate to decrease the background fluorescence. To compensate for low emission, we decreased the resolution of the CCD-camera from a maximum of 16 MP resolution to 2×2 binning settings, thus allowing for a fast acquisition time of 1 s while maintaining the brightness of the test lines to be detected. The CRP concentration in blood samples is of interest if it exceeds 500 nM; therefore, the detectable concentration needed to be adjusted to accommodate higher amounts. This was achieved by dilution of the Qdot-525-anti-CRP conjugates with additional anti-CRP antibodies, which competed with the QD-conjugates for the target protein (the sample composition of all three assay types can be found in Table 1). Using these simple modifications, we were able to adjust the CRP/IL-6 assay to the clinically relevant range (examples of test strips in Fig. 4; linear calibration models of both analytes in Fig. 5 and key measures in Table 3), thus enabling the immediate applicability of our assay.

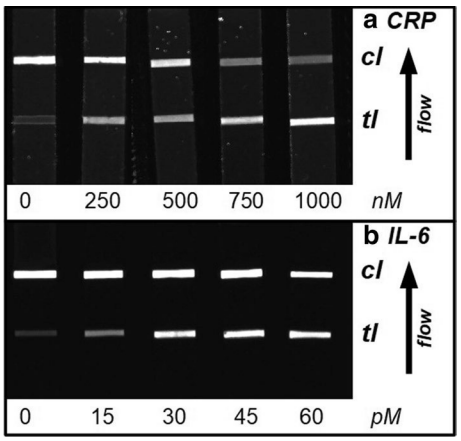

Fig. 4 CRP/IL-6 duplex LFA strips (0–1000 nM CRP/0–60 pM IL-6); top, CRP-assay (readout 513–557 nm bandpass filter); bottom, IL-6-assay (readout 565–625 nm bandpass filter); *cl* control line, *tl* test line. Brightness and contrast were adjusted for better visibility of lines

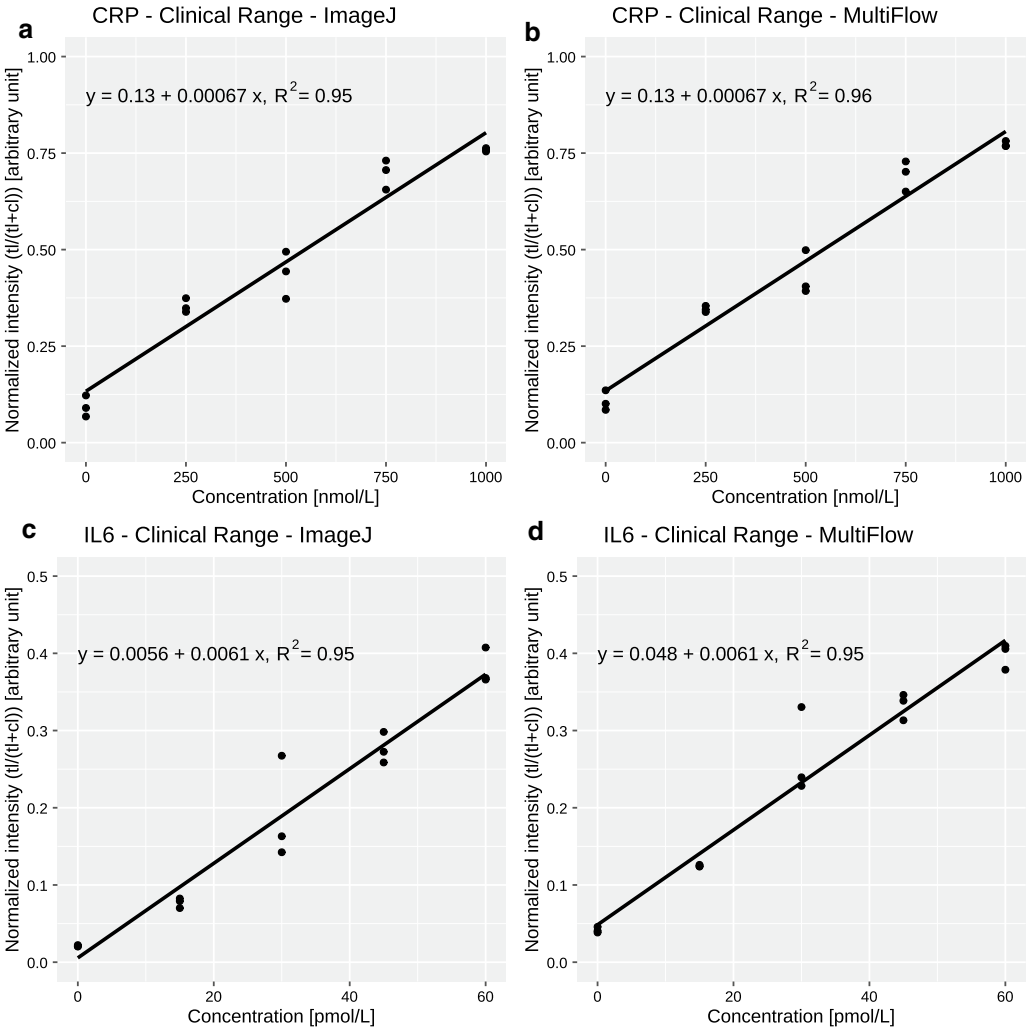

Fig. 5 Calibration curves of the clinical range LFA assay: CRP range, 0–1000 nM; IL-6 range, 0–60 pM

Table 3 Key measures for the clinical range LFA

Clinical range assay	Green channel QD-525-anti-CRP (nM)		Red channel QD-605-anti-IL-6 (pM)	
Image processing software	**ImageJ**	**MultiFlow app**	**ImageJ**	**MultiFlow app**
LOB	7.9	22.8	2.8	Negative
LOD	52.9	42.5	4.5	0.21
LOQ	556.4	527.7	15.3	16.4
R^2 of linear fit	0.96	0.95	0.95	0.95

Performance of the MultiFlow-Shiny app

The MultiFlow-Shiny app provides an all in one solution for the analysis of images taken from LFAs that may include up to six lines, a restriction we chose since we are not aware of any LFA having more than six lines. It works for grayscale as well as color images and can handle images that include several well aligned strips in one batch. Overall, it clearly speeds up the analysis process compared to other image analysis software such as ImageJ. It provides various tools for processing the images, handling the intensity and the experimental data, conducting a calibration analysis by arbitrary linear models and generating automatic.html reports of the calibration analysis. Furthermore, the app offers various options to start the analysis. Instead of starting with the raw images, one can also start with already existing intensity data (e.g. from ImageJ) or further preprocessed intensity data (e.g. after averaging technical replicates). The results of the MultiFlow-Shiny app are also well reproducible, since the analysis is fully automatic except for the cropping of the images. We found that the app especially outperforms the manual analysis with ImageJ when the analyzed LFAs contain very weak signal intensities or broad and blurred lines and consequently leads to better calibration with higher measures of determination. Figure 6 shows screenshots of the user interface of the MultiFlow-Shiny app.

Conclusion

The presented LFAs were designed to detect the sepsis biomarkers CRP and IL-6 simultaneously on one test line, by using two different QDs as labels. We calibrated the LFAs (streptavidin, sandwich assay and clinical range assay) by using linear models, and we demonstrated that optical duplex imaging using emission filters for signal separation did not indicate any mutual disturbance between different QD-dyed antibody probes. The results therefore indicated that the presented setup is suitable for quantitative readout. Data processing with our MultiFlow-Shiny app with automated report generation significantly increased the test performance relative to that of a general-purpose standard software solution, such as *ImageJ*. This improvement was particularly evident in the detection of LFA lines with very weak signal intensities or wide and blurred lines. Accordingly, we not only achieved but exceeded the sensitivity required for the detection of CRP in clinical diagnostics. We furthermore demonstrated that, with simple adjustments (e.g., varying the sample volume, amount of probes applied, addition of unlabeled antibodies and different lateral flow membranes), this method can be made suitable for detecting clinically relevant concentration ranges,

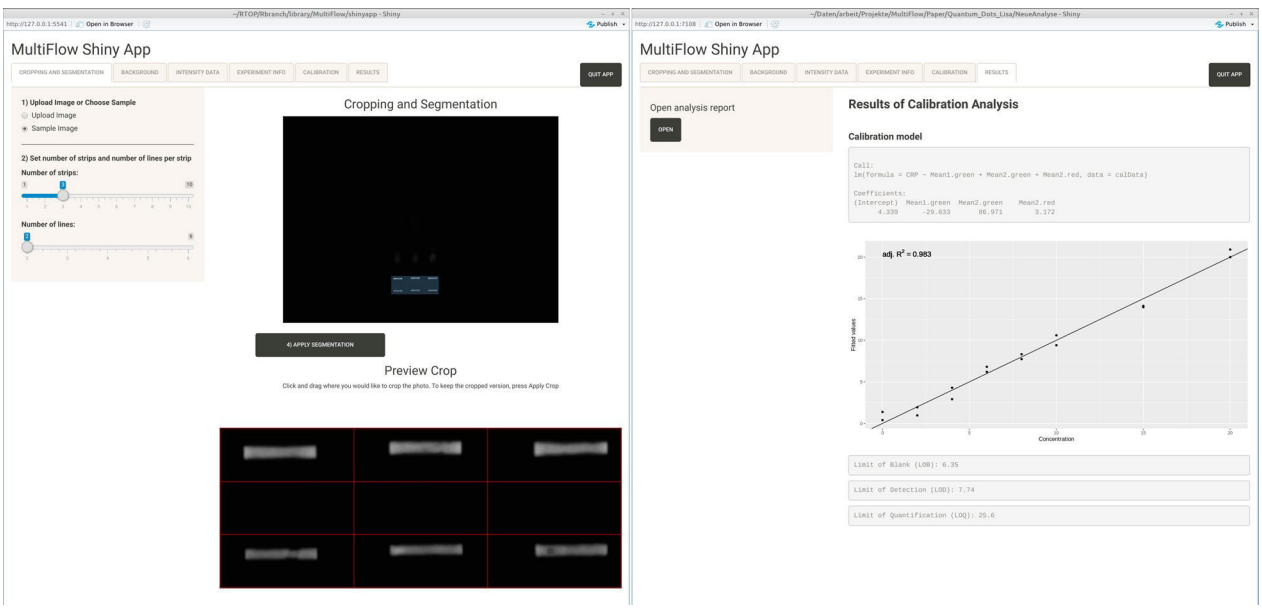

Fig. 6 Screenshot of the MultiFlow-Shiny app: left, cropping and segmentation; right, result report generation

thus providing a highly useful POC assay. Similar approaches should be feasible for other targets. The setup presented, with its optimization to clinical parameters, has potential for increased number of analytical targets and optimized readout workflow through our app. Together with the downsizing of readout equipment, the assay has promise as a robust, inexpensive and rapid POC sensing system for sepsis and other diagnostic challenges.

Supplementary information

Supplementary information accompanies this paper at https://doi.org/10.1186/s12951-020-00688-1.

Additional file 1. Supplementing information of material characterization, imaging hardware settings and results of data processing for the streptavidin and clinical range assay.

Abbreviations

CRP: C-reactive protein; IL-6: Interleukin-6; LF(I)A: Lateral flow (immune) assay; QD: Quantum dot; LOD: Limit of detection; LOB: Limit of blank; LOQ: Limit of quantification; POC: Point of care; PBS: Phosphate buffered saline; EDTA: Ethylenediaminetetraacetic acid; SMCC: *N*-Succinimidyl 4-(maleimidomethyl) cyclohexanecarboxylate; BSA: Bovine serum albumin; MES: 2-(*N*-Morpholino) ethanesulfonic acid; EDC: *N*-Ethyl-*N*′-(3-dimethylaminopropyl)carbodiimide; sulfo-NHS: *N*-Hydroxysulfosuccinimide; HEPES: 4-(2-Hydroxyethyl)piperazine-1-ethanesulfonic acid; Tween 20: Polyethylene glycol sorbitan monolaurate; Bis-Tris: 2,2-Bis(hydroxymethyl)-2,2′,2″-nitrilotriethanol; Triton X-100: *t*-Octylphenoxypolyethoxyethanol.

Acknowledgements

Support from Bundesministerium für Bildung und Forschung (MultiFlow project: 03FH046PX4 and FlowArray project: 13FH121PX8) is gratefully acknowledged. We thank Weronika Schary and Filip Paskali for their support in developing and testing the Shiny app. We thank R-Biopharm (Darmstadt Germany) and especially Steffen Rameil for their support.

Authors' contributions

CR performed most of the experiments, performed analysis of data through ImageJ and wrote this article. LK performed particle characterization experiments and contributed to writing and editing of this article. LJJ performed streptavidin assay pre-experiments. MK performed statistical data analysis, programmed R-packages and apps, and contributed to writing of data processing parts. SL and HPD revised the manuscript and contributed to editing. All authors read and approved the final manuscript.

Funding

Open access funding provided by Projekt DEAL.

Availability of data and materials

MultiFlow-Shiny app download: https://github.com/stamats/MultiFlow
Manual at: https://stamats.github.io/MultiFlow/MultiFlow.html
Video tutorial: https://www.youtube.com/playlist?list=PLRgOZXM8LZ0gv2OJts1c62n0gsXO9VrAN
Additional charts and tables referred to in the text are available in Additional file 1.

Ethics approval and consent to participate

Not applicable.

Consent for publication

Not applicable.

Competing interests

The authors declare no conflicts of interest.

Author details

[1] Medical and Life Sciences Faculty, Furtwangen University, Jakob-Kienzle Str. 17, 78054 Villingen-Schwenningen, Germany. [2] Institute of Precision Medicine, Furtwangen University, Jakob-Kienzle Str. 17, 78054 Villingen-Schwenningen, Germany. [3] Department of Pharmaceutical Chemistry, Pharmaceutical Institute, University of Tuebingen, Auf der Morgenstelle 8, 72076 Tübingen, Germany. [4] Institute of Pharmaceutical Sciences, University of Freiburg, Albertstraße 25, 79104 Freiburg, Germany. [5] EXIM Department, Fraunhofer Institute IZI, Leipzig, Schillingallee 68, 18057 Rostock, Germany. [6] Faculty of Science, Tuebingen University, Auf der Morgenstelle 8, 72076 Tübingen, Germany.

Received: 16 June 2020 Accepted: 30 August 2020
Published online: 10 September 2020

References

1. Driessen RGH, van de Poll MCG, Mol MF, van Mook WNKA, Schnabel RM. The influence of a change in septic shock definitions on intensive care epidemiology and outcome: comparison of sepsis-2 and sepsis-3 definitions. Infect Dis. 2018;50:207–13. https://doi.org/10.1080/23744235.2017.1383630.
2. Singer M, Deutschman CS, Seymour C, Shankar-Hari M, Annane D, Bauer M, Bellomo R, Bernard GR, Chiche JD, Coopersmith CM, et al. The third international consensus definitions for sepsis and septic shock (sepsis-3). JAMA J Am Med Assoc. 2016;315:801–10.
3. Soong J, Soni N. Sepsis: recognition and treatment. Clin Med J R Coll Physicians Lond. 2012;12:276–80.
4. Hu B, Huang S, Yin L. The cytokine storm and COVID-19. J Med Virol. 2020. https://doi.org/10.1002/jmv.26232.
5. Deigner HP, Kohl M. The molecular sepsis signature. Crit Care Med. 2009;37:1137–8.
6. Póvoa P. C-reactive protein: a valuable marker of sepsis. Intensive Care Med. 2002;28:235–43.
7. Kibe S, Adams K, Barlow G. Diagnostic and prognostic biomarkers of sepsis in critical care. J Antimicrob Chemother. 2011;66:ii33–ii40. https://doi.org/10.1093/jac/dkq523.
8. Pfäfflin A, Schleicher E. Inflammation markers in point-of-care testing (POCT). Anal Bioanal Chem. 2009;393:1473–80. https://doi.org/10.1007/s00216-008-2561-3.
9. Yang Y, Xie J, Guo F, Longhini F, Gao Z, Huang Y, Qiu H. Combination of C-reactive protein, procalcitonin and sepsis-related organ failure score for the diagnosis of sepsis in critical patients. Ann Intensive Care. 2016;6:51. https://doi.org/10.1186/s13613-016-0153-5.
10. Lamping F, Jack T, Rübsamen N, Sasse M, Beerbaum P, Mikolajczyk RT, Boehne M, Karch A. Development and validation of a diagnostic model for early differentiation of sepsis and non-infectious SIRS in critically ill children—a data-driven approach using machine-learning algorithms. BMC Pediatr. 2018;18:112. https://doi.org/10.1186/s12887-018-1082-2.
11. Suhua Z, Lefeng Z, Qingli C, Yueying W. The prognostic value of serum PCT, hs-CRP, and IL-6 in patients with sepsis. Open Life Sci. 2017;12:425–8. https://doi.org/10.1515/biol-2017-0050.
12. Herold T, Jurinovic V, Arnreich C, Lipworth BJ, Hellmuth JC, von Bergwelt-Baildon M, Klein M, Weinberger T. Elevated levels of IL-6 and CRP predict the need for mechanical ventilation in COVID-19. J Allergy Clin Immunol. 2020;146:128–136.e4. https://doi.org/10.1016/j.jaci.2020.05.008.
13. Luo P, Liu Y, Qiu L, Liu X, Liu D, Li J. Tocilizumab treatment in COVID-19: a single center experience. J Med Virol. 2020;92:814–8. https://doi.org/10.1002/jmv.25801.
14. Hall TC, Bilku DK, Al-Leswas D, Horst C, Dennison AR. Biomarkers for the differentiation of sepsis and SIRS: the need for the standardisation of diagnostic studies. Ir J Med Sci. 2011;180:793–8.
15. Buttaro MA, Tanoira I, Comba F, Piccaluga F. Combining C-reactive protein and interleukin-6 may be useful to detect periprosthetic hip infection. In: Proceedings of the clinical orthopaedics and related research, Vol. 468. Springer New York LLC. 2010; pp. 3263–7.
16. Fonseca FAH, de Izar MCO. High-sensitivity C-reactive protein and cardiovascular disease across countries and ethnicities. Clinics. 2016;71:235–42.

17. Cozlea DL, Farcas DM, Nagy A, Keresztesi AA, Tifrea R, Cozlea L, Carașca E. The impact of C reactive protein on global cardiovascular risk on patients with coronary artery disease. Curr Health Sci J. 2013;39:225–31. https://doi.org/10.12865/CHSJ.39.04.06.
18. Wainstein MV, Mossmann M, Araujo GN, Gonçalves SC, Gravina GL, Sangalli M, Veadrigo F, Matte R, Reich R, Costa FG, et al. Elevated serum interleukin-6 is predictive of coronary artery disease in intermediate risk overweight patients referred for coronary angiography. Diabetol Metab Syndr. 2017;9:67. https://doi.org/10.1186/s13098-017-0266-5.
19. Posthuma-Trumpie GA, Korf J, Van Amerongen A. Lateral flow (immuno) assay: its strengths, weaknesses, opportunities and threats. A literature survey. Anal Bioanal Chem. 2009;393:569–82. https://doi.org/10.1007/s00216-008-2287-2.
20. Li J, Macdonald J. Multiplexed lateral flow biosensors: Technological advances for radically improving point-of-care diagnoses. Biosens Bioelectron. 2016;83:177–92.
21. Qi XP, Huang YY, Lin ZS, Xu L, Yu H. Dual-quantum-dots-labeled lateral flow strip rapidly quantifies procalcitonin and C-reactive protein. Nanoscale Res Lett. 2016. https://doi.org/10.1186/s11671-016-1383-z.
22. Panfilova E, Shirokov A, Khlebtsov B, Matora L, Khlebtsov N. Multiplexed dot immunoassay using Ag nanocubes, Au/Ag alloy nanoparticles, and Au/Ag nanocages. Nano Res. 2012;5:124–34. https://doi.org/10.1007/s12274-012-0193-6.
23. Yen CW, De Puig H, Tam JO, Gómez-Márquez J, Bosch I, Hamad-Schifferli K, Gehrke L. Multicolored silver nanoparticles for multiplexed disease diagnostics: distinguishing dengue, yellow fever, and Ebola viruses. Lab Chip. 2015;15:1638–41. https://doi.org/10.1039/c5lc00055f.
24. Taranova NA, Berlina AN, Zherdev AV, Dzantiev BB. "Traffic light" immunochromatographic test based on multicolor quantum dots for the simultaneous detection of several antibiotics in milk. Biosens Bioelectron. 2015;63:255–61. https://doi.org/10.1016/j.bios.2014.07.049.
25. Ruppert C, Kohl M, Jacob L, Deigner HP. Multiplexing in bioassays. Biosens J. 2015. https://doi.org/10.4172/2090-4967.1000124.
26. Lim YT, Kim S, Nakayama A, Stott NE, Bawendi MG, Frangioni JV. Selection of quantum dot wavelengths for biomedical assays and imaging. Mol Imaging. 2003;2:153535002003021. https://doi.org/10.1162/153535002003021.
27. R Core Team. R: a language and environment for statistical computing. Vienna: R Foundation for Statistical Computing; 2018.
28. Chang W, Cheng J, Allaire J, Xie Y, McPherson J. Shiny: web application framework for R. R package version 1.5.0. https://cran.r-project.org/package=shiny.
29. Fu A, Shin A, Matloff N. ShinyImage: image manipulation, with an emphasis on journaling. R package version 0.1.1. https://cran.r-project.org/package=ShinyImage.
30. Kohl M. MultiFlow: multiplex lateral flow assays. R package version 0.2.
31. Armbruster DA, Pry T. Limit of blank, limit of detection and limit of quantitation. Clin Biochem Rev. 2008;29(Suppl 1):S49–52.
32. Little T. Method validation essentials, limit of blank, limit of detection, and limit of quantitation. BioPharm Int. 2015;28:48–51.
33. Otsu N. Threshold selection method from gray-level histograms. IEEE Trans Syst Man Cybern. 1979;9:62–6. https://doi.org/10.1109/tsmc.1979.4310076.

Publisher's Note

3.3 Publication 3: Combining aptamers and antibodies: lateral flow quantification for thrombin and interleukin-6 with smartphone readout

Mahmoud M, Ruppert C, Rentschler S, Laufer S and Deigner HP

Sensors and Actuators B: Chemical 333, 129246 (2020)

https://doi.org/10.1016/j.snb.2020.129246

Status: published ***Manuscript pages:*** ***48-54***

Sensors & Actuators: B. Chemical 333 (2021) 129246

Contents lists available at ScienceDirect

Sensors and Actuators: B. Chemical

journal homepage: www.elsevier.com/locate/snb

Combining aptamers and antibodies: Lateral flow quantification for thrombin and interleukin-6 with smartphone readout

Mostafa Mahmoud [a,b,c], Christoph Ruppert [a,b,c], Simone Rentschler [a,b,c], Stefan Laufer [c], Hans-Peter Deigner [a,b,d,e,*]

[a] Furtwangen University, Medical and Life Sciences Faculty, Jakob-Kienzle Str. 17, D-78054, Villingen Schwenningen, Germany
[b] Institute of Precision Medicine, Jakob-Kienzle Str. 17, D-78054, Villingen-Schwenningen, Germany
[c] University of Tuebingen, Pharmaceutical Institute, Department of Pharmaceutical Chemistry, Auf der Morgenstelle 8, D-72076, Tuebingen, Germany
[d] Fraunhofer Institute IZI, Leipzig, EXIM Department, Schillingallee 68, D-18057, Rostock, Germany
[e] University of Tuebingen, Faculty of Science, Auf der Morgenstelle 8, D-72076, Tuebingen, Germany

ARTICLE INFO

Keywords:
Duplex lateral flow assay
Point-of-care diagnostics
Nanoparticles
Quantum dots image processing
Immunoassay
Aptamer assay
3D-printing
Smartphone imaging

ABSTRACT

Modern strategies in precision medicine require diagnostic tools for fast assessment of biomarkers. A popular and well-established assay format for the rapid detection of disease markers directly at the point of care is the lateral flow assay, which enables medical staff to directly use body fluids such as blood or urine for diagnosis, without the need for a professional laboratory environment. Interleukin-6 and thrombin are clinically relevant biomarkers that are associated with infectious diseases, inflammation, and blood coagulation, and can provide valuable information on the status and treatment responses of patients with COVID-19. This work presents a novel method for the quantification of these biomarkers by using fluorescent green and red quantum dots as labels for interleukin-6 antibodies and thrombin binding aptamers, respectively. For readout, a 3D printed smartphone imager with a built in UV-LED light source is used. Through separation of RGB-channels, the acquired images can be processed to achieve a fully functional duplex lateral flow assay for simultaneous quantification of interleukin-6 and thrombin on the same test line (optical multiplexing). Furthermore, the assay performs well in complex samples (10 % serum samples). In conclusion, this novel combination of antibody and aptamer-based detection in a single lateral flow assay reduces turnaround time, and the user-friendly smartphone imager facilitates availability, particularly in low resource settings.

1. Introduction

Fast, inexpensive, and readily available diagnostic tools for biomarker assessment are becoming increasingly important in precision medicine. Point-of-care (POC) tests are of particular interest, especially in disease epidemics, because they are designed to be used at sites of patient care and to provide rapid results, thus enabling better clinical decision-making and improved clinical outcomes [1,2]. Lateral flow assays (LFAs) meet all the criteria necessary for application as POC tests [3]. They have been applied in early detection of complex diseases, such as cancer [4,5] and sepsis [6,7], through high sensitivity and specificity multiplex quantification of various analytes.

If reliable quantitative results are necessary for analytes such as blood biomarkers, readout hardware, such as professional LFA readers, must be used. Optical strip readers can enable precise signal quantification, thus overcoming the drawback of operator dependent result interpretation, and can also improve the detectability and sensitivity of multiplex LFA sensors [8,9]. Because smartphones have become an ubiquitous part of everyday life, even in remote areas and low resource settings, smartphone-based readout of LFAs presents a major opportunity for use in POC tests [10,11].

Numerous approaches exist for smartphone-based analysis of LFAs without additional hardware; some include using simple aids, such as a cardboard dark box, or 3D-printed accessories for applications in food analysis, drug monitoring or diagnostics [11–14]. Recently, aptamers have been explored as replacements for antibodies in LFA [15,16].

Aptamers are in vitro selected single strand oligonucleotides that bind various target molecules, e.g., proteins, small molecules, and toxins [15,17–19]. The thrombin binding aptamer (TBA) used in this work is a 15mer DNA aptamer identified in 1992 to bind thrombin exosite I [20].

* Corresponding author at: Furtwangen University, Medical and Life Sciences Faculty, Jakob-Kienzle Str. 17, D-78054, Villingen Schwenningen, Germany.
E-mail addresses: dei@hs-furtwangen.de, hans-peter.deigner@hs-furtwangen.de (H.-P. Deigner).

https://doi.org/10.1016/j.snb.2020.129246
Received 30 August 2020; Received in revised form 10 November 2020; Accepted 20 November 2020
Available online 30 November 2020

TBA has been studied extensively, and its binding structure has been characterized by NMR spectroscopy [21] and X-ray crystallography [22]. According to these studies, TBA binds α-thrombin in an antiparallel quadruplex structure but shows no detectable binding to γ-thrombin or to other serum proteins or enzymes [23].

Interleukin (IL) 6 and thrombin are both relevant in multiple diseases, such as chronic inflammation, autoimmunity, infectious diseases, cancer, neurodegenerative diseases, and sepsis [24–27]. More recently, both molecules have been found to play important roles in severe coronavirus disease 2019 (COVID-19) and to serve as potential biomarkers [28].

COVID-19 can lead to a variety of complications, such as pneumonia, sepsis, respiratory arrest, and acute respiratory distress syndrome (ARDS). COVID-19 results in significant mortality, and ARDS is the main cause of death [29]. Clinical data suggest that is one of the main mechanisms of ARDS is cytokine storm syndrome, which involves an uncontrolled systemic inflammatory response resulting from the extensive release of pro-inflammatory cytokines and chemokines (e.g., tumor necrosis factor, IL-6, and IL-1β) [29,30] and correlates with COVID-19 severity [31]. Blood levels of IL-6, a pro-inflammatory mediator, are lower in patients with mild disease but significantly elevated in critically ill patients [32]. Even higher IL-6 levels are found in patients who die in the course of the disease [33]. IL-6 levels therefore might be predictive of fatal outcomes, and initial determination of IL-6 might provide an opportunity to assess worsening clinical symptoms and COVID-19 progression [34,35]. IL-6 detection might even be used to identify patients eligible for a specific immunosuppressive treatment [36]. Moreover, IL-6 stimulates coagulation cascades in response to SARS-CoV-2-induced inflammation by disrupting the production of tissue factor and ultimately thrombin production [37], thus contributing to coagulation abnormalities, coagulopathy, and thrombotic complications in patients with severe COVID-19 [38,39]. Early detection of patients with increased risk of coagulopathy by measuring thrombin might allow for timely therapeutic intervention and thus decrease SARS-CoV-2 microthrombosis and the associated poor outcomes. Quantification of IL-6 and thrombin levels [40] therefore may be highly useful in COVID-19 treatment and monitoring of therapy. For IL-6, the clinical range in healthy adults is 1.0–5.0 pg/mL, but levels rapidly increase in disease and can reach concentrations on the order of μg/mL in extreme conditions (e.g., septic shock) [24]. Similarly, thrombin circulates at picomolar concentrations in the blood and regulates coagulation. However, at sites of injury, thrombin concentrations as high as several hundred nanomolar can be found. This process is regulated by natural thrombin inhibitors and is localized. Nevertheless, free thrombin levels of 5–20 nM indicate a high risk of thrombosis, and concentrations above 20 nM indicate thrombosis [41]. We therefore set out to develop a straightforward and fast test for both parameters that requires minimal hardware for quantitative readout.

We present a duplex LFA system for detecting IL-6 and thrombin on the basis of red and green quantum dot (QD) labels and readout through a 3D printed smartphone reader with a built-in UV-LED light source. By splitting the colored pictures through RGB-channels, we achieved quantitative optical duplex detection on the same test line. Therefore, the system is suitable for multiparameter diagnostic applications while providing all benefits associated with POC testing.

2. Materials and methods

2.1. Materials

Carboxyl modified QDs (Qdot 525 ITK, Qdot 605 ITK) were purchased from Thermo Fisher Scientific, (Waltham, USA). Two anti-human IL-6 antibodies (biotinylated goat polyclonal or mouse monoclonal) were purchased from Peprotech (Hamburg, Germany). An amine modified thrombin binding aptamer (TBA: (5`-amine-TT TTT TTT TTT TTT TTT TTT GGT TGG TGT GGT TGG-3`)) and corresponding biotin labeled detection aptamer (HD22: 5`-biotin-AGT CCG TGG TAG GGC AGG TTG GGG TGA CT-3`) were purchased from Integrated DNA Technologies IDT (Leuven, Belgium). Buffers and reagents were purchased from Sigma Aldrich. All buffers and reagents were prepared with milliQ water (≥ 18 MΩ). Lateral flow test strips with a streptavidin test line and anti-mouse-antibody control line were provided by R-Biopharm (Darmstadt, Germany). A human IL-6 ELISA kit was purchased from PeproTech (Hamburg, Germany), and a human thrombin ELISA kit was purchased from Abcam (Cambridge, MA).

2.2. Synthesis of QD labeled antibodies and aptamers

Carboxyl QD conjugates (*Qdot ITK 525* for conjugation to anti-IL-6 antibody, *Qdot ITK 605* for conjugation to thrombin aptamer) were produced according to the following protocol:

Qdot ITK carboxyl stock solution (5 μL of 8 μM stock) was diluted in 50 μL MES (2-(N-morpholino)ethanesulfonic acid) buffer (50 mM, pH 6.4). Then 5 μL EDC (N-ethyl-N′-(3-dimethylaminopropyl)carbodiimide) (10 mg/mL in milliQ water) and 5 μL N-hydroxysulfosuccinimide (sulfo-NHS) (10 mg/L, in milliQ water) were added, and the mixture was incubated for 30 min under 500 rpm orbital mixing, at 22 °C.

Then 80 μL antibody solution (monoclonal mouse anti-IL6, 0.5 mg/mL in phosphate buffered saline (PBS) pH 7.4) was added to activated *Qdot ITK 525* solution for QD-525-anti-IL-6-conjugate synthesis, or 80 μL TBA (100 nM, in milliQ water) was added to activated *Qdot ITK 605* solution for QD-605-TBA-conjugate synthesis. Both reaction mixes were adjusted to 200 μL with MES buffer (pH 6.4) and incubated for 90 min under 500 rpm, at 22 °C. Then 150 μL HEPES (4-(2-hydroxyethyl) piperazine-1-ethanesulfonic acid) buffer (50 mM, 0.1 % Tween 20 (polyethylene glycol sorbitan monolaurate), and 10 mg/mL bovine serum albumin (BSA), pH 7.4) were added. The conjugates were then stored at 4 °C overnight.

2.3. Characterization of the QDs

Agarose gel electrophoresis of QDs before and after conjugation to the IL-6 antibody and TBA was performed on a 1% (w/v) agarose gel in 1× Tris-acetate-EDTA buffer. Electrophoresis was performed at 10 V/cm for 20 min, and pictures were taken with a Gel iX20 Imager device (Intas, Göttingen, Germany). Fluorescence spectrum measurements were collected with a TECAN Infinite 200Pro plate reader from Tecan Group Ltd. (Männedorf, Switzerland). The prepared conjugates were diluted in ddH_2O to 100 μL. Afterward, the QDs were excited at 365 nm, and the fluorescence emission between 450 and 600 nm for QD525, or 550 and 700 nm for QD605, was recorded. Emission peaks were normalized to the peak maximum and plotted against the wavelength. DLS-spectra were acquired with a Zetasizer Nano ZS instrument (Malvern, Worcestershire UK).

2.4. Running buffer and assay component optimization

The buffer volume was 90 μL for single-plex experiments and 80 μL for duplex experiments. For all experiments, a volume of 10 μL of each QD conjugate (QD-525-anti-IL-6-conjugate or QD-605-TBA-conjugate) was used per lateral flow strip.

The following buffers were tested: LFA running buffer (50 mM bis-Tris, 8% Triton X-100 (t-octylphenoxypolyethoxyethanol), and 0.3 % BSA, pH 7.5), aptamer binding buffer (20 mM Tris−HCl, 140 mM NaCl, and 2 mM $MgCl_2$, pH 7.5), and aptamer binding buffer with an additional 8% Triton X-100, a mix of 50 % aptamer binding buffer and 50 % LFA running buffer, and PBST (1 × PBS with 0.1 % Tween20). A 20 μL volume of buffer was replaced with the corresponding analyte (IL-6 250 nM, thrombin 866 nM). A 2.5 μL volume of the buffer was replaced with IL-6 detection antibody (50 μg/mL) for the IL-6 experiments, and a 0.625 μL volume was replaced with HD22 (1 μM) for the thrombin experiments.

2.5. LFA assay procedure

In the single-plex experiments, 10 µL of either QD-525-anti-IL-6-conjugate or QD-605-TBA-conjugate was added to the prepared samples in aptamer binding buffer with 8% Triton X-100 and either 0.625 µL HD22 (1 µM) in thrombin assays or 2.5 µL IL-6 detection antibody (50 µg/mL) in IL-6 assays, in a 2 mL flat bottom reaction vessel. Similarly, in the duplex experiments, 10 µL of each QD conjugate was added to the prepared samples in aptamer binding buffer with 8% Triton X-100 containing 0.625 µL HD22 (1 µM) and 2.5 µL IL-6 detection antibody (50 µg/mL) in a 2 mL flat bottom reaction vessel. The final volume of the prepared reaction mixes was fixed at 100 µL. For serum experiments, 10 µL of buffer was replaced by human serum to achieve a content of 10 % serum. Lateral flow strips were then placed in the prepared mixture. Samples were given 15 min to flow through the LFA strips, and were then allowed to dry for 5 min and imaged for further analysis.

2.6. Specificity experiments

To assess the specificity of the assay, we challenged the LFA strips with structurally similar molecules as controls. For the thrombin response, prothrombin at a final concentration of 173.2 nM; a mix of thrombin (86.6 nM) and antithrombin III (200 nM); and a mix of prothrombin (86.6 nM) with antithrombin III (100 nM) were used. For the IL-6 response, IL-2 (50 nM) and IL-8 (50 nM) were used. The thrombin/antithrombin III mixes were preincubated for 30 min at room temperature. Similarly to the protocol for the duplex experiments, 10 µL of each QD conjugate was added to the prepared samples in aptamer binding buffer with 8% Triton X-100 containing 0.625 µL HD22 (1 µM) and 2.5 µL of IL-6 detection antibody (50 µg/mL) in a 2 mL flat bottom reaction vessel. The final volume of the prepared reaction mixes was fixed at 100 µL.

2.7. ELISA experiments

The thrombin ELISA kit was used according to the manufacturer's protocol. Thrombin was diluted in 1× diluent to final amounts of 0, 0.00215, 0.0043, 0.0086, 0.0172, and 0.0258 pmol. For the recovery experiments, thrombin was diluted to the same concentrations in 1× diluent containing 10 % serum. To account for variability, each concentration was assayed in quintuplicate, with 50 µL sample per well. The samples were incubated for 2 h at room temperature. The biotinylated detection antibody was incubated for 1 h, and this was followed by a 30 min incubation step with streptavidin-peroxidase conjugate. After each step, the plates were washed five times with 200 µL 1× wash buffer per well; 15 min after the addition of the chromogen substrate, the stop solution was added. The absorbance was measured on a TECAN infinite 200Pro plate reader at a wavelength of 450 nm with 570 nm as the reference wavelength.

A Human IL-6 Standard ABTS ELISA kit was used according to the manufacturer's protocol. A Nunc-MaxiSorp™ flat bottom 96-well plate (Thermo Fisher) was coated with 100 µL capture antibody at a concentration of 0.5 µg/mL overnight at room temperature. Unbound sites were blocked with 300 µL blocking buffer (1x PBS and 1% BSA, pH 7.2) per well for 1 h at room temperature. IL6 was diluted in diluent (1x PBS, 0.05 % Tween-20, and 0.1 % BSA, pH 7.2) to final amounts of 0, 0.000625, 0.00125, 0.0025, 0.005, and 0.0075 pmol. For the recovery experiment, the IL-6 was diluted to the same concentrations in diluent containing 10 % serum. To account for variability, each concentration was assayed in quintuplicate, with 100 µL sample per well. The samples were incubated for 2 h at room temperature. The biotinylated detection antibody (1 µg/mL) was incubated for 2 h, and this was followed by a 30 min incubation step with avidin-HRP conjugate. After each step, the plates were washed four times with 300 µL wash buffer (PBS and 0.05 % Tween-20, pH 7.2) per well. A 100 µL volume of ABTS solution was added per well, and the absorbance was measured after 30 min at a wavelength of 405 nm, with 650 nm as the reference wavelength.

2.8. Smartphone imager: 3D-printed LFA reader for Huawei P30 pro

Pictures of the LFA test strips were taken with a *Huawei P30 Pro* smartphone by using a 3D-printed dark box (Fig. 1). The developed smartphone imager was composed of four 3D-printed parts (bottom part, top part (consisting of a lid and exchangeable smartphone adapter), and sample plate for seven LFA strips) and was equipped with a 365 nm UV-LED light source consisting of a UV-LED, ∅ 50 mm aluminum heatsink, 350 mA power supply, and power supply cable with a switch for connection to the European standard 220 V power grid. The *Huawei P30 Pro* camera provided 40 M P resolution. Pictures were taken without zoom and with the flash disabled, under standard settings. The 3D-models for download and the technical specifications of the electronic components are provided in the Electronic Supplementary Material. All 3D-printed parts were produced with an *Ultimaker 3* printer with black and red PLA filament at 0.2 mm layer height resolution. As a reference readout system, a BioImager (ChemStudio Plus, Analytic Jena) equipped with suitable emission bandpass filters was used.

2.9. Data processing: color separation

Images captured with the BioImager (*ChemStudio Plus*, Analytik Jena) and the smartphone imager were analyzed in ImageJ. With the BioImager, images were captured with the corresponding emission filters (565–625 nm bandpass, Omega Optical nr. 595BP60/50 for red particles; 514–557 nm bandpass, Omega Optical nr. 535BP60/50 for green particles). This process resulted in separate images for each

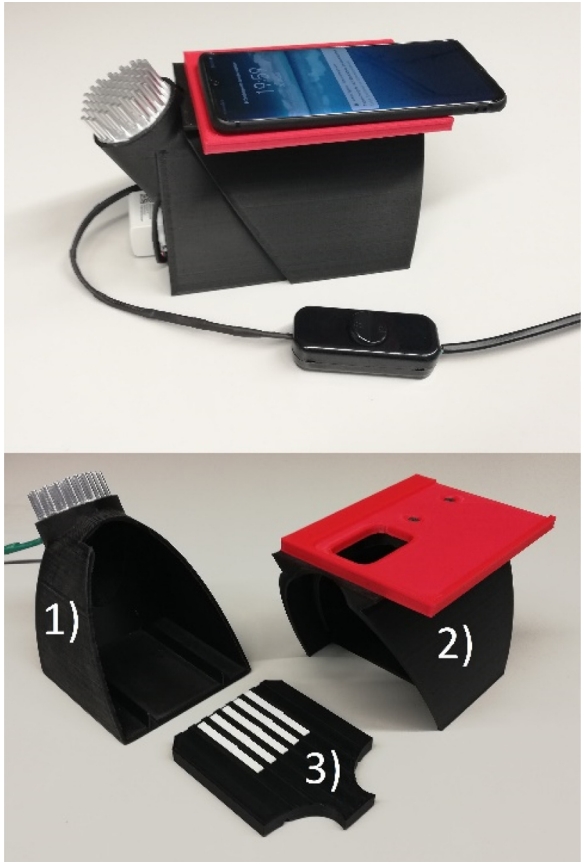

Fig. 1. Smartphone imager consisting of 1) a bottom part equipped with a UV-LED light source, 2) a top part comprising a darkbox lid equipped with an exchangeable adapter for a Huawei P30 Pro smartphone, and 3) a sample plate for up to seven LFA strips (5 mm width).

analyte. The images were quantified with the gel analyzer tool, and the signal was plotted against the concentration. In the case of the smartphone dark box, no physical emission filters were used. The smartphone images were first split into RGB channels and then analyzed with the gel analyzer tool.

Data analysis (plotting, fitting with linear and non-linear regression analysis, and statistical significance analysis) was performed in GraphPad Prism version 8.02 for Windows, La Jolla California USA, www.graphpad.com.

3. Results and discussion

3.1. QD conjugate characterization

Fluorescence emission spectra, agarose gel electrophoresis, and dynamic light scattering were used to verify the successful conjugation of the IL-6 antibody and TBA to the QDs. The emission spectra showed a shift of approximately 2 nm for the IL-6 QD conjugates and 1 nm for the TBA QD conjugates (Fig. S2). This behavior is in agreement with reports in previous publications, reviewed in [42]. Because most modern QDs are synthesized to avoid any significant changes to their optical properties after bioconjugation, agarose gel electrophoresis was used to further study the conjugates and confirm successful conjugation. A band shift was observed (Fig. S2) after conjugation for both QD conjugates. DLS spectra (Fig. S2) further confirmed the successful conjugation of the antibodies and aptamers (diameters: QD525-unconjugated, 11.7 nm; QD525-anti IL-6, 15.7 nm; QD605-unconjugated, 21.0 nm; and QD605-TBA, 28.2 nm).

3.2. Running buffer optimization

The binding of aptamers as well as antibodies is highly dependent on the buffer's salt concentration. Different buffers were tested in a single-plex format with either the QD-605-TBA-conjugate for thrombin detection or the QD-525-anti-IL-6-conjugate for IL-6 detection, to identify the optimal multiplex running buffer.

For the QD-605-TBA-conjugates, as shown in Fig. S2, no signal was detected with the LFA running buffer, owing to a lack of monovalent and divalent cations in the buffer. The aptamer binding buffer showed a high signal, albeit with a very high background because of the lack of surfactants and the passive adsorption of the QD conjugates on the lateral flow membrane. The highest binding was obtained with the aptamer binding buffer containing 8% Triton X-100; this result was attributable to the aptamer's dependence on the salt concentration for proper folding and subsequent binding, and the blocking of non-specific adsorption by the surfactant. A mix of 50 % LFA buffer and 50 % aptamer binding buffer showed a deterioration in binding, owing to the decrease in salt concentration, whereas PBST showed suboptimal binding, thus indicating the aptamer's dependency on cations.

In contrast, the QD-525-anti-IL-6 conjugates showed optimal binding with the LFA running buffer. The aptamer binding buffer led to aggregation of the conjugates, and no signal was detected. The aptamer binding buffer with 8% Triton X-100 as well as the 50 % aptamer binding buffer-50 % LFA running buffer showed comparable signals and slightly inhibited binding. PBST had a lower signal than both buffers.

The data clearly indicated that a trade-off was necessary, because no buffer conditions were simultaneously optimal for both the antibody and the aptamer conjugates. The aptamer running buffer with Triton X-100 was chosen for further experiments. This buffer showed the highest signal for the thrombin binding conjugates and acceptable performance for the IL-6 conjugates.

3.3. Optimization of the amounts of HD22 and IL-6 detection antibody

Different amounts of the detection aptamer and the IL-6 detection antibody were tested in a single-plex format. In the case of the detection aptamer (Fig. S3), increasing amounts led to inhibition of the test line signal, because the free HD22 saturated the test line and inhibited the binding of the QDs. Decreasing the amount led to a constant signal, thus indicating that all the HD22 was bound to the QD-TBA-thrombin complex. However, there was no significant difference in the signals obtained with different IL-6 detection antibody concentrations (Fig. S4). Therefore, volumes of 2.5 µL detection antibody and 0.625 µL HD22 per strip were used for developing the assay.

3.4. Single-plex and setup testing

To test the optimized assay conditions, we challenged the lateral flow strips with different concentrations of the analyte in a single-plex format. Then images were captured with the smartphone setup (RGB photos) and the BioImager with the corresponding filters (grayscale photos). To validate the designed smartphone box imaging setup, we compared the signals with the BioImager results. For IL-6 (Fig. S5), the data showed a concentration dependent signal for both setups; however, the smartphone signals were slightly higher than the imager signals. In contrast, for thrombin (Fig. S6), the results with the two setups agreed well; nevertheless, the smartphone showed a relatively higher signal attributable to the sizes of the camera sensors in both setups. The smartphone setup thus was comparable to the BioImager and therefore could be used for quantification of the QD-labeled aptamers and antibodies.

3.5. Duplex LFA IL-6/thrombin

Under the optimized assay conditions, the lateral flow strips were simultaneously challenged with increasing concentrations of thrombin and IL-6 (1:1 ratio). After a buffer running time of 15 min, the strips were allowed to dry for 5 min, and images were captured with the smartphone setup; the images then were processed (RGB splitting) and analyzed in ImageJ (Fig. S8). As seen in Figs. 2 and 3, a concentration dependent response from both the red and green channels was detected. For IL6, the data showed a linear response with a limit of detection (limit of detection = blank mean value + $3*SD_{blank}$) of 100 pM. In contrast, thrombin showed a typical binding curve with exponential behavior, a limit of detection of 3 nM, and a K_D value of 146 ± 21 nM, which is comparable to previously published K_D values in the nanomolar range

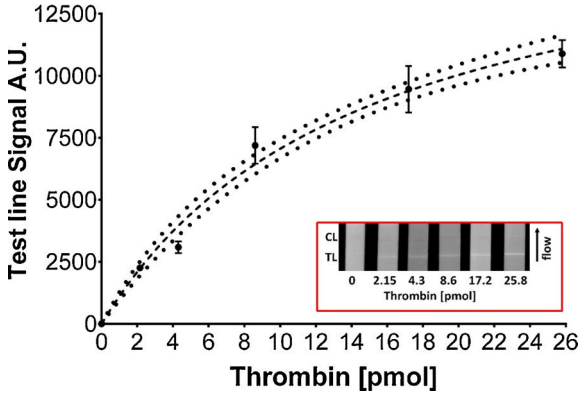

Fig. 2. Plot of test line signal intensity (A.U.) against the amount of thrombin (pmol) in the sample (100 µL). The test line intensity was measured in ImageJ software (gel analyzer tool). The points show the mean values, and the error bars represent the standard deviation n = 5. The line represents the best fit with the one site total binding equation Y = Bmax*X/(Kd + X) + NS*X + background, adjusted $r^2 = 0.9948$. The dashed lines represent the 95 % CI of the best fitting lines. The inset shows a monochromatic image of the LFA strips' red channel after digital RGB splitting in ImageJ (CL: control line, TL: test line) (For interpretation of the references to colour in this figure legend, the reader is referred to the web version of this article.).

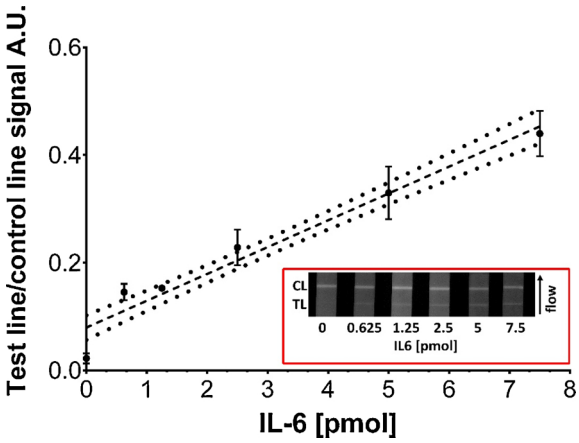

Fig. 3. Plot of test line signal intensity normalized to that of the control line (A.U.) versus the IL-6 amount (pmol) in the sample (100 μL). The test line and control line intensity values were measured in ImageJ software (gel analyzer tool). The points show the mean values, and the error bars represent the standard deviation n = 5. The line represents the best fit with the equation Y = 0.05X + 0.0784 r^2 = 0.9520. The dashed lines represent the 95 % CI of the best fitting lines. The inset shows a monochromatic image of the LFA strips' green channel after digital RGB splitting in ImageJ (CL: control line, TL: test line) (For interpretation of the references to colour in this figure legend, the reader is referred to the web version of this article.).

(97.6 ± 2.2 nM [43] and 102.6 ± 5.1 nM [44]). In addition, the limits of detection and quantification for thrombin were comparable to those of published aptamer LFA methods (2.5 nM [45] and 0.85 nM [46]).

3.6. Serum experiments and recovery

To test the matrix effect in the assay, we challenged the lateral flow strips with 10 % serum content in samples containing IL-6 and thrombin in increasing concentrations. The recovery rates and coefficients of variation are shown in Table 1. The recovery rates for IL-6 and thrombin were 86–130 % and 80–120 % (Figs. S9 and S10), with a CV % average of 9.8 ± 3.4 and 14.2 ± 3.1, respectively.

3.7. Specificity of the response of the LFA

The specificity of thrombin binding aptamers has been extensively studied [41]. TTBA has been found to cross react with prothrombin, and binding to thrombin has been found to be inhibited by antithrombin III. In contrast, HD22 is more selective toward free thrombin and shows no cross reactivity to prothrombin. Because both aptamers were used in the LFA, the specificity of the response was tested. For prothrombin as well as thrombin/antithrombin III and prothrombin/antithrombin III, no test line was detected at concentrations of 173.2 nM (17.2 pmol), 86.6 nM (8.6 pmol)/200 nM (20 pmol), and 86.6 nM (8.6 pmol)/100 nM (10 pmol), respectively (Fig. S11). These results were consistent with previously published results [41], in which the use of both aptamers in a sandwich assay increased the selectivity for free thrombin. Additionally, when we challenged the LFA strips with IL-2 and IL-8 at a concentration of 50 nM, we observed a clear control line but no detectable test lines (Fig. S12). This result was expected because the monoclonal antibodies used are highly specific for IL-6.

Table 1
Percentage recovery for IL-6 (pmol) and thrombin (pmol) and the coefficients of variation n = 5.

IL6 (pmol)/thrombin (pmol)	Recovery %	CV %
0.625/2.15	86.64/126	13.41/17.84
1.25/ 4.3	108.5/105.33	10.25/15.98
2.5/8.6	96.55/86.71	4.17/13.39
5/17.2	135.76/80.45	11.66/9.56

3.8. Comparison with published assays and ELISA

Various approaches to design a POC assay for IL-6 and thrombin have been described in the literature (Table 2). Nevertheless, no duplex assay for both analytes has been described. For IL-6 and thrombin, the most sensitive approaches are based on ELISA with detection limits reaching low pg/mL and ng/mL concentrations, respectively. However, most of these assays are time intensive, including incubation, washing, and detection steps requiring up to 5 h. In contrast, lateral flow approaches provide faster results with lower sensitivity. Nevertheless, these approaches can be used to detect and quantify abnormal concentrations and disease conditions. In comparison to the published methods, this method can detect both analytes simultaneously in 20 min through smartphone-based quantification.

To further compare the LFA method to well established assays, we used ELISA as a reference method for both analytes. The assay was performed in single-plex format, because no duplex ELISA kit is available for both analytes. The results (Figs. S13 and S14) showed high agreement between the ELISA and the LFA methods (r = 0.996 and P = 0.004 for thrombin; r = 0.992 and P = 0.0077 for IL-6).

4. Conclusion

This work presents a simple, cost efficient LFA combined with an affordable smartphone detection system for determination of thrombin and IL-6. Although IL-6 quantification displayed a higher limit of detection, owing to the buffer components and the affinity of the antibodies, the assay performed well in complex media (10 % serum). Therefore, this assay could be applied to analyze real samples. The simplicity and efficiency, combined with smartphone quantification, make this assay ideal for POC application in low resource settings. A novel combination of aptamers and antibodies with QD labels allows for smartphone-based quantification. The 3D printed dark box could be modified to fit other smartphones for the simultaneous quantification of IL-6 and thrombin.

Availability of data and materials

Charts and tables referred to in the text as well as files used for the 3D printing are available in the Electronic Supplementary Material (ESM).

CRediT authorship contribution statement

Mostafa Mahmoud: Conceptualization, Investigation, Writing - original draft, Writing - review & editing. **Christoph Ruppert:** Conceptualization, Investigation, Writing - original draft, Writing - review & editing. **Simone Rentschler:** Investigation, Writing - original draft. **Stefan Laufer:** Conceptualization, Writing - review & editing.

Table 2
Comparison of assays reported for the quantification of IL-6 and thrombin.

Analyte/assay format	LOD	Reference
IL-6/LFA	0.38 ng/mL	[47]
IL-6/LFA	15 pM (0.31 ng/mL)	[6]
IL6- electrochemiluminescence immunoassay	2.63 pg/mL	[48]
IL-6/LFA	100 pM (2.1 ng/mL)	This work
Thrombin/microfluidic aptasensor	8.21 nM	[49]
Thrombin/LFA	0.85 nM	[46]
Thrombin/LFA	1.5 nM	[50]
Thrombin/electrochemiluminescence aptasensor	10 nM	[51]
Thrombin/LFA	3 nM	This work

Hans-Peter Deigner: Conceptualization, Writing - review & editing.

Declaration of Competing Interest

The authors declare no competing interests.

Acknowledgements

Partial support provided by Bundesministerium für Bildung und Forschung (FlowArray project 13FH121PX8, and by the MultiFlow project 03FH046PX4) is gratefully acknowledged. HPD is grateful to Prof. Friedhelm Beyersdorf and Bartosz Rylski,Freiburg, for facilitating this work. We thank Mrs. Ayesha Talib from MPI Potsdam for support with DLS measurements.

Appendix A. Supplementary data

Supplementary material related to this article can be found, in the online version, at doi:https://doi.org/10.1016/j.snb.2020.129246.

References

[1] C.P. Price, Clinical Review Point of Care Testing, 2001, pp. 1285–1288.
[2] A.C. Sun, D.A. Hall, Point-of-Care Smartphone-Based Electrochemical Biosensing, 2019, pp. 2–16.
[3] V. Borse, R. Srivastava, Fluorescence lateral flow immunoassay based point-of-care nanodiagnostics for orthopedic implant-associated infection, Sens. Actuators B Chem. 280 (2019) 24–33.
[4] M. Stobiecka, K. Ratajczak, S. Jakiela, Toward early cancer detection: Focus on biosensing systems and biosensors for an anti-apoptotic protein survivin and survivin mRNA, Biosens. Bioelectron. 137 (2019) 58–71.
[5] K. Ratajczak, M. Stobiecka, High-performance modified cellulose paper-based biosensors for medical diagnostics and early cancer screening: a concise review, Carbohydr. Polym. 229 (2020), 115463.
[6] C. Ruppert, L. Kaiser, L.J. Jacob, S. Laufer, M. Kohl, H.-P. Deigner, Duplex Shiny app quantification of the sepsis biomarkers C-reactive protein and interleukin-6 in a fast quantum dot labeled lateral flow assay, J. Nanobiotechnol. 18 (1) (2020) 130.
[7] T.-T. Tsai, T.-H. Huang, N.Y.-J. Ho, Y.-P. Chen, Y.-P. Chen, Y.-P. Chen, Development of a multiplex and sensitive lateral flow immunoassay for the diagnosis of periprosthetic joint infection, Sci. Rep. 9 (1) (2019) 15679.
[8] H. Kim, D.-R. Chung, M. Kang, A new point-of-care test for the diagnosis of infectious diseases based on multiplex lateral flow immunoassays, Analyst 144 (8) (2019) 2460–2466.
[9] M. Drancourt, A. Michel-lepage, S. Boyer, The point-of-care laboratory in clinical microbiology, Clin. Microbiol. Rev. 29 (3) (2016) 429–447.
[10] K. Mohd Hanafiah, N. Arifin, Y. Bustami, R. Noordin, M. Garcia, D. Anderson, Development of multiplexed infectious disease lateral flow assays: challenges and opportunities, Diagnostics (Basel) 7 (3) (2017) 51.
[11] V.K. Rajendran, P. Bakthavathsalam, B. Mohammed, J. Ali, Smartphone based bacterial detection using biofunctionalized fluorescent nanoparticles, Microchim. Acta (2014) 1815–1821.
[12] S. Lee, G. Kim, J. Moon, Development of a smartphone-based reading system for lateral flow immunoassay, J. Nanosci. Nanotechnol. 14 (11) (2014) 8453–8457.
[13] L. Yu, Z. Shi, C. Fang, Y. Zhang, Y. Liu, C. Li, Disposable lateral flow-through strip for smartphone-camera to quantitatively detect alkaline phosphatase activity in milk, Biosens. Bioelectron. 69 (2015) 307–315.
[14] C. Ruppert, N. Phogat, S. Laufer, M. Kohl, H.-P. Deigner, A smartphone readout system for gold nanoparticle-based lateral flow assays: application to monitoring of digoxigenin, Microchimica Acta. 186 (2) (2019) 119.
[15] A. Chen, S. Yang, Replacing antibodies with aptamers in lateral flow immunoassay, Biosens. Bioelectron. 71 (2015) 230–242.
[16] T. Schüling, A. Eilers, T. Scheper, J. Walter, Aptamer-based lateral flow assays, AIMS Bioeng. 5 (2) (2018) 78–102.
[17] F. Radom, P.M. Jurek, M.P. Mazurek, J. Otlewski, F. Jeleń, Aptamers: molecules of great potential, Biotechnol. Adv. 31 (8) (2013) 1260–1274.
[18] S.Y. Toh, M. Citartan, S.C.B. Gopinath, T.-H. Tang, Aptamers as a replacement for antibodies in enzyme-linked immunosorbent assay, Biosens. Bioelectron. 64 (0) (2015) 392–403.
[19] S. Tombelli, M. Minunni, M. Mascini, Analytical applications of aptamers, Biosens. Bioelectron. 20 (12) (2005) 2424–2434.
[20] S. Nagatoishi, Y. Tanaka, K. Tsumoto, Circular dichroism spectra demonstrate formation of the thrombin-binding DNA aptamer G-quadruplex under stabilizing-cation-deficient conditions, Biochem. Biophys. Res. Commun. 352 (3) (2007) 812–817.
[21] K.Y. Wang, S. McCurdy, R.G. Shea, S. Swaminathan, P.H. Bolton, A DNA aptamer which binds to and inhibits thrombin exhibits a new structural motif for DNA, Biochemistry 32 (8) (1993) 1899–1904.
[22] K. Padmanabhan, K.P. Padmanabhan, J.D. Ferrara, J.E. Sadler, A. Tulinsky, The structure of alpha-thrombin inhibited by a 15-mer single-stranded DNA aptamer, J. Biol. Chem. 268 (24) (1993) 17651–17654.
[23] A. Anna, F. Carme, T. Maria, E. Ramon, Thrombin binding aptamer, more than a simple aptamer: chemically modified derivatives and biomedical applications, Curr. Pharm. Des. 18 (14) (2012) 2036–2047.
[24] C.A. Hunter, S.A. Jones, IL-6 as a keystone cytokine in health and disease, Nat. Immunol. 16 (5) (2015) 448–457.
[25] D.E. Johnson, R.A. O'Keefe, J.R. Grandis, Targeting the IL-6/JAK/STAT3 signalling axis in cancer, Nat. Rev. Clin. Oncol. 15 (4) (2018) 234–248.
[26] S. Saibeni, V. Saladino, V. Chantarangkul, F. Villa, S. Bruno, M. Vecchi, et al., Increased thrombin generation in inflammatory bowel diseases, Thromb. Res. 125 (3) (2010) 278–282.
[27] J. Chapman, Thrombin in inflammatory brain diseases, Autoimmun. Rev. 5 (8) (2006) 528–531.
[28] S. Colafrancesco, R. Scrivo, C. Barbati, F. Conti, R. Priori, Targeting the immune system for pulmonary inflammation and cardiovascular complications in COVID-19 patients, Front. Immunol. 11 (1439) (2020).
[29] X. Li, M. Geng, Y. Peng, L. Meng, S. Lu, Molecular immune pathogenesis and diagnosis of COVID-19, J. Pharm. Anal. 10 (2) (2020) 102–108.
[30] R.J. Jose, A. Manuel, COVID-19 cytokine storm: the interplay between inflammation and coagulation, Lancet Respir. Med. 8 (6) (2020) e46-e7.
[31] P. Mehta, D.F. McAuley, M. Brown, E. Sanchez, R.S. Tattersall, J.J. Manson, COVID-19: consider cytokine storm syndromes and immunosuppression, Lancet 395 (10229) (2020) 1033–1034.
[32] F. Liu, L. Li, M. Xu, J. Wu, D. Luo, Y. Zhu, et al., Prognostic value of interleukin-6, C-reactive protein, and procalcitonin in patients with COVID-19, J. Clin. Virol. 127 (January) (2020), 104370-.
[33] J. Zhu, J. Pang, P. Ji, Z. Zhong, H. Li, B. Li, et al., Elevated interleukin-6 is associated with severity of COVID-19: a meta-analysis, J. Med. Virol. 2019 (2020) 0–2.
[34] Q. Ruan, K. Yang, W. Wang, L. Jiang, J. Song, Clinical predictors of mortality due to COVID-19 based on an analysis of data of 150 patients from Wuhan, China, Intensive Care Med. 46 (5) (2020) 846–848.
[35] Z.S. Ulhaq, G.V. Soraya, Interleukin-6 as a potential biomarker of COVID-19 progression, Médecine et Maladies Infectieuses. 50 (4) (2020) 382–383.
[36] P. Sarzi-Puttini, V. Giorgi, S. Sirotti, D. Marotto, S. Ardizzone, G. Rizzardini, et al., COVID-19, cytokines and immunosuppression: what can we learn from severe acute respiratory syndrome? Clin. Exp. Rheumatol. 38 (2) (2020) 337–342.
[37] M. Abbasifard, H. Khorramdelazad, The bio-mission of interleukin-6 in the pathogenesis of COVID-19: a brief look at potential therapeutic tactics, Life Sci. 257 (2020), 118097.
[38] J.M. Connors, J.H. Levy, COVID-19 and its implications for thrombosis and anticoagulation, Blood 135 (23) (2020) 2033–2040.
[39] F. Zhou, T. Yu, R. Du, G. Fan, Y. Liu, Z. Liu, et al., Clinical course and risk factors for mortality of adult inpatients with COVID-19 in Wuhan, China: a retrospective cohort study, Lancet 395 (10229) (2020) 1054–1062.
[40] S.M. Russell, A. Alba-Patiño, E. Barón, M. Borges, M. Gonzalez-Freire, R. de la Rica, Biosensors for managing the COVID-19 cytokine storm: challenges ahead, ACS Sens. 5 (6) (2020) 1506–1513.
[41] A. Trapaidze, J.P. Hérault, J.M. Herbert, A. Bancaud, A.M. Gué, Investigation of the selectivity of thrombin-binding aptamers for thrombin titration in murine plasma, Biosens. Bioelectron. 78 (2016) 58–66.
[42] A. Foubert, N.V. Beloglazova, A. Rajkovic, B. Sas, A. Madder, I.Y. Goryacheva, et al., Bioconjugation of quantum dots: review & impact on future application, Trac. Trends Anal. Chem. 83 (2016) 31–48.
[43] K. Derszniak, K. Przyborowski, K. Matyjaszczyk, M. Moorlag, B. de Laat, M. Nowakowska, et al., Comparison of effects of anti-thrombin aptamers HD1 and HD22 on aggregation of human platelets, thrombin generation, fibrin formation, and thrombus formation under flow conditions, Front. Pharmacol. 10 (68) (2019).
[44] A. Pasternak, F.J. Hernandez, L.M. Rasmussen, B. Vester, J. Wengel, Improved thrombin binding aptamer by incorporation of a single unlocked nucleic acid monomer, Nucleic Acids Res. 39 (3) (2011) 1155–1164.
[45] H. Xu, X. Mao, Q. Zeng, S. Wang, A.N. Kawde, G. Liu, Aptamer-functionalized gold nanoparticles as probes in a dry-reagent strip biosensor for protein analysis, Anal. Chem. 81 (2) (2009) 669–675.
[46] Y. Gao, Z. Zhu, X. Xi, T. Cao, W. Wen, X. Zhang, et al., An aptamer-based hook-effect-recognizable three-line lateral flow biosensor for rapid detection of thrombin, Biosens. Bioelectron. 133 (2019) 177–182.
[47] I. de Souza Sene, V. Costa, D.C. Brás, E.A. de Oliveira Farias, G.E. Nunes, I. H. Bechtold, A point of care lateral flow assay for rapid and colorimetric detection of interleukin 6 and perspectives in bedside diagnostics, J. Clin. Med. Res. 2 (2) (2020) 1–16.
[48] B. Prieto, D. Miguel, M. Costa, D. Coto, F.V. Álvarez, New quantitative electrochemiluminescence method (ECLIA) for interleukin-6 (IL-6) measurement, Clin. Chem. Lab. Med. (CCLM) 48 (6) (2010) 835.
[49] N. Yu, J. Wu, Rapid and reagentless detection of thrombin in clinic samples via microfluidic aptasensors with multiple target-binding sites, Biosens. Bioelectron. 146 (2019), 111726.
[50] G. Liu, A.S. Gurung, W. Qiu, Lateral Flow aptasensor for simultaneous detection of platelet-derived growth factor-BB (PDGF-BB) and thrombin, Mol. (Basel Switz.) 24 (4) (2019) 756.
[51] L. Fang, Z. Lü, H. Wei, E. Wang, A electrochemiluminescence aptasensor for detection of thrombin incorporating the capture aptamer labeled with gold nanoparticles immobilized onto the thio-silanized ITO electrode, Anal. Chim. Acta 628 (1) (2008) 80–86.

Mostafa Mahmoud is a PhD student at University of Tuebingen and Furtwangen University. His work is focused on aptamer assays for point of care applications.

Christoph Ruppert is a PhD student at University of Tuebingen and Furtwangen University. His work is focused on Lateral Flow assay systems.

Simone Rentschler is a PhD student at University of Tuebingen and Furtwangen University. Her primary research interest is in molecular diagnostics.

Stefan Laufer is Professor for Pharmaceutical/Medicinal Chemistry at Tuebingen University. He received his degrees from Regensburg University. After 10 years in Pharmaceutical Industry he joined in 1999 Tuebingen University as Chairman Pharm./Med. Chemistry. His research interests are anti-inflammatory and cancer drug discovery with various eicosanoid (COX-1,2,3, LOXs, mPGES1, cPLA2) and protein kinase targets (p38, JAKs, JNKs, CK1d, mtEGRFs) . Three compounds from his lab entered clinical development phases. Dr. Laufer chairs the ICEPHA (Interfaculty Center for Pharmacogenomics and Drug Research) and TüCADD, Tuebingen Center for Academic Drug Discovery. As part of this work, a proprietary kinase inhibitor collections is established (TüKIC, 10.000 cpds). He authored more than 500 publications, 14 books/bookchapters and is inventor in 42 patent families.

Hans-Peter Deigner is professor in pharmacology, deputy director of the Institute of Precision Medicine and dean of the faculty of Medical and Life Sciences at Furtwangen University. After PhD at Heidelberg University and post doc at Harvard Medical School, Boston, he finished his habilitation in pharmaceutical chemistry (Heidelberg University). He led research in molecular diagnostics in several biotech companies, held a professorship in biomedicinal chemistry at the University of East Anglia, Norwich, UK (2004-2006) and is professor at Furtwangen University since 2011; in 2020 he became also associated member of the science faculty, Tuebingen University. His research interest is in molecular diagnostics, functional genomics/metabolomics and chemical biology.

4. Concluding remarks

In the three included projects that led to Publications 1, 2 & 3, we first demonstrated the capabilities of imaging with smartphones compared with professional laboratory equipment. We next identified suitable multiplex dyes and used QDs as strong and reliable fluorescent labels. Then we transferred the characterized components of our novel LFAs to the newly designed 3D-printed duplex platform for smartphone readout, in which we were able to use aptamer-QD based biosensors for detection of thrombin from human serum in a functional hybrid assay.

Crucially, the systems should be inexpensive and easy to operate, to ensure their suitability for POC diagnostics. The assays from Publications 1 & 3 enable operators to perform home testing of harmful drugs in close intervals, thus enabling adherence to an ideal schedule for administration of therapeutics or monitoring of important associated biomarkers. Treatment of numerous diseases would benefit from the availability of inexpensive, uncomplicated self-monitoring devices; these conditions include chronic inflammation, autoimmune related diseases, bacterial and viral infections, or chronic cardiovascular issues. The use of smartphones, which are widely present in daily life and do not require further investment, unlocks massive potential for the close interval testing necessary in precision medicine.

The chosen inflammation and coagulation biomarkers (Publications 2 & 3) provide useful diagnostic data within 30 min; therefore, they could potentially help medical professionals in their decision-making at the POC. In sepsis, for example, a physician is currently limited to assessing physical symptoms, such as respiratory or heart rates, but cannot immediately acquire important blood biomarker values, such as CRP and IL-6, which might affect treatment decisions. Our rapid assays and portable readout devices address this urgent medical need, thereby enabling better treatment in emergency medicine and in remote areas. Because the LFAs can be produced at a low price per unit, and the open source readout hardware is affordable, the investigated assays are ideally suited to strengthen the scope of LFAs for POC diagnostics.

The use of QD labels had exceptional performance in the investigated optical duplex platforms. Although approaches using QDs for multiplexing approaches previously existed, our open source reader from distributable 3D-printing patterns in combination with smartphone readout provides a new diagnostic system with high performance. The designed upgrades in the LFA platform technology therefore provide major improvements enabling easy and available lateral flow diagnostics.

5. References

1. Bahadır, E.B.; Sezgintürk, M.K. Lateral flow assays: Principles, designs and labels. *TrAC Trends in Analytical Chemistry* **2016**, *82*, 286–306, doi:10.1016/j.trac.2016.06.006.
2. Posthuma-Trumpie, G.A.; Korf, J.; van Amerongen, A. Lateral flow (immuno)assay: its strengths, weaknesses, opportunities and threats. A literature survey. *Anal. Bioanal. Chem.* **2009**, *393*, 569–582, doi:10.1007/s00216-008-2287-2.
3. Sajid, M.; Kawde, A.-N.; Daud, M. Designs, formats and applications of lateral flow assay: A literature review. *Journal of Saudi Chemical Society* **2015**, *19*, 689–705, doi:10.1016/j.jscs.2014.09.001.
4. Guo, J.; Chen, S.; Guo, J.; Ma, X. Nanomaterial Labels in Lateral Flow Immunoassays for Point-of-Care-Testing. *Journal of Materials Science & Technology* **2021**, *60*, 90–104, doi:10.1016/j.jmst.2020.06.003.
5. Huang, X.; Aguilar, Z.P.; Xu, H.; Lai, W.; Xiong, Y. Membrane-based lateral flow immunochromatographic strip with nanoparticles as reporters for detection: A review. *Biosens. Bioelectron.* **2016**, *75*, 166–180, doi:10.1016/j.bios.2015.08.032.
6. Mak, W.C.; Beni, V.; Turner, A.P. Lateral-flow technology: From visual to instrumental. *TrAC Trends in Analytical Chemistry* **2016**, *79*, 297–305, doi:10.1016/j.trac.2015.10.017.
7. Link, S.; El-Sayed, M.A. Size and Temperature Dependence of the Plasmon Absorption of Colloidal Gold Nanoparticles. *J. Phys. Chem. B* **1999**, *103*, 4212–4217, doi:10.1021/jp984796o.
8. Yang, W.; Li, X.; Liu, G.; Zhang, B.; Zhang, Y.; Kong, T.; Tang, J.; Li, D.; Wang, Z. A colloidal gold probe-based silver enhancement immunochromatographic assay for the rapid detection of abrin-a. *Biosens. Bioelectron.* **2011**, *26*, 3710–3713, doi:10.1016/j.bios.2011.02.016.
9. Liu, R.; Zhang, Y.; Zhang, S.; Qiu, W.; Gao, Y. Silver Enhancement of Gold Nanoparticles for Biosensing: From Qualitative to Quantitative. *Applied Spectroscopy Reviews* **2014**, *49*, 121–138, doi:10.1080/05704928.2013.807817.
10. Zhang, C.; Zhang, Y.; Wang, S. Development of multianalyte flow-through and lateral-flow assays using gold particles and horseradish peroxidase as tracers for the rapid determination of carbaryl and endosulfan in agricultural products. *Journal of agricultural and food chemistry* **2006**, *54*, 2502–2507, doi:10.1021/jf0531407.
11. Zhu, J.; Zou, N.; Zhu, D.; Wang, J.; Jin, Q.; Zhao, J.; Mao, H. Simultaneous detection of high-sensitivity cardiac troponin I and myoglobin by modified sandwich lateral flow immunoassay: proof of principle. *Clinical chemistry* **2011**, *57*, 1732–1738, doi:10.1373/clinchem.2011.171694.
12. Medintz, I.L.; Clapp, A.R.; Mattoussi, H.; Goldman, E.R.; Fisher, B.; Mauro, J.M. Self-assembled nanoscale biosensors based on quantum dot FRET donors. *Nat. Mater.* **2003**, *2*, 630–638, doi:10.1038/nmat961.
13. He, Y.; Zhang, S.; Zhang, X.; Baloda, M.; Gurung, A.S.; Xu, H.; Zhang, X.; Liu, G. Ultrasensitive nucleic acid biosensor based on enzyme-gold nanoparticle dual

label and lateral flow strip biosensor. *Biosens. Bioelectron.* **2011**, *26*, 2018–2024, doi:10.1016/j.bios.2010.08.079.
14. Mao, X.; Ma, Y.; Zhang, A.; Zhang, L.; Zeng, L.; Liu, G. Disposable nucleic acid biosensors based on gold nanoparticle probes and lateral flow strip. *Anal. Chem.* **2009**, *81*, 1660–1668, doi:10.1021/ac8024653.
15. Liu, H.; Zhan, F.; Liu, F.; Zhu, M.; Zhou, X.; Da Xing. Visual and sensitive detection of viable pathogenic bacteria by sensing of RNA markers in gold nanoparticles based paper platform. *Biosens. Bioelectron.* **2014**, *62*, 38–46, doi:10.1016/j.bios.2014.06.020.
16. Trapaidze, A.; Hérault, J.-P.; Herbert, J.-M.; Bancaud, A.; Gué, A.-M. Investigation of the selectivity of thrombin-binding aptamers for thrombin titration in murine plasma. *Biosens. Bioelectron.* **2016**, *78*, 58–66, doi:10.1016/j.bios.2015.11.017.
17. Chen, A.; Yang, S. Replacing antibodies with aptamers in lateral flow immunoassay. *Biosens. Bioelectron.* **2015**, *71*, 230–242, doi:10.1016/j.bios.2015.04.041.
18. Sefah, K.; Shangguan, D.; Xiong, X.; O'Donoghue, M.B.; Tan, W. Development of DNA aptamers using Cell-SELEX. *Nat. Protoc.* **2010**, *5*, 1169–1185, doi:10.1038/nprot.2010.66.
19. Wang, L.; Ma, W.; Chen, W.; Liu, L.; Ma, W.; Zhu, Y.; Xu, L.; Kuang, H.; Xu, C. An aptamer-based chromatographic strip assay for sensitive toxin semi-quantitative detection. *Biosens. Bioelectron.* **2011**, *26*, 3059–3062, doi:10.1016/j.bios.2010.11.040.
20. Gao, X.; Xu, L.-P.; Wu, T.; Wen, Y.; Ma, X.; Zhang, X. An enzyme-amplified lateral flow strip biosensor for visual detection of microRNA-224. *Talanta* **2016**, *146*, 648–654, doi:10.1016/j.talanta.2015.06.060.
21. Oliveira, J.P.; Prado, A.R.; Keijok, W.J.; Antunes, P.W.P.; Yapuchura, E.R.; Guimarães, M.C.C. Impact of conjugation strategies for targeting of antibodies in gold nanoparticles for ultrasensitive detection of 17β-estradiol. *Sci. Rep.* **2019**, *9*, 13859, doi:10.1038/s41598-019-50424-5.
22. Zhang, L.; Mazouzi, Y.; Salmain, M.; Liedberg, B.; Boujday, S. Antibody-Gold Nanoparticle Bioconjugates for Biosensors: Synthesis, Characterization and Selected Applications. *Biosens. Bioelectron.* **2020**, *165*, 112370, doi:10.1016/j.bios.2020.112370.
23. Li, S.; Liu, H.; He, N. Covalent binding of streptavidin on gold magnetic nanoparticles for bead array fabrication. *J. Nanosci. Nanotechnol.* **2010**, *10*, 4875–4882, doi:10.1166/jnn.2010.2385.
24. Turcu, I.; Zarafu, I.; Popa, M.; Chifiriuc, M.C.; Bleotu, C.; Culita, D.; Ghica, C.; Ionita, P. Lipoic Acid Gold Nanoparticles Functionalized with Organic Compounds as Bioactive Materials. *Nanomaterials (Basel)* **2017**, *7*, doi:10.3390/nano7020043.
25. Larsson, J.A.; Nolan, M.; Greer, J.C. Interactions between Thiol Molecular Linkers and the Au 13 Nanoparticle. *J. Phys. Chem. B* **2002**, *106*, 5931–5937, doi:10.1021/jp014483k.
26. Wang, Y.; Dave, R.N.; Pfeffer, R. Polymer coating/encapsulation of nanoparticles using a supercritical anti-solvent process. *The Journal of Supercritical Fluids* **2004**, *28*, 85–99, doi:10.1016/S0896-8446(03)00011-1.

27. Eltzov, E.; Guttel, S.; Low Yuen Kei, A.; Sinawang, P.D.; Ionescu, R.E.; Marks, R.S. Lateral Flow Immunoassays - from Paper Strip to Smartphone Technology. *Electroanalysis* **2015**, *27*, 2116–2130, doi:10.1002/elan.201500237.
28. Urusov, A.E.; Zherdev, A.V.; Dzantiev, B.B. Towards Lateral Flow Quantitative Assays: Detection Approaches. *Biosensors (Basel)* **2019**, *9*, doi:10.3390/bios9030089.
29. Wang, Y.; Xu, H.; Wei, M.; Gu, H.; Xu, Q.; Zhu, W. Study of superparamagnetic nanoparticles as labels in the quantitative lateral flow immunoassay. *Materials Science and Engineering: C* **2009**, *29*, 714–718, doi:10.1016/j.msec.2009.01.011.
30. Fernández-Sánchez, C.; McNeil, C.J.; Rawson, K.; Nilsson, O. Disposable noncompetitive immunosensor for free and total prostate-specific antigen based on capacitance measurement. *Anal. Chem.* **2004**, *76*, 5649–5656, doi:10.1021/ac0494937.
31. Huang, Y.; Xu, T.; Wang, W.; Wen, Y.; Li, K.; Qian, L.; Zhang, X.; Liu, G. Lateral flow biosensors based on the use of micro- and nanomaterials: a review on recent developments. *Mikrochim. Acta* **2019**, *187*, 70, doi:10.1007/s00604-019-3822-x.
32. Liu, Z.; Hua, Q.; Wang, J.; Liang, Z.; Li, J.; Wu, J.; Shen, X.; Lei, H.; Li, X. A smartphone-based dual detection mode device integrated with two lateral flow immunoassays for multiplex mycotoxins in cereals. *Biosens. Bioelectron.* **2020**, *158*, 112178, doi:10.1016/j.bios.2020.112178.
33. Rong, Z.; Wang, Q.; Sun, N.; Jia, X.; Wang, K.; Xiao, R.; Wang, S. Smartphone-based fluorescent lateral flow immunoassay platform for highly sensitive point-of-care detection of Zika virus nonstructural protein 1. *Anal. Chim. Acta* **2019**, *1055*, 140–147, doi:10.1016/j.aca.2018.12.043.
34. Zangheri, M.; Cevenini, L.; Anfossi, L.; Baggiani, C.; Simoni, P.; Di Nardo, F.; Roda, A. A simple and compact smartphone accessory for quantitative chemiluminescence-based lateral flow immunoassay for salivary cortisol detection. *Biosens. Bioelectron.* **2015**, *64*, 63–68, doi:10.1016/j.bios.2014.08.048.
35. Ross, G.M.S.; Salentijn, G.I.; Nielen, M.W.F. A Critical Comparison between Flow-through and Lateral Flow Immunoassay Formats for Visual and Smartphone-Based Multiplex Allergen Detection. *Biosensors (Basel)* **2019**, *9*, doi:10.3390/bios9040143.
36. Hiemke, C.; Bergemann, N.; Clement, H.W.; Conca, A.; Deckert, J.; Domschke, K.; Eckermann, G.; Egberts, K.; Gerlach, M.; Greiner, C.; et al. Consensus Guidelines for Therapeutic Drug Monitoring in Neuropsychopharmacology: Update 2017. *Pharmacopsychiatry* **2018**, *51*, 9–62, doi:10.1055/s-0043-116492.
37. Jerling, M.; Bertilsson, L.; Sjöqvist, F. The use of therapeutic drug monitoring data to document kinetic drug interactions: an example with amitriptyline and nortriptyline. *Ther. Drug Monit.* **1994**, *16*, 1–12, doi:10.1097/00007691-199402000-00001.
38. Patsalos, P.N.; Spencer, E.P.; Berry, D.J. Therapeutic Drug Monitoring of Antiepileptic Drugs in Epilepsy: A 2018 Update. *Ther. Drug Monit.* **2018**, *40*, 526–548, doi:10.1097/FTD.0000000000000546.

39. Brunet, M.; van Gelder, T.; Åsberg, A.; Haufroid, V.; Hesselink, D.A.; Langman, L.; Lemaitre, F.; Marquet, P.; Seger, C.; Shipkova, M.; et al. Therapeutic Drug Monitoring of Tacrolimus-Personalized Therapy: Second Consensus Report. *Ther. Drug Monit.* **2019**, *41*, 261–307, doi:10.1097/FTD.0000000000000640.
40. Iisalo, E. Clinical pharmacokinetics of digoxin. *Clin. Pharmacokinet.* **1977**, *2*, 1–16, doi:10.2165/00003088-197702010-00001.
41. Dasgupta, A. Therapeutic drug monitoring of digoxin: impact of endogenous and exogenous digoxin-like immunoreactive substances. *Toxicol. Rev.* **2006**, *25*, 273–281, doi:10.2165/00139709-200625040-00007.
42. Bauman, J.L.; Didomenico, R.J.; Galanter, W.L. Mechanisms, manifestations, and management of digoxin toxicity in the modern era. *Am. J. Cardiovasc. Drugs* **2006**, *6*, 77–86, doi:10.2165/00129784-200606020-00002.
43. Smith, T.W.; Haber, E. Digoxin intoxication: the relationship of clinical presentation to serum digoxin concentration. *J. Clin. Invest.* **1970**, *49*, 2377–2386, doi:10.1172/JCI106457.
44. Kibe, S.; Adams, K.; Barlow, G. Diagnostic and prognostic biomarkers of sepsis in critical care. *J. Antimicrob. Chemother.* **2011**, *66 Suppl 2*, ii33-40, doi:10.1093/jac/dkq523.
45. Singer, M.; Deutschman, C.S.; Seymour, C.W.; Shankar-Hari, M.; Annane, D.; Bauer, M.; Bellomo, R.; Bernard, G.R.; Chiche, J.-D.; Coopersmith, C.M.; et al. The Third International Consensus Definitions for Sepsis and Septic Shock (Sepsis-3). *JAMA* **2016**, *315*, 801–810, doi:10.1001/jama.2016.0287.
46. Soong, J.; Soni, N. Sepsis: recognition and treatment. *Clin. Med. (Lond)* **2012**, *12*, 276–280, doi:10.7861/clinmedicine.12-3-276.
47. Driessen, R.G.H.; van de Poll, M.C.G.; Mol, M.F.; van Mook, W.N.K.A.; Schnabel, R.M. The influence of a change in septic shock definitions on intensive care epidemiology and outcome: comparison of sepsis-2 and sepsis-3 definitions. *Infect. Dis. (Lond)* **2018**, *50*, 207–213, doi:10.1080/23744235.2017.1383630.
48. Deigner, H.P.; Kohl, M. The molecular sepsis signature. *Crit. Care Med.* **2009**, *37*, 1137–1138, doi:10.1097/CCM.0b013e31819bb705.
49. Póvoa, P. C-reactive protein: a valuable marker of sepsis. *Intensive Care Med.* **2002**, *28*, 235–243, doi:10.1007/s00134-002-1209-6.
50. Pfäfflin, A.; Schleicher, E. Inflammation markers in point-of-care testing (POCT). *Anal. Bioanal. Chem.* **2009**, *393*, 1473–1480, doi:10.1007/s00216-008-2561-3.
51. White, D.; MacDonald, S.; Edwards, T.; Bridgeman, C.; Hayman, M.; Sharp, M.; Cox-Morton, S.; Duff, E.; Mahajan, S.; Moore, C.; et al. Evaluation of COVID-19 coagulopathy; laboratory characterization using thrombin generation and nonconventional haemostasis assays. *Int. J. Lab. Hematol.* **2020**, doi:10.1111/ijlh.13329.
52. Nougier, C.; Benoit, R.; Simon, M.; Desmurs-Clavel, H.; Marcotte, G.; Argaud, L.; David, J.S.; Bonnet, A.; Negrier, C.; Dargaud, Y. Hypofibrinolytic state and high thrombin generation may play a major role in SARS-COV2 associated thrombosis. *J. Thromb. Haemost.* **2020**, doi:10.1111/jth.15016.

6. Appendix

6.1 Supplementary material publication 1

Ruppert C, Phogat N, Laufer S, Kohl M and Deigner HP. A smartphone readout system for gold nanoparticle-based lateral flow assays: application to monitoring of digoxigenin. *Microchim Acta* **186,** 119 (2019). https://doi.org/10.1007/s00604-018-3195-6

Status: published ***Manuscript pages:*** ***61-101***

Electronic Supplementary Material (ESM) on the Microchimica Acta publication entitled:

A smartphone readout system for gold nanoparticle-based lateral flow assays: application to monitoring of digoxigenin

Christoph Ruppert[a,b,c], Navneet Phogat[a,b,c], Stefan Laufer[c], Matthias Kohl[a,b] and Hans-Peter Deigner[a,b,d]

a. **Furtwangen University, Medical and Life Sciences Faculty, Jakob-Kienzle Str. 17, D-78054 Villingen-Schwenningen, Germany**
b. **Furtwangen University, Institute of Precision Medicine, Jakob-Kienzle Str. 17, D-78054 Villingen-Schwenningen, Germany**
c. **University of Tuebingen, Pharmaceutical Institute, Department of Pharmaceutical Chemistry, Auf der Morgenstelle 8, D-72076 Tuebingen, Germany**
d. **Fraunhofer Institute IZI, Leipzig, EXIM Department, Schillingallee 68, D-18057 Rostock, Germany**

The electronic supplementary includes the exported report files that can be produced with our Shiny App. It includes all normalized concentration vs. intensity graphs and additionally graphs for standardized intensity vs. concentration both with included linear fits. Additionally the assay parameters like limit of detection (LOD), limit of quantification (LOQ) and limit of blank (LOB).
The GNSplex R-Package can be downloaded from:

https://github.com/NPhogat/GNSplex

Data sets of the performed experiments are arranged as follows:

S1-Shiny app report: Imager_ImageJ_Calibration

Analysis of the data of lateral flow assay

Initial Data:

Replicate	Test	Control	Conc
R1	12819480	814577	0
R1	14326359	1185355	1
R1	13504823	1313891	20
R1	13770773	1142355	40
R1	13454238	1073477	60
R2	13875238	1391477	80
R2	13587187	787456	100
R2	13449238	1176355	NA
R2	13729652	1132477	NA
R2	12543066	972820	NA
R3	15777702	2357134	NA
R3	15684945	2172305	NA
R3	15922530	2273255	NA
R3	16134167	2437548	NA
R3	15916066	2485305	NA
R4	18939288	7613154	NA
R4	19005803	6334619	NA
R4	18720267	6102740	NA
R4	18869288	6302912	NA
R4	19328459	7455497	NA
R5	19944974	10378983	NA
R5	18514075	11656861	NA
R5	18435146	11673447	NA
R5	18430024	11652983	NA
R5	17556853	11262326	NA
R6	16017539	11280811	NA
R6	14704246	12080397	NA
R6	16332731	12576518	NA
R6	15552024	12087569	NA
R6	13211660	11650861	NA
R7	12343196	11994933	NA
R7	12865711	11579326	NA
R7	13871418	12373933	NA
R7	12513418	11912154	NA
R7	11460296	11752154	NA

Combined replicates:

	NI.crep	SI.crep	NI.sdns	SI.sdns	NI.sd	SI.sd	Concn
R1	0.0812629	12.538054	0.0120222	1.9862343	546165.3	184947.7	0
R2	0.0811499	12.735234	0.0154814	2.7457642	524290.4	226600.7	1
R3	0.1475786	6.788277	0.0069760	0.3235095	170272.6	125865.7	20
R4	0.3562058	2.828357	0.0349840	0.2672936	225384.7	712993.9	40
R5	0.6113959	1.645927	0.0510716	0.1545336	859903.2	556326.4	60
R6	0.7909906	1.271267	0.0658407	0.1058906	1251801.5	491085.8	80
R7	0.9482524	1.057357	0.0548080	0.0603023	874484.4	298300.0	100

Normalized Intensity Plot (Standardized Intensity vs Concentration):

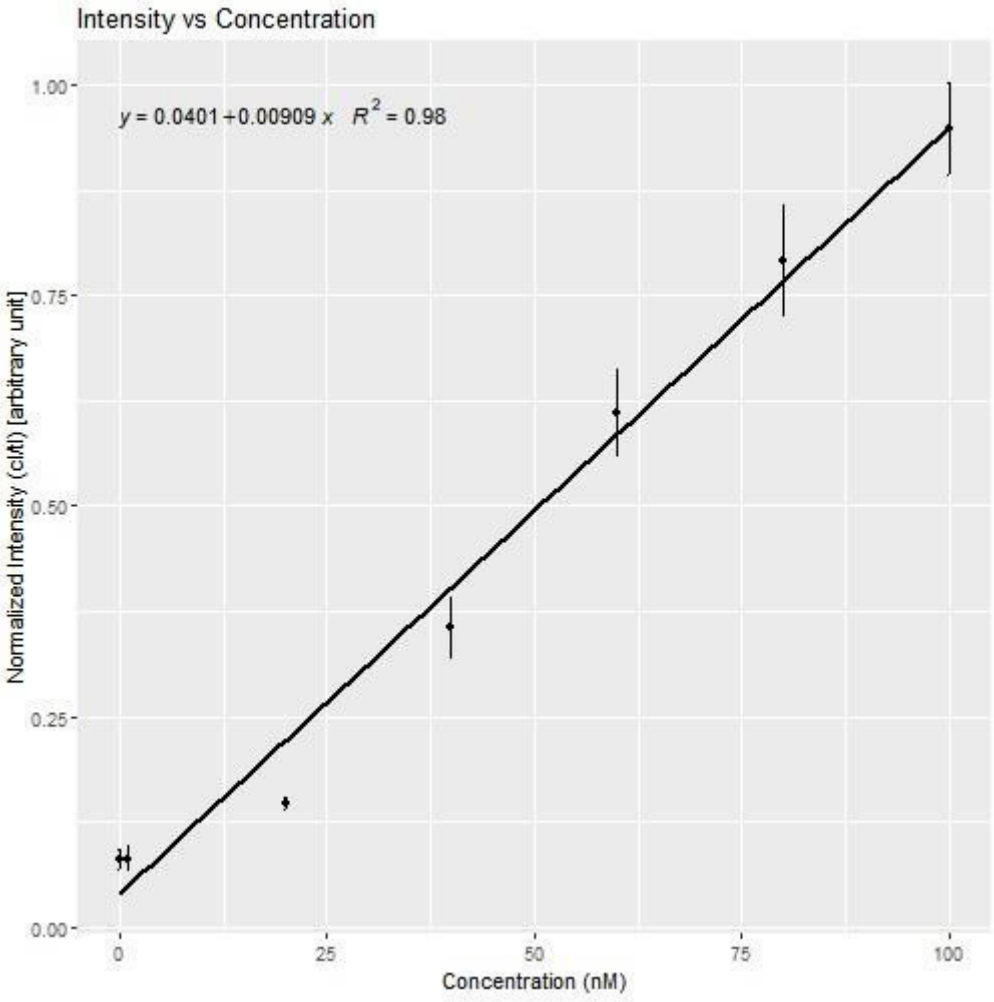

Standardized Intensity Plot (Normalized Intensity vs Concentration):

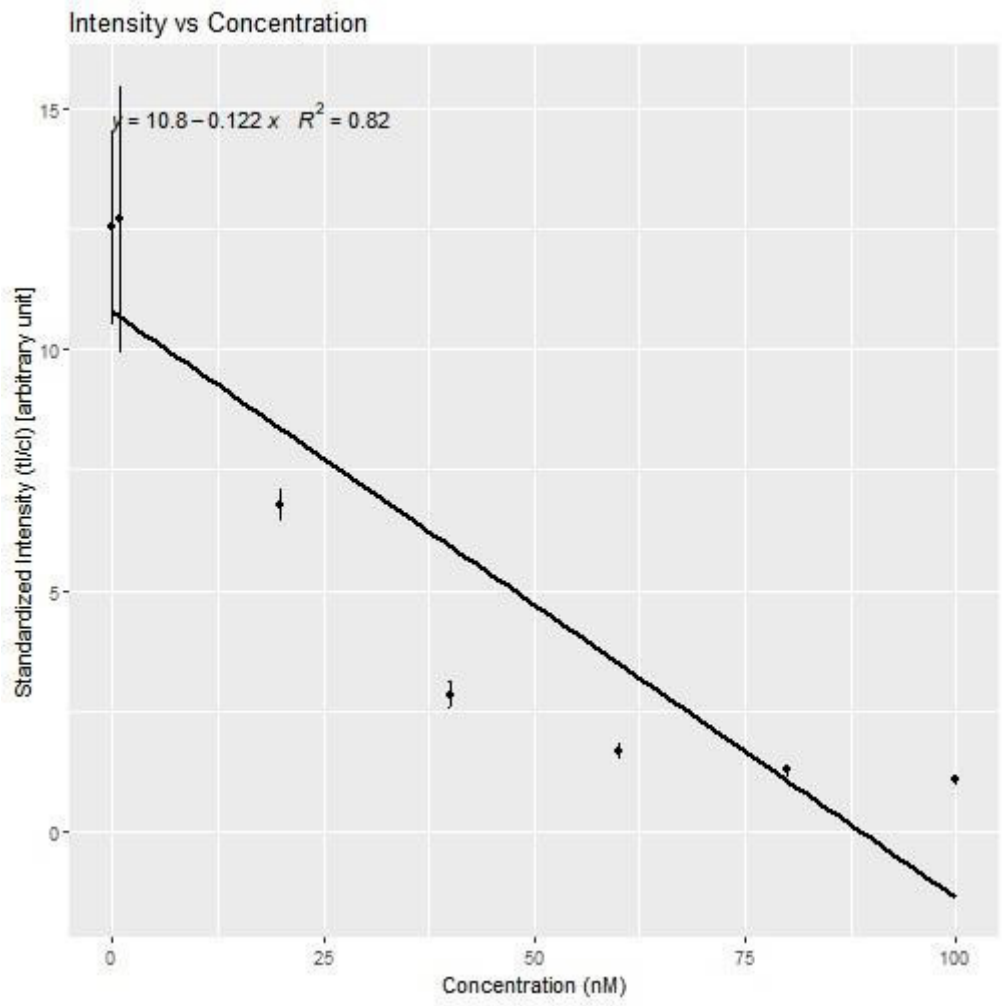

95% Confidence Interval:

	Min.Value	Max.Value
NI	0.161883	0.7000701
SI	1.610418	9.4937171

95% Confidence Interval:

	Min.Value	Max.Value
NI	0.161883	0.7000701
SI	1.610418	9.4937171

Correlation:

NI_cor	SI_cor
0.9922576	0.9076582

LOD_First Method:

lod_ni	loq_ni	lod_si	loq_si
0.1173294	0.2014846	1.238264	1.66038

LOD_Second Method:

lob_ni	lod_ni	loq_ni	lob_si	lod_si	loq_si
0.1010394	0.1265062	0.2014846	1.156555	1.330745	1.66038

Settings used during implementation

Select the type of file: .csv

Intensity value: 1

Slope value: 1

Intercept value: 1

Session Information:

R version 3.5.1 (2018-07-02) Platform: x86_64-w64-mingw32/x64 (64-bit) Running under: Windows >= 8 x64 (build 9200)

Matrix products: default

locale: [1] LC_COLLATE=English_Germany.1252 LC_CTYPE=English_Germany.1252
[3] LC_MONETARY=English_Germany.1252 LC_NUMERIC=C
[5] LC_TIME=English_Germany.1252

attached base packages: character(0)

other attached packages: [1] GNSplex_0.1.0

loaded via a namespace (and not attached): [1] tidyselect_0.2.4 locfit_1.5-9.1 purrr_0.2.5
[4] lattice_0.20-35 colorspace_1.3-2 htmltools_0.3.6
[7] yaml_2.2.0 grDevices_3.5.1 rlang_0.2.2
[10] pillar_1.3.0 later_0.7.5 glue_1.3.0
[13] withr_2.1.2 EBImage_4.22.1 BiocGenerics_0.26.0 [16] RColorBrewer_1.1-2
bindrcpp_0.2.2 jpeg_0.1-8
[19] bindr_0.1.1 plyr_1.8.4 stringr_1.3.1
[22] munsell_0.5.0 gtable_0.2.0 htmlwidgets_1.2
[25] evaluate_0.11 labeling_0.3 Biobase_2.40.0
[28] knitr_1.20 httpuv_1.4.5 parallel_3.5.1
[31] markdown_0.8 highr_0.7 methods_3.5.1
[34] Rcpp_0.12.18 xtable_1.8-3 polynom_1.3-9
[37] ggpmisc_0.3.0 scales_1.0.0 promises_1.0.1
[40] jsonlite_1.5 abind_1.4-5 mime_0.5
[43] ggplot2_3.0.0 stats_3.5.1 datasets_3.5.1

[46] graphics_3.5.1 png_0.1-7 digest_0.6.17
[49] stringi_1.1.7 tiff_0.1-5 dplyr_0.7.6
[52] shiny_1.1.0 grid_3.5.1 tools_3.5.1
[55] bitops_1.0-6 magrittr_1.5 lazyeval_0.2.1
[58] RCurl_1.95-4.11 tibble_1.4.2 crayon_1.3.4
[61] pkgconfig_2.0.2 utils_3.5.1 assertthat_0.2.0
[64] base_3.5.1 rstudioapi_0.7 R6_2.2.2
[67] fftwtools_0.9-8 compiler_3.5.1

S2-Shiny app report: iPhone_ImageJ_Calibration

Analysis of the data of lateral flow assay

Initial Data:

Replicate	Test	Control	Conc
R1	19849957	628920	0
R1	20209421	928648	1
R1	17242057	1217355	20
R1	18451936	966406	40
R1	21477271	1138648	60
R2	20175371	1168820	80
R2	17886936	877234	100
R2	20728957	1284891	NA
R2	18457421	1046062	NA
R2	22558220	1119477	NA
R3	23369563	2424276	NA
R3	26038756	2703861	NA
R3	28845605	2992589	NA
R3	23761371	2608397	NA
R3	22600886	2779518	NA
R4	30055312	11393066	NA
R4	28549664	9383045	NA
R4	31830635	9358803	NA
R4	28814342	8482510	NA
R4	25131714	9992631	NA
R5	28579271	15226945	NA
R5	29707371	22186057	NA
R5	26940785	21022208	NA
R5	26856907	19979673	NA
R5	30144664	22591137	NA
R6	26158593	22059723	NA
R6	21369643	22826894	NA
R6	24382836	23808401	NA
R6	23511785	22188430	NA
R6	22259078	22584300	NA
R7	20811744	24079380	NA
R7	19167350	23064865	NA
R7	19337886	20622208	NA
R7	17003401	21214844	NA
R7	19796643	201648029	NA

Combined replicates:

	NI.crep	SI.crep	NI.sdns	SI.sdns	NI.sd	SI.sd	Concn
R1	0.0507259	21.0886304	0.0140401	6.4622003	1636886	227763.8	0
R2	0.0550524	18.3159343	0.0055801	1.8706501	1867067	151518.8	1
R3	0.1088158	9.2299661	0.0083351	0.6552132	2539021	209968.0	20
R4	0.3387482	2.9987605	0.0478572	0.4142733	2462246	1078058.5	40
R5	0.7106566	1.4352015	0.1005035	0.2481936	1523579	2963013.6	60
R6	0.9692533	1.0382675	0.0842802	0.0943725	1865432	694530.7	80
R7	2.9720837	0.7065397	4.0332446	0.3438572	1396074	80243373.8	100

Normalized Intensity Plot (Standardized Intensity vs Concentration):

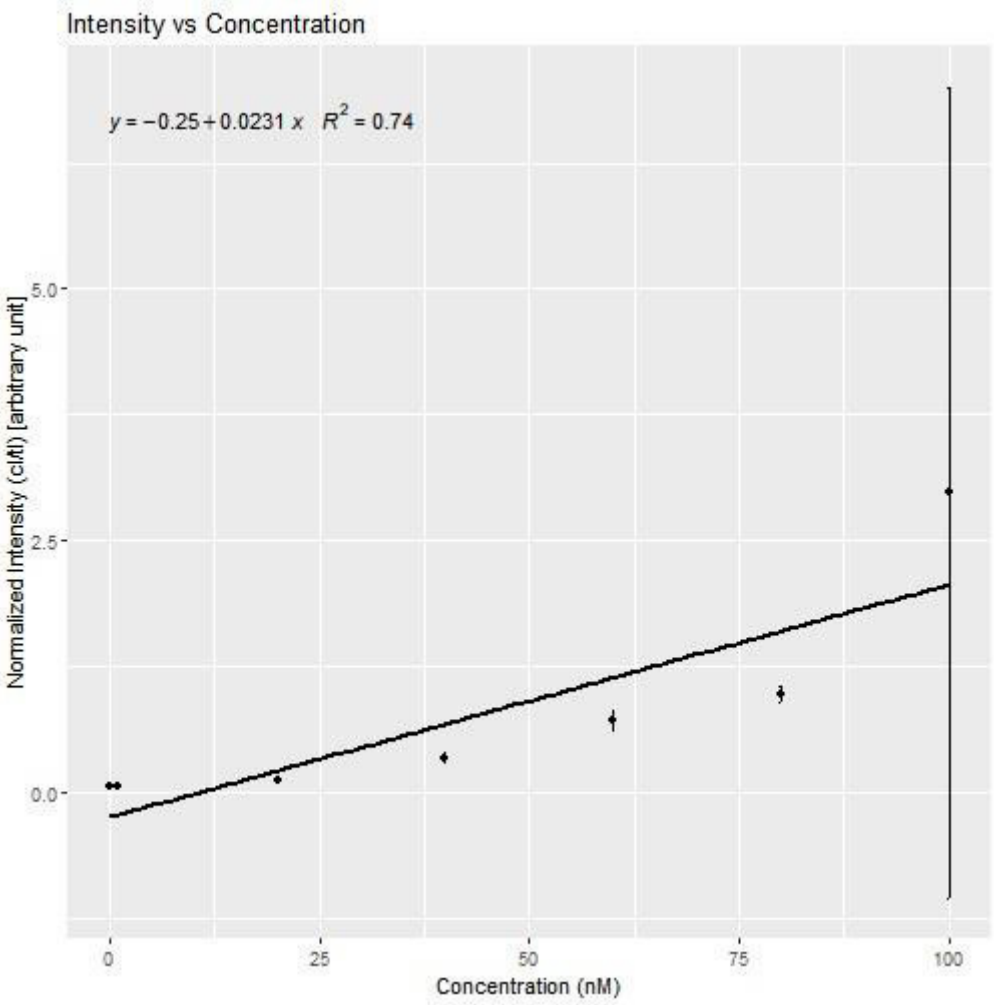

Standardized Intensity Plot (Normalized Intensity vs Concentration):

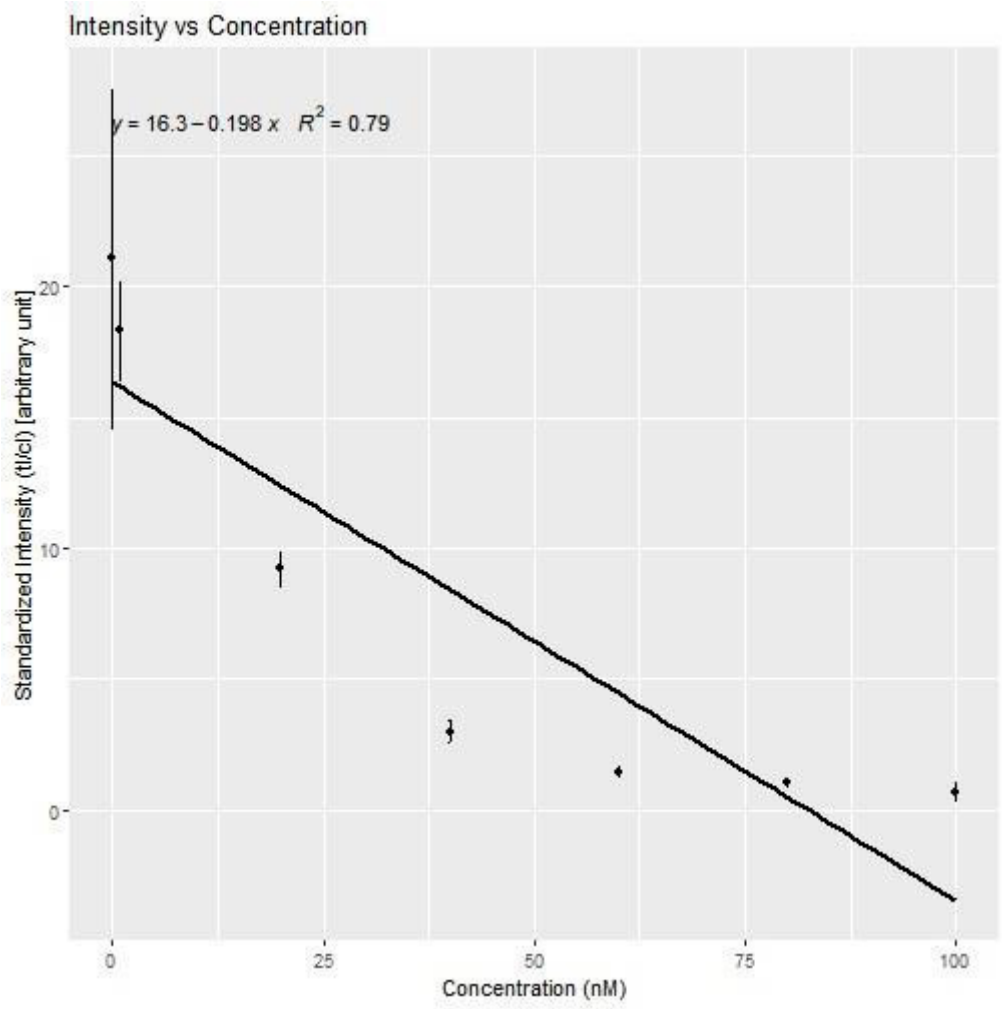

95% Confidence Interval:

Min.Value	Max.Value
-0.0455437	1.532782
1.2925845	14.368358

95% Confidence Interval:

Min.Value	Max.Value
-0.0455437	1.532782
1.2925845	14.368358

Correlation:

NI_cor	SI_cor
0.8601504	0.889901

LOD_First Method:

lod_ni	loq_ni	lod_si	loq_si
0.0928462	0.1911269	1.738111	4.145111

LOD_Second Method:

lob_ni	lod_ni	loq_ni	lob_si	lod_si	loq_si
0.0738218	0.083001	0.1911269	1.272185	1.427427	4.145111

Settings used during implementation:

Select the type of file: .csv

Intensity value: 1

Slope value: 1

Intercept value: 1

Session Information:

R version 3.5.1 (2018-07-02) Platform: x86_64-w64-mingw32/x64 (64-bit) Running under: Windows >= 8 x64 (build 9200)

Matrix products: default

locale: [1] LC_COLLATE=English_Germany.1252 LC_CTYPE=English_Germany.1252
[3] LC_MONETARY=English_Germany.1252 LC_NUMERIC=C
[5] LC_TIME=English_Germany.1252

attached base packages: character(0)

other attached packages: [1] GNSplex_0.1.0

loaded via a namespace (and not attached): [1] tidyselect_0.2.4 locfit_1.5-9.1 purrr_0.2.5
[4] lattice_0.20-35 colorspace_1.3-2 htmltools_0.3.6
[7] yaml_2.2.0 grDevices_3.5.1 rlang_0.2.2
[10] pillar_1.3.0 later_0.7.5 glue_1.3.0
[13] withr_2.1.2 EBImage_4.22.1 BiocGenerics_0.26.0 [16] RColorBrewer_1.1-2
bindrcpp_0.2.2 jpeg_0.1-8
[19] bindr_0.1.1 plyr_1.8.4 stringr_1.3.1
[22] munsell_0.5.0 gtable_0.2.0 htmlwidgets_1.2
[25] evaluate_0.11 labeling_0.3 Biobase_2.40.0
[28] knitr_1.20 httpuv_1.4.5 parallel_3.5.1
[31] markdown_0.8 highr_0.7 methods_3.5.1
[34] Rcpp_0.12.18 xtable_1.8-3 polynom_1.3-9
[37] ggpmisc_0.3.0 scales_1.0.0 promises_1.0.1

[40] jsonlite_1.5 abind_1.4-5 mime_0.5
[43] ggplot2_3.0.0 stats_3.5.1 datasets_3.5.1
[46] graphics_3.5.1 png_0.1-7 digest_0.6.17
[49] stringi_1.1.7 tiff_0.1-5 dplyr_0.7.6
[52] shiny_1.1.0 grid_3.5.1 tools_3.5.1
[55] bitops_1.0-6 magrittr_1.5 lazyeval_0.2.1
[58] RCurl_1.95-4.11 tibble_1.4.2 crayon_1.3.4
[61] pkgconfig_2.0.2 utils_3.5.1 assertthat_0.2.0
[64] base_3.5.1 rstudioapi_0.7 R6_2.2.2
[67] fftwtools_0.9-8 compiler_3.5.1

S3-Shiny app report: Imager_GNSplex_Calibration

Analysis of the data of lateral flow assay

Initial Data:

Replicate	Test	Control	Conc
R1	2.665618	1.972250	0
R1	2.686467	1.802999	1
R1	2.982301	2.274860	20
R1	2.565966	1.776844	40
R1	2.573689	1.842936	60
R2	2.430503	1.853013	80
R2	2.416658	1.709303	100
R2	2.390548	1.711391	NA
R2	2.449333	1.782119	NA
R2	2.722949	2.139932	NA
R3	2.491461	1.836071	NA
R3	2.578742	1.809790	NA
R3	2.604295	1.788031	NA
R3	2.533569	1.855411	NA
R3	2.848490	2.161237	NA
R4	2.370671	2.022635	NA
R4	2.463702	1.999698	NA
R4	2.372856	1.994070	NA
R4	2.448968	2.070735	NA
R4	2.593987	2.377702	NA
R5	2.277622	2.123299	NA
R5	2.219586	2.276303	NA
R5	2.191259	2.133412	NA
R5	2.252434	2.276235	NA
R5	2.655807	2.692046	NA
R6	2.161167	2.328301	NA
R6	2.154898	2.376353	NA
R6	1.983065	2.033739	NA
R6	2.184675	2.419267	NA
R6	2.454299	2.662822	NA
R7	2.068945	2.345260	NA
R7	2.078979	2.310772	NA
R7	1.936355	2.104124	NA
R7	2.097462	2.399156	NA
R7	2.356825	2.681556	NA

Combined replicates:

	NI.crep	SI.crep	NI.sdns	SI.sdns	NI.sd	SI.sd	Concn
R1	0.7164693	1.3986347	0.0364847	0.0712727	0.1694432	0.2048173	0
R2	0.7398159	1.3538322	0.0332087	0.0597395	0.1363896	0.1782534	1
R3	0.7232777	1.3843692	0.0288702	0.0555885	0.1394379	0.1537087	20
R4	0.8534793	1.1735368	0.0386335	0.0514672	0.0910568	0.1620143	40
R5	0.9911220	1.0101923	0.0382247	0.0400302	0.1909073	0.2311930	60
R6	1.0795999	0.9269663	0.0326476	0.0288263	0.1693662	0.2251934	80
R7	1.1226620	0.8910581	0.0235472	0.0189521	0.1531780	0.2077923	100

Normalized Intensity Plot (Standardized Intensity vs Concentration):

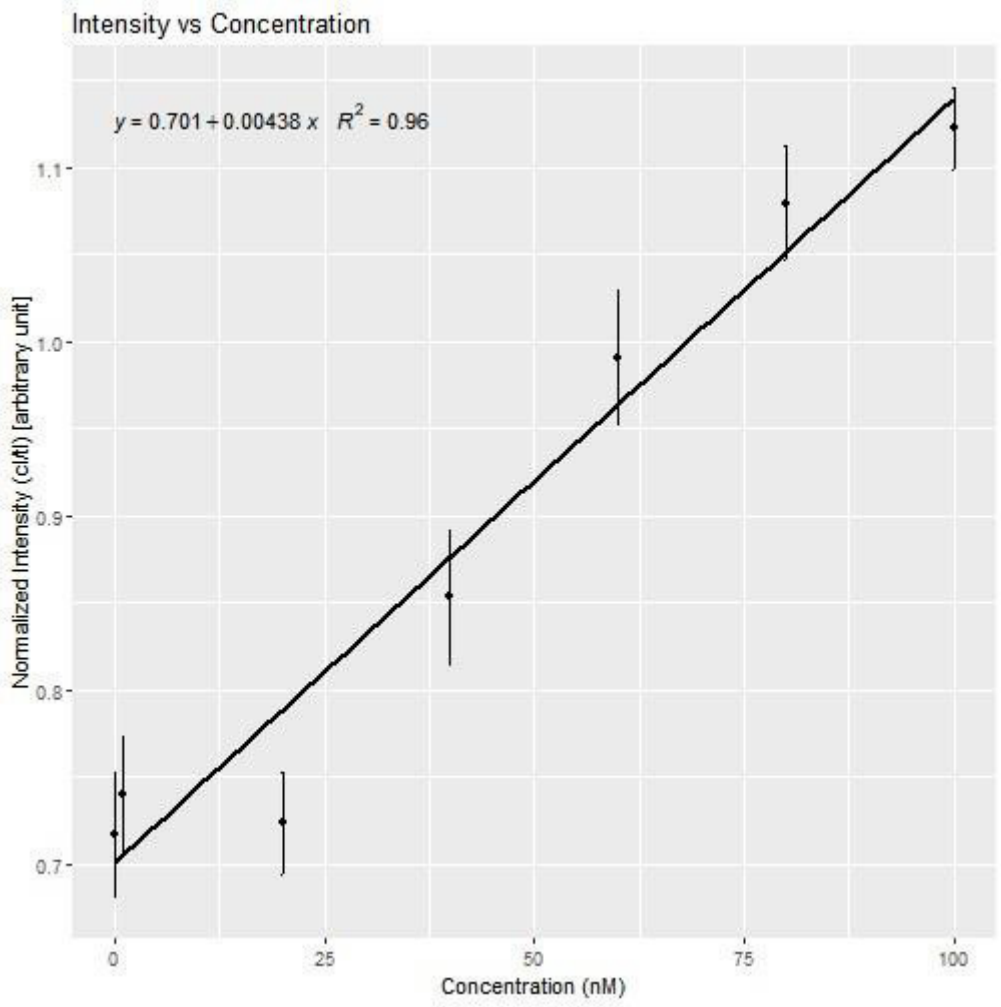

Standardized Intensity Plot (Normalized Intensity vs Concentration):

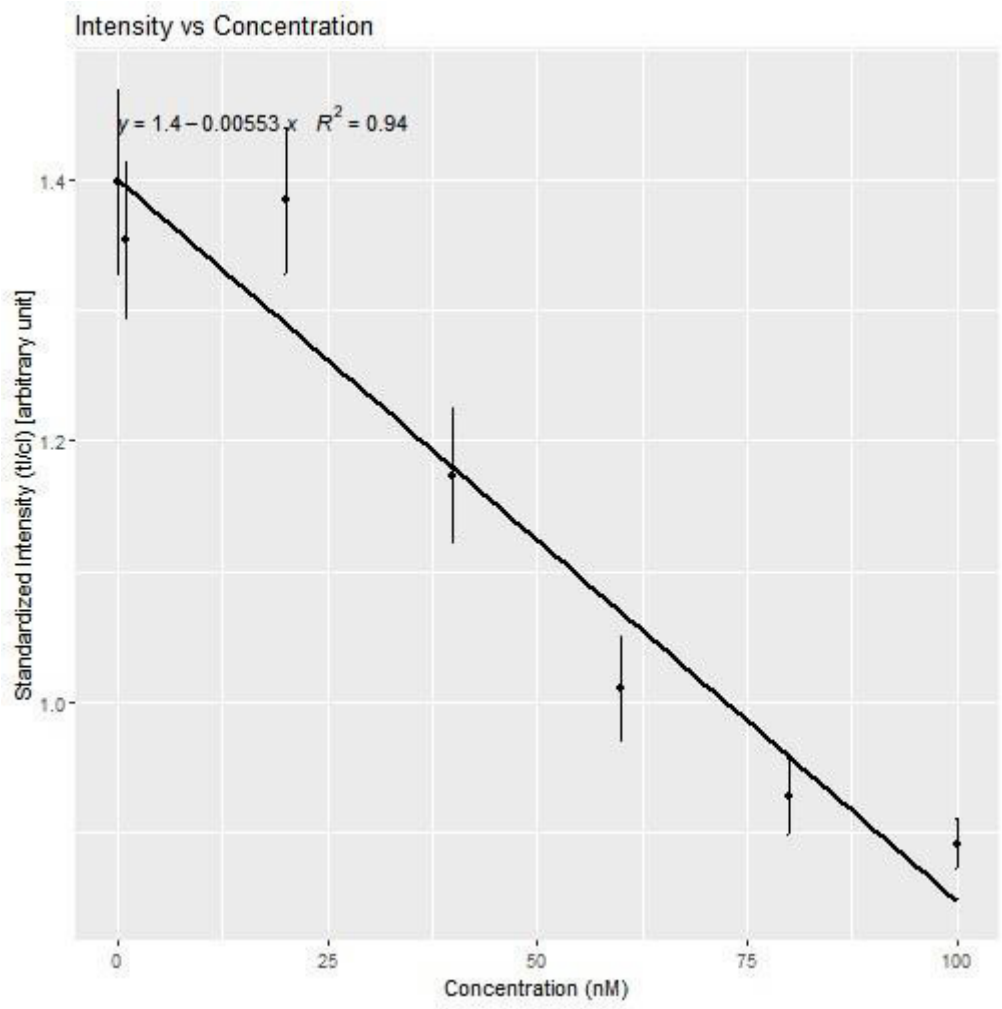

95% Confidence Interval:

Min.Value	Max.Value
0.7577965	1.021182
0.9953038	1.330008

95% Confidence Interval:

Min.Value	Max.Value
0.7577965	1.021182
0.9953038	1.330008

Correlation:

NI_cor	SI_cor
0.9777406	0.9707645

LOD_First Method:

lod_ni	loq_ni	lod_si	loq_si
0.8259236	1.081317	0.9479143	1.080579

LOD_Second Method:

lob_ni	lod_ni	loq_ni	lob_si	lod_si	loq_si
0.7764867	0.831115	1.081317	0.9222343	0.9696535	1.080579

Settings used during implementation:

Select the type of file: .txt

Intensity value: 1

Slope value: 1

Intercept value: 1

Session Information:

R version 3.5.1 (2018-07-02) Platform: x86_64-w64-mingw32/x64 (64-bit) Running under: Windows >= 8 x64 (build 9200)

Matrix products: default

locale: [1] LC_COLLATE=English_Germany.1252 LC_CTYPE=English_Germany.1252
[3] LC_MONETARY=English_Germany.1252 LC_NUMERIC=C
[5] LC_TIME=English_Germany.1252

attached base packages: character(0)

other attached packages: [1] GNSplex_0.1.0

loaded via a namespace (and not attached): [1] tidyselect_0.2.4 locfit_1.5-9.1 purrr_0.2.5
[4] lattice_0.20-35 colorspace_1.3-2 htmltools_0.3.6
[7] yaml_2.2.0 grDevices_3.5.1 rlang_0.2.2
[10] pillar_1.3.0 later_0.7.5 glue_1.3.0
[13] withr_2.1.2 EBImage_4.22.1 BiocGenerics_0.26.0 [16] RColorBrewer_1.1-2
bindrcpp_0.2.2 jpeg_0.1-8
[19] bindr_0.1.1 plyr_1.8.4 stringr_1.3.1
[22] munsell_0.5.0 gtable_0.2.0 htmlwidgets_1.2
[25] evaluate_0.11 labeling_0.3 Biobase_2.40.0
[28] knitr_1.20 httpuv_1.4.5 parallel_3.5.1
[31] markdown_0.8 highr_0.7 methods_3.5.1
[34] Rcpp_0.12.18 xtable_1.8-3 polynom_1.3-9
[37] ggpmisc_0.3.0 scales_1.0.0 promises_1.0.1
[40] jsonlite_1.5 abind_1.4-5 mime_0.5
[43] ggplot2_3.0.0 stats_3.5.1 datasets_3.5.1
[46] graphics_3.5.1 png_0.1-7 digest_0.6.17
[49] stringi_1.1.7 tiff_0.1-5 dplyr_0.7.6

[52] shiny_1.1.0 grid_3.5.1 tools_3.5.1
[55] bitops_1.0-6 magrittr_1.5 lazyeval_0.2.1
[58] RCurl_1.95-4.11 tibble_1.4.2 crayon_1.3.4
[61] pkgconfig_2.0.2 utils_3.5.1 assertthat_0.2.0
[64] base_3.5.1 rstudioapi_0.7 R6_2.2.2
[67] fftwtools_0.9-8 compiler_3.5.1

S4-Shiny app report: iPhone_GNSplex_Calibration

Analysis of the data of lateral flow assay

Initial Data:

Replicate	Test	Control	Conc
R1	2.253461	1.667461	0
R1	2.253461	1.666799	1
R1	2.040317	1.636620	20
R1	2.115741	1.664692	40
R1	2.050332	1.664525	60
R2	2.063235	1.652308	80
R2	2.068786	1.633346	100
R2	2.107026	1.639472	NA
R2	2.130163	1.670773	NA
R2	1.894965	1.604337	NA
R3	2.009606	1.656089	NA
R3	1.997425	1.671873	NA
R3	1.913738	1.624843	NA
R3	1.995282	1.668776	NA
R3	1.939495	1.653739	NA
R4	1.901865	1.752297	NA
R4	1.978616	1.789533	NA
R4	1.928561	1.730834	NA
R4	1.899058	1.733774	NA
R4	1.874816	1.750269	NA
R5	1.877766	1.809685	NA
R5	1.783899	1.776576	NA
R5	1.809998	1.793537	NA
R5	1.820237	1.810064	NA
R5	1.808478	1.802381	NA
R6	1.735298	1.760593	NA
R6	1.787728	1.817140	NA
R6	1.747525	1.759287	NA
R6	1.824096	1.849292	NA
R6	1.739770	1.760294	NA
R7	1.735752	1.770822	NA
R7	1.795284	1.823320	NA
R7	1.751836	1.762549	NA
R7	1.714216	1.781534	NA
R7	1.805152	1.873045	NA

Combined replicates:

	NI.crep	SI.crep	NI.sdns	SI.sdns	NI.sd	SI.sd	Concn
R1	0.7760804	1.2905599	0.0342921	0.0575385	0.1052104	0.0131435	0
R2	0.7998845	1.2513173	0.0274313	0.0414408	0.0924687	0.0245706	1
R3	0.8398336	1.1908873	0.0113733	0.0161701	0.0419814	0.0186191	20
R4	0.9139604	1.0943489	0.0141657	0.0169053	0.0395594	0.0233978	40
R5	0.9883168	1.0119847	0.0139122	0.0145033	0.0349035	0.0139568	60
R6	1.0126739	0.9874954	0.0037177	0.0036349	0.0381291	0.0416543	80
R7	1.0237635	0.9769414	0.0143415	0.0136821	0.0388376	0.0459590	100

Normalized Intensity Plot (Standardized Intensity vs Concentration):

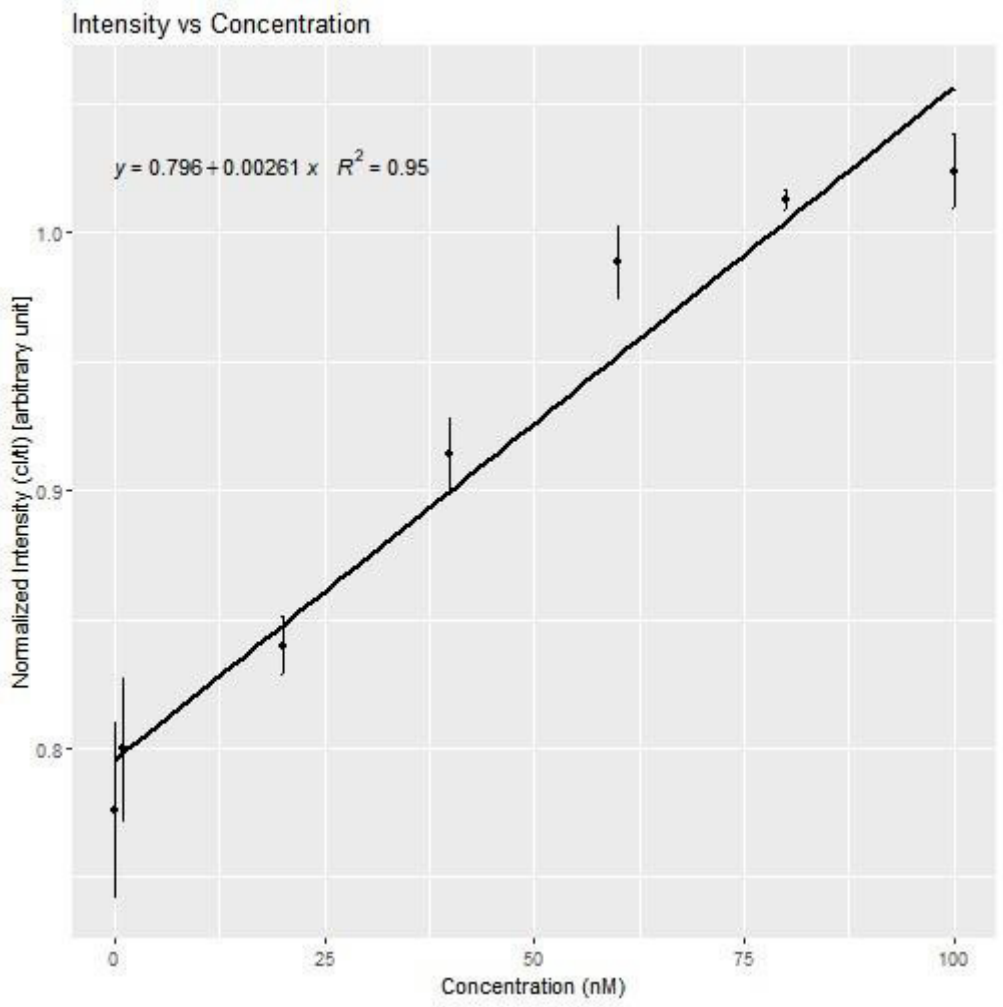

Standardized Intensity Plot (Normalized Intensity vs Concentration):

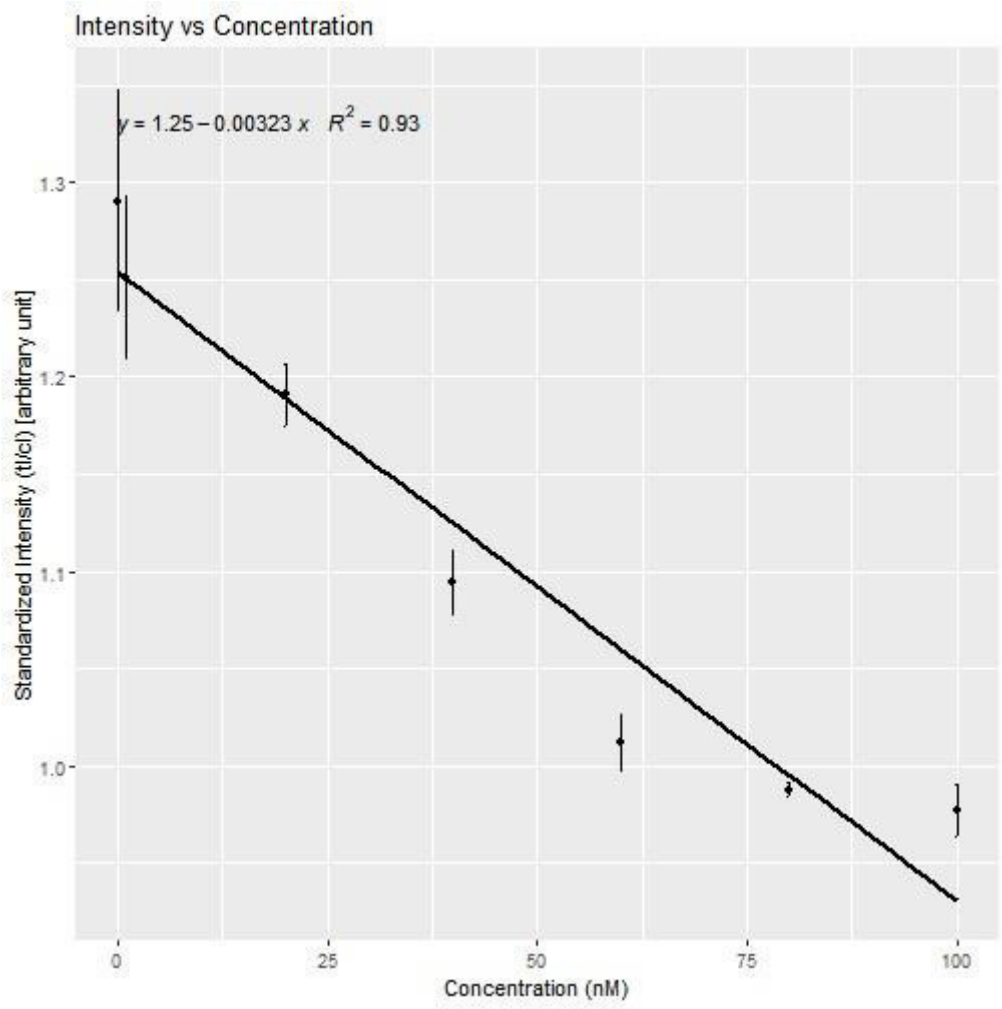

95% Confidence Interval:

Min.Value	Max.Value
0.8293613	0.9862139
1.0164626	1.2131188

95% Confidence Interval:

Min.Value	Max.Value
0.8293613	0.9862139
1.0164626	1.2131188

Correlation:

NI_cor	SI_cor
0.9757593	0.9660987

LOD_First Method:

lod_ni	loq_ni	lod_si	loq_si
0.8789566	1.119001	1.017988	1.113762

LOD_Second Method:

lob_ni	lod_ni	loq_ni	lob_si	lod_si	loq_si
0.8324909	0.8776154	1.119001	0.9994485	1.005428	1.113762

Settings used during implementation:

Select the type of file: .txt

Intensity value: 1

Slope value: 1

Intercept value: 1

Session Information:

R version 3.5.1 (2018-07-02) Platform: x86_64-w64-mingw32/x64 (64-bit) Running under: Windows >= 8 x64 (build 9200)

Matrix products: default

locale: [1] LC_COLLATE=English_Germany.1252 LC_CTYPE=English_Germany.1252
[3] LC_MONETARY=English_Germany.1252 LC_NUMERIC=C
[5] LC_TIME=English_Germany.1252

attached base packages: character(0)

other attached packages: [1] GNSplex_0.1.0

loaded via a namespace (and not attached): [1] tidyselect_0.2.4 locfit_1.5-9.1 purrr_0.2.5
[4] lattice_0.20-35 colorspace_1.3-2 htmltools_0.3.6
[7] yaml_2.2.0 grDevices_3.5.1 rlang_0.2.2
[10] pillar_1.3.0 later_0.7.5 glue_1.3.0
[13] withr_2.1.2 EBImage_4.22.1 BiocGenerics_0.26.0 [16] RColorBrewer_1.1-2
bindrcpp_0.2.2 jpeg_0.1-8
[19] bindr_0.1.1 plyr_1.8.4 stringr_1.3.1
[22] munsell_0.5.0 gtable_0.2.0 htmlwidgets_1.2
[25] evaluate_0.11 labeling_0.3 Biobase_2.40.0
[28] knitr_1.20 httpuv_1.4.5 parallel_3.5.1
[31] markdown_0.8 highr_0.7 methods_3.5.1
[34] Rcpp_0.12.18 xtable_1.8-3 polynom_1.3-9
[37] ggpmisc_0.3.0 scales_1.0.0 promises_1.0.1
[40] jsonlite_1.5 abind_1.4-5 mime_0.5
[43] ggplot2_3.0.0 stats_3.5.1 datasets_3.5.1

[46] graphics_3.5.1 png_0.1-7 digest_0.6.17
[49] stringi_1.1.7 tiff_0.1-5 dplyr_0.7.6
[52] shiny_1.1.0 grid_3.5.1 tools_3.5.1
[55] bitops_1.0-6 magrittr_1.5 lazyeval_0.2.1
[58] RCurl_1.95-4.11 tibble_1.4.2 crayon_1.3.4
[61] pkgconfig_2.0.2 utils_3.5.1 assertthat_0.2.0
[64] base_3.5.1 rstudioapi_0.7 R6_2.2.2
[67] fftwtools_0.9-8 compiler_3.5.1

S5-Shiny app report: Imager_ImageJ_Serum

Analysis of the data of lateral flow assay

Initial Data:

Replicate	Control	Test	Conc
R1	3.304790	12.57558	0
R1	2.927962	11.61563	1
R1	2.324374	12.88241	5
R2	3.209134	12.51863	10
R2	3.168548	12.72105	15
R2	3.047426	12.63887	20
R3	2.284255	13.39434	25
R3	3.421669	12.93004	30
R3	2.040255	12.24482	40
R4	3.581790	13.05705	60
R4	3.621841	13.42092	80
R4	3.833912	12.87734	100
R5	3.615962	13.36729	NA
R5	3.789912	13.47992	NA
R5	3.856255	13.69051	NA
R6	4.274548	14.03180	NA
R6	4.015669	13.97092	NA
R6	4.341790	14.02622	NA
R7	4.783497	14.45309	NA
R7	4.814033	14.68563	NA
R7	4.843083	14.40132	NA
R8	5.939205	15.14144	NA
R8	4.408740	15.82995	NA
R8	5.440497	14.10468	NA
R9	7.009740	15.16856	NA
R9	6.647447	15.42109	NA
R9	6.320083	14.92415	NA
R10	9.058447	15.54256	NA
R10	8.502397	15.04863	NA
R10	8.208447	15.78887	NA
R11	10.360276	14.71515	NA
R11	9.652397	15.13817	NA
R11	10.073690	15.22595	NA
R12	10.443861	13.54049	NA
R12	9.145225	16.54265	NA
R12	10.262640	13.51956	NA

Combined replicates:

	NI.crep	SI.crep	NI.sdns	SI.sdns	NI.sd	SI.sd	Concn
R1	0.2317650	4.438237	0.0447795	0.9595780	0.4945593	0.6608547	0
R2	0.2488477	4.021039	0.0076193	0.1233468	0.0841301	0.1018020	1
R3	0.2005967	5.214750	0.0554885	1.2454169	0.7372868	0.5782851	5
R4	0.2806364	3.569916	0.0149661	0.1852907	0.1354890	0.2769441	10
R5	0.2777781	3.601248	0.0063012	0.0827679	0.1240972	0.1640659	15
R6	0.3005372	3.330753	0.0116138	0.1310918	0.1721892	0.0336521	20
R7	0.3316890	3.015207	0.0042902	0.0388793	0.0297961	0.1514312	25
R8	0.3521592	2.910841	0.0638686	0.5890683	0.7805506	0.8684703	30
R9	0.4388884	2.281721	0.0204757	0.1041054	0.3449759	0.2484856	40
R10	0.5558995	1.803076	0.0324347	0.1077362	0.4316824	0.3769607	60
R11	0.6677628	1.500044	0.0336419	0.0746519	0.3560693	0.2731219	80
R12	0.6944096	1.474248	0.1227660	0.2899911	0.7033151	1.7393728	100

Normalized Intensity Plot (Standardized Intensity vs Concentration):

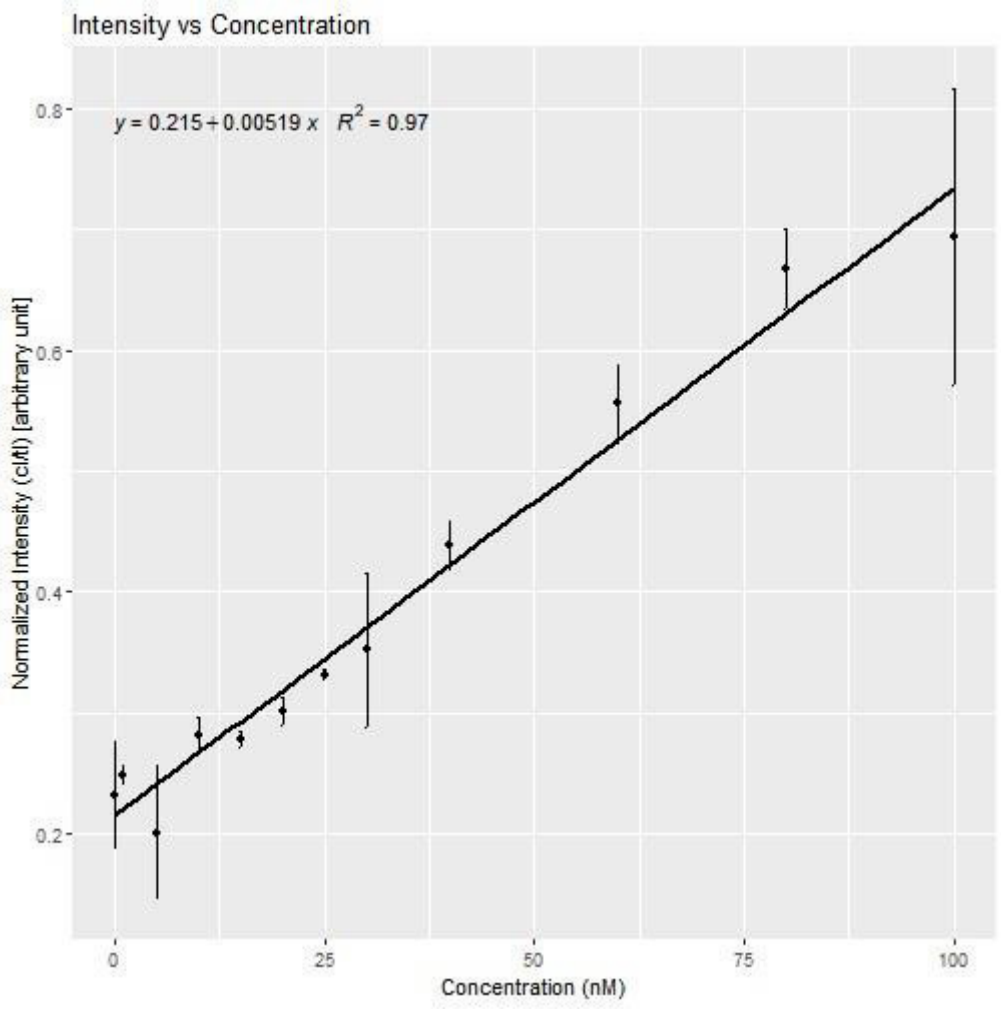

Standardized Intensity Plot (Normalized Intensity vs Concentration):

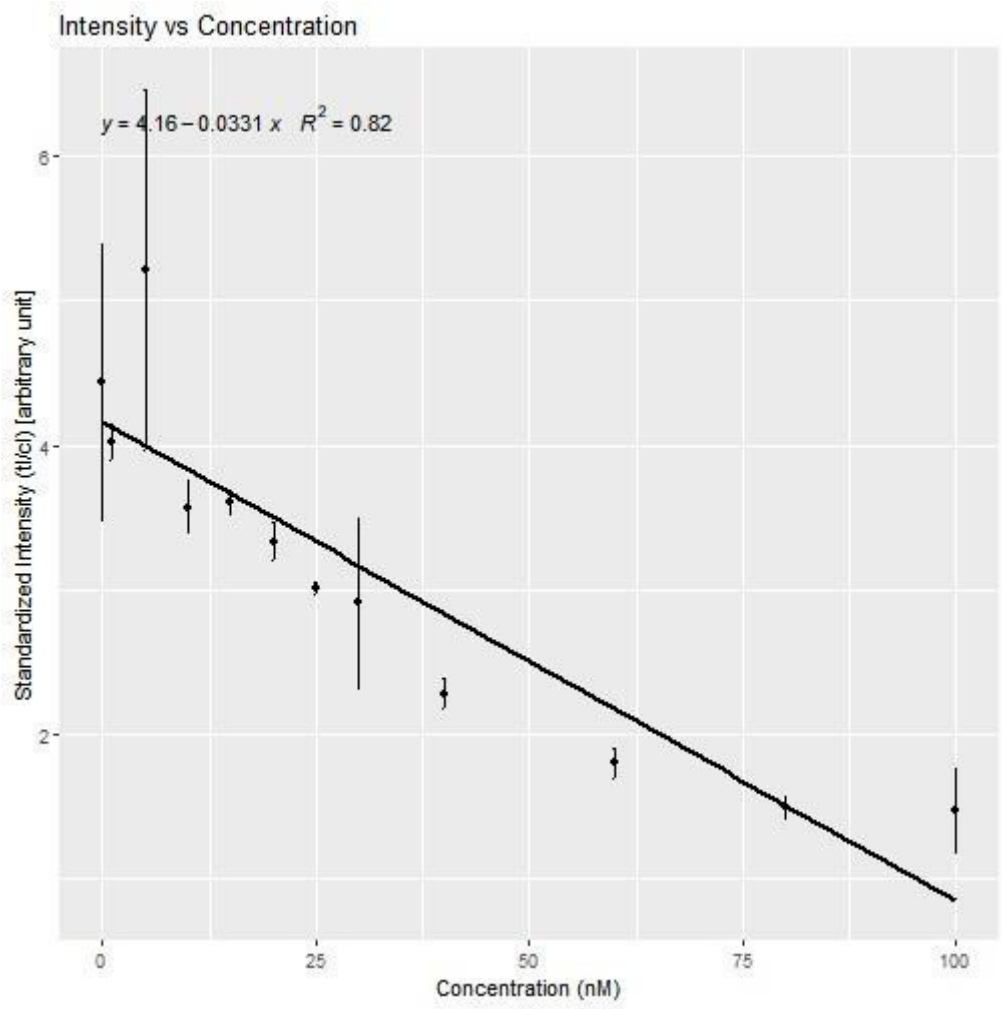

95% Confidence Interval:

Min.Value	Max.Value
0.2837155	0.4797794
2.4173174	3.7761959

95% Confidence Interval:

Min.Value	Max.Value
0.2837155	0.4797794
2.4173174	3.7761959

Correlation:

NI_cor	SI_cor
0.9871345	0.9078776

LOD_First Method:

lod_ni	loq_ni	lod_si	loq_si
0.3661037	0.6795605	2.344221	4.374159

LOD_Second Method:

lob_ni	lod_ni	loq_ni	lob_si	lod_si	loq_si
0.3054274	0.3179611	0.6795605	1.951283	2.074085	4.374159

Settings used during implementation:

Select the type of file: .txt

Intensity value: 1

Slope value: 1

Intercept value: 1

Session Information:

R version 3.5.1 (2018-07-02) Platform: x86_64-w64-mingw32/x64 (64-bit) Running under: Windows >= 8 x64 (build 9200)

Matrix products: default

locale: [1] LC_COLLATE=English_Germany.1252 LC_CTYPE=English_Germany.1252
[3] LC_MONETARY=English_Germany.1252 LC_NUMERIC=C
[5] LC_TIME=English_Germany.1252

attached base packages: character(0)

other attached packages: [1] GNSplex_0.1.0

loaded via a namespace (and not attached): [1] tidyselect_0.2.4 locfit_1.5-9.1 purrr_0.2.5
[4] lattice_0.20-35 colorspace_1.3-2 htmltools_0.3.6
[7] yaml_2.2.0 grDevices_3.5.1 rlang_0.2.2
[10] pillar_1.3.0 later_0.7.5 glue_1.3.0
[13] withr_2.1.2 EBImage_4.22.1 BiocGenerics_0.26.0 [16] RColorBrewer_1.1-2
bindrcpp_0.2.2 jpeg_0.1-8
[19] bindr_0.1.1 plyr_1.8.4 stringr_1.3.1
[22] munsell_0.5.0 gtable_0.2.0 htmlwidgets_1.2
[25] evaluate_0.11 labeling_0.3 Biobase_2.40.0
[28] knitr_1.20 httpuv_1.4.5 parallel_3.5.1
[31] markdown_0.8 highr_0.7 methods_3.5.1
[34] Rcpp_0.12.18 xtable_1.8-3 polynom_1.3-9
[37] ggpmisc_0.3.0 scales_1.0.0 promises_1.0.1
[40] jsonlite_1.5 abind_1.4-5 mime_0.5
[43] ggplot2_3.0.0 stats_3.5.1 datasets_3.5.1
[46] graphics_3.5.1 png_0.1-7 digest_0.6.17
[49] stringi_1.1.7 tiff_0.1-5 dplyr_0.7.6

[52] shiny_1.1.0 grid_3.5.1 tools_3.5.1
[55] bitops_1.0-6 magrittr_1.5 lazyeval_0.2.1
[58] RCurl_1.95-4.11 tibble_1.4.2 crayon_1.3.4
[61] pkgconfig_2.0.2 utils_3.5.1 assertthat_0.2.0
[64] base_3.5.1 rstudioapi_0.7 R6_2.2.2
[67] fftwtools_0.9-8 compiler_3.5.1

S6-Shiny app report: iPhone_ImageJ_Serum

Analysis of the data of lateral flow assay

Initial Data:

Replicate	Control	Test	Conc
R1	3.655782	18.23130	0
R1	2.723397	15.03921	1
R1	2.238912	19.25371	5
R2	3.249296	16.32562	10
R2	3.340175	17.10187	15
R2	3.008933	16.99386	20
R3	2.806054	20.21449	25
R3	3.629589	17.90752	30
R3	2.102740	18.41913	40
R4	3.405054	17.68823	60
R4	4.081180	19.50425	80
R4	4.078539	18.41547	100
R5	4.197044	19.65837	NA
R5	4.059418	18.33676	NA
R5	4.437953	19.20935	NA
R6	4.971660	18.93552	NA
R6	4.446953	18.47677	NA
R6	4.951368	20.44071	NA
R7	5.718853	19.27906	NA
R7	5.731489	20.85752	NA
R7	6.069196	22.00054	NA
R8	8.272924	24.29020	NA
R8	5.319196	23.12944	NA
R8	5.757125	17.42850	NA
R9	9.160681	20.03211	NA
R9	8.568974	19.74645	NA
R9	9.643167	22.69484	NA
R10	15.171359	23.87086	NA
R10	15.102894	23.21654	NA
R10	14.302702	23.22196	NA
R11	17.204823	21.00291	NA
R11	16.489409	21.02323	NA
R11	18.676359	22.04011	NA
R12	21.782673	19.89194	NA
R12	15.729409	24.47032	NA
R12	20.421966	19.25157	NA

Combined replicates:

	NI.crep	SI.crep	NI.sdns	SI.sdns	NI.sd	SI.sd	Concn
R1	0.1659645	6.369595	0.0441078	1.9496828	0.7201375	2.1983646	0
R2	0.1904670	5.264070	0.0117589	0.3357500	0.1711503	0.4204692	1
R3	0.1518866	6.965743	0.0456872	1.9239974	0.7642129	1.2115543	5
R4	0.2077410	4.829661	0.0145433	0.3425561	0.3896014	0.9139887	10
R5	0.2219704	4.509793	0.0087807	0.1778300	0.1916015	0.6720202	15
R6	0.2484887	4.030638	0.0122085	0.1926719	0.2972551	1.0273880	20
R7	0.2824312	3.545068	0.0123130	0.1507916	0.1987234	1.3665367	25
R8	0.3002967	3.437232	0.0611159	0.7903209	1.5940272	3.6726693	30
R9	0.4387186	2.281541	0.0167152	0.0856780	0.5380211	1.6260737	40
R10	0.6339986	1.578082	0.0173578	0.0433794	0.4829699	0.3762146	60
R11	0.8169623	1.225273	0.0315767	0.0475840	1.1150475	0.5930489	80
R12	0.9328802	1.137198	0.2518040	0.3627374	3.1757839	2.8462553	100

Normalized Intensity Plot (Standardized Intensity vs Concentration):

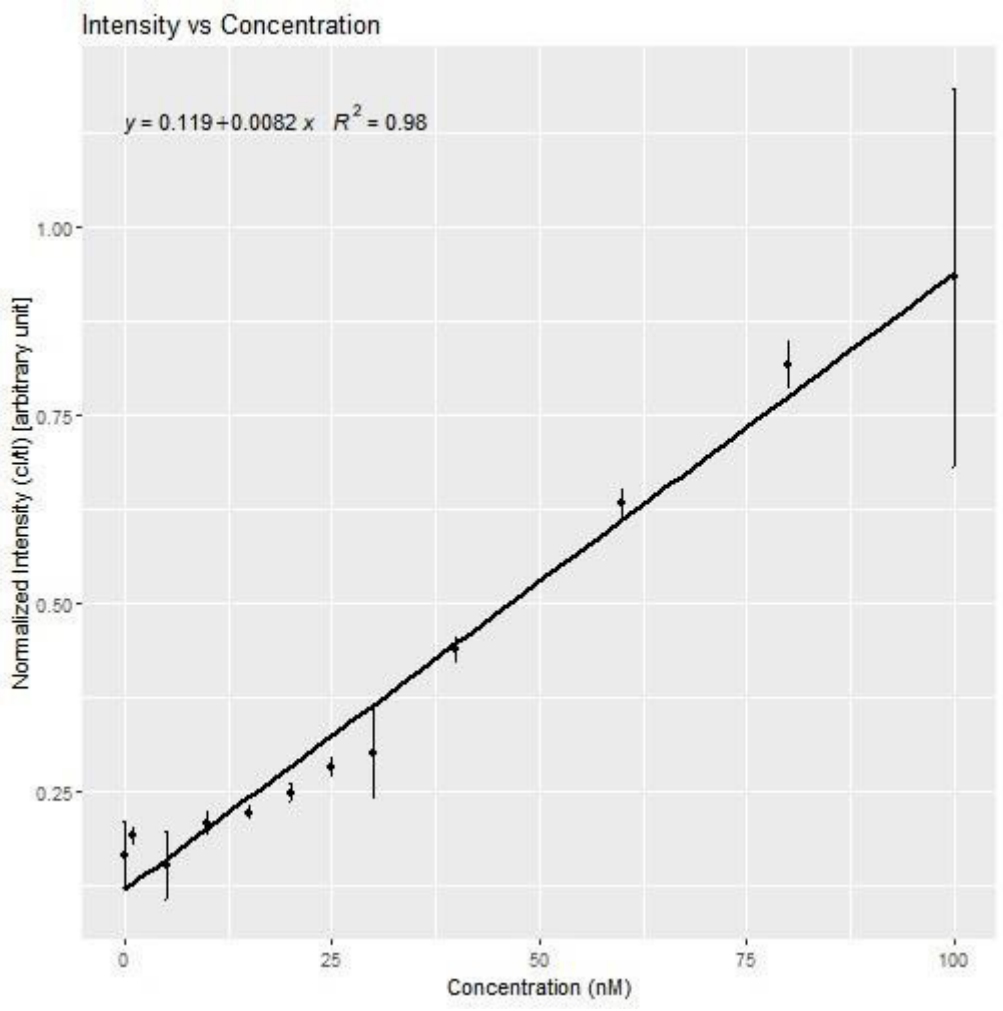

Standardized Intensity Plot (Normalized Intensity vs Concentration):

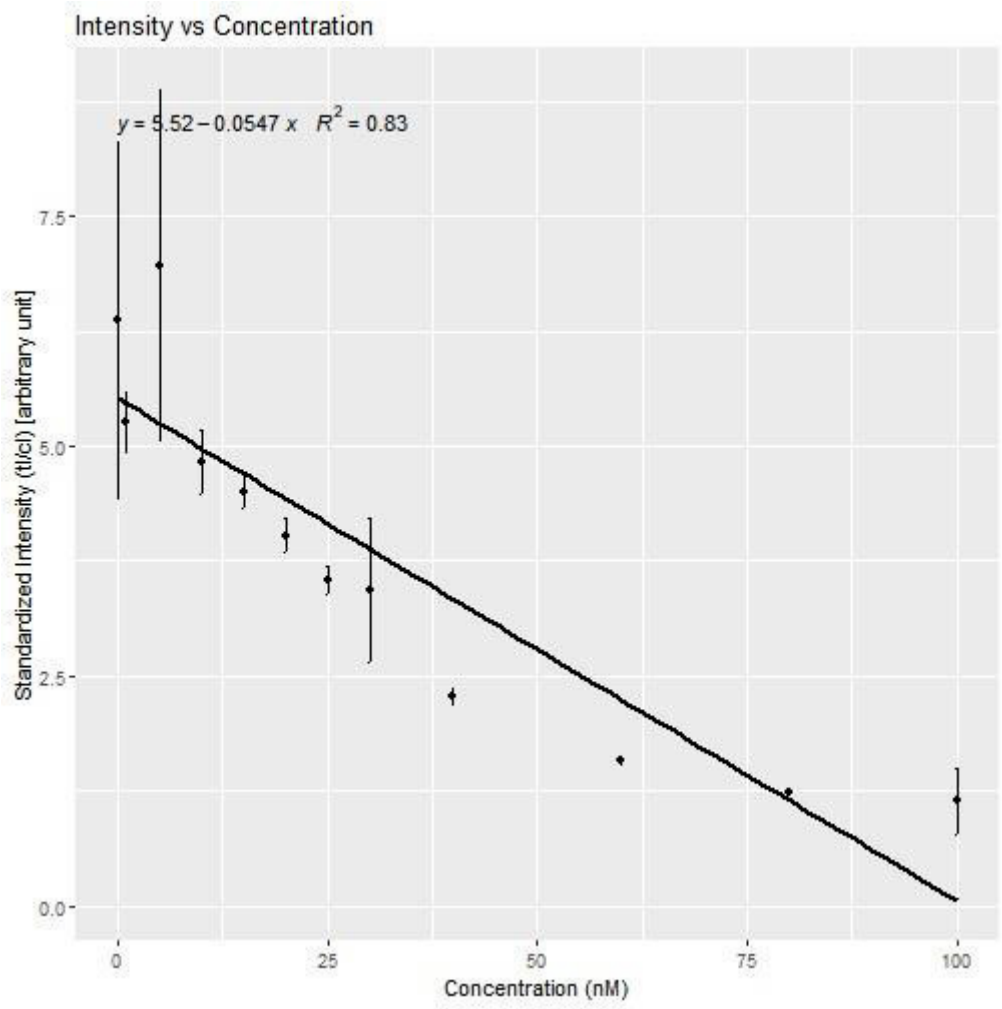

95% Confidence Interval:

Min.Value	Max.Value
0.2283117	0.5369893
2.6426789	4.8863038

95% Confidence Interval:

Min.Value	Max.Value
0.2283117	0.5369893
2.6426789	4.8863038

Correlation:

NI_cor	SI_cor
0.989628	0.9088938

LOD_First Method:

lod_ni	loq_ni	lod_si	loq_si
0.2982879	0.6070426	2.22541	4.764572

LOD_Second Method:

lob_ni	lod_ni	loq_ni	lob_si	lod_si	loq_si
0.2385218	0.2578652	0.6070426	1.733901	1.812177	4.764572

Settings used during implementation:

Select the type of file: .txt

Intensity value: 1

Slope value: 1

Intercept value: 1

Session Information:

R version 3.5.1 (2018-07-02) Platform: x86_64-w64-mingw32/x64 (64-bit) Running under: Windows >= 8 x64 (build 9200)

Matrix products: default

locale: [1] LC_COLLATE=English_Germany.1252 LC_CTYPE=English_Germany.1252
[3] LC_MONETARY=English_Germany.1252 LC_NUMERIC=C
[5] LC_TIME=English_Germany.1252

attached base packages: character(0)

other attached packages: [1] GNSplex_0.1.0

loaded via a namespace (and not attached): [1] tidyselect_0.2.4 locfit_1.5-9.1 purrr_0.2.5
[4] lattice_0.20-35 colorspace_1.3-2 htmltools_0.3.6
[7] yaml_2.2.0 grDevices_3.5.1 rlang_0.2.2
[10] pillar_1.3.0 later_0.7.5 glue_1.3.0
[13] withr_2.1.2 EBImage_4.22.1 BiocGenerics_0.26.0 [16] RColorBrewer_1.1-2
bindrcpp_0.2.2 jpeg_0.1-8
[19] bindr_0.1.1 plyr_1.8.4 stringr_1.3.1
[22] munsell_0.5.0 gtable_0.2.0 htmlwidgets_1.2
[25] evaluate_0.11 labeling_0.3 Biobase_2.40.0
[28] knitr_1.20 httpuv_1.4.5 parallel_3.5.1
[31] markdown_0.8 highr_0.7 methods_3.5.1
[34] Rcpp_0.12.18 xtable_1.8-3 polynom_1.3-9
[37] ggpmisc_0.3.0 scales_1.0.0 promises_1.0.1
[40] jsonlite_1.5 abind_1.4-5 mime_0.5
[43] ggplot2_3.0.0 stats_3.5.1 datasets_3.5.1

[46] graphics_3.5.1 png_0.1-7 digest_0.6.17
[49] stringi_1.1.7 tiff_0.1-5 dplyr_0.7.6
[52] shiny_1.1.0 grid_3.5.1 tools_3.5.1
[55] bitops_1.0-6 magrittr_1.5 lazyeval_0.2.1
[58] RCurl_1.95-4.11 tibble_1.4.2 crayon_1.3.4
[61] pkgconfig_2.0.2 utils_3.5.1 assertthat_0.2.0
[64] base_3.5.1 rstudioapi_0.7 R6_2.2.2
[67] fftwtools_0.9-8 compiler_3.5.1

S7-Shiny app report: Imager_GNSplex_Serum

Analysis of the data of lateral flow assay

Initial Data:

Replicate	Test	Control	Conc
R1	2.495087	2.192661	0
R1	2.709717	2.193412	1
R1	2.698113	2.231806	5
R2	2.508678	2.114448	10
R2	2.713118	2.194251	15
R2	2.677233	2.290130	20
R3	2.544692	2.075266	25
R3	2.617144	2.236919	30
R3	2.818819	2.197077	40
R4	2.600412	2.101003	60
R4	2.554399	2.204841	80
R4	2.555401	2.316758	100
R5	2.627631	2.179235	NA
R5	2.543842	2.259638	NA
R5	2.650721	2.239813	NA
R6	2.467461	2.218733	NA
R6	2.641235	2.275245	NA
R6	2.678383	2.307905	NA
R7	2.533235	2.248420	NA
R7	2.765401	2.332045	NA
R7	2.673531	2.315511	NA
R8	2.475173	2.224196	NA
R8	2.690972	2.325040	NA
R8	2.639707	2.444197	NA
R9	2.447104	2.292898	NA
R9	2.755486	2.531030	NA
R9	2.693439	2.414114	NA
R10	2.333501	2.343541	NA
R10	2.600692	2.547074	NA
R10	2.569431	2.592836	NA
R11	2.278629	2.409436	NA
R11	2.467937	2.575594	NA
R11	2.620096	2.692390	NA
R12	2.328753	2.478548	NA
R12	2.527264	2.747437	NA
R12	2.473426	2.571805	NA

Combined replicates:

	NI.crep	SI.crep	NI.sdns	SI.sdns	NI.sd	SI.sd	Concn
R1	0.8384753	1.1940842	0.0360203	0.0504003	0.1207064	0.0223867	0
R2	0.8356730	1.1973145	0.0241412	0.0350069	0.1091591	0.0879635	1
R3	0.8165589	1.2263878	0.0376535	0.0565047	0.1420491	0.0842190	5
R4	0.8592390	1.1664162	0.0494475	0.0676909	0.0262811	0.1079027	10
R5	0.8542046	1.1716630	0.0305254	0.0412757	0.0562389	0.0418875	15
R6	0.8741025	1.1444956	0.0217326	0.0280527	0.1125948	0.0451145	20
R7	0.8656498	1.1557060	0.0221408	0.0295916	0.1169217	0.0442864	25
R8	0.8961840	1.1167388	0.0310308	0.0388460	0.1127451	0.1101275	30
R9	0.9172736	1.0905468	0.0203746	0.0242794	0.1631105	0.1190725	40
R10	0.9975982	1.0025800	0.0159567	0.0161710	0.1460772	0.1327076	60
R11	1.0428735	0.9590201	0.0149210	0.0137374	0.1710700	0.1421928	80
R12	1.0637392	0.9403910	0.0236778	0.0209546	0.1026608	0.1365313	100

Normalized Intensity Plot (Standardized Intensity vs Concentration):

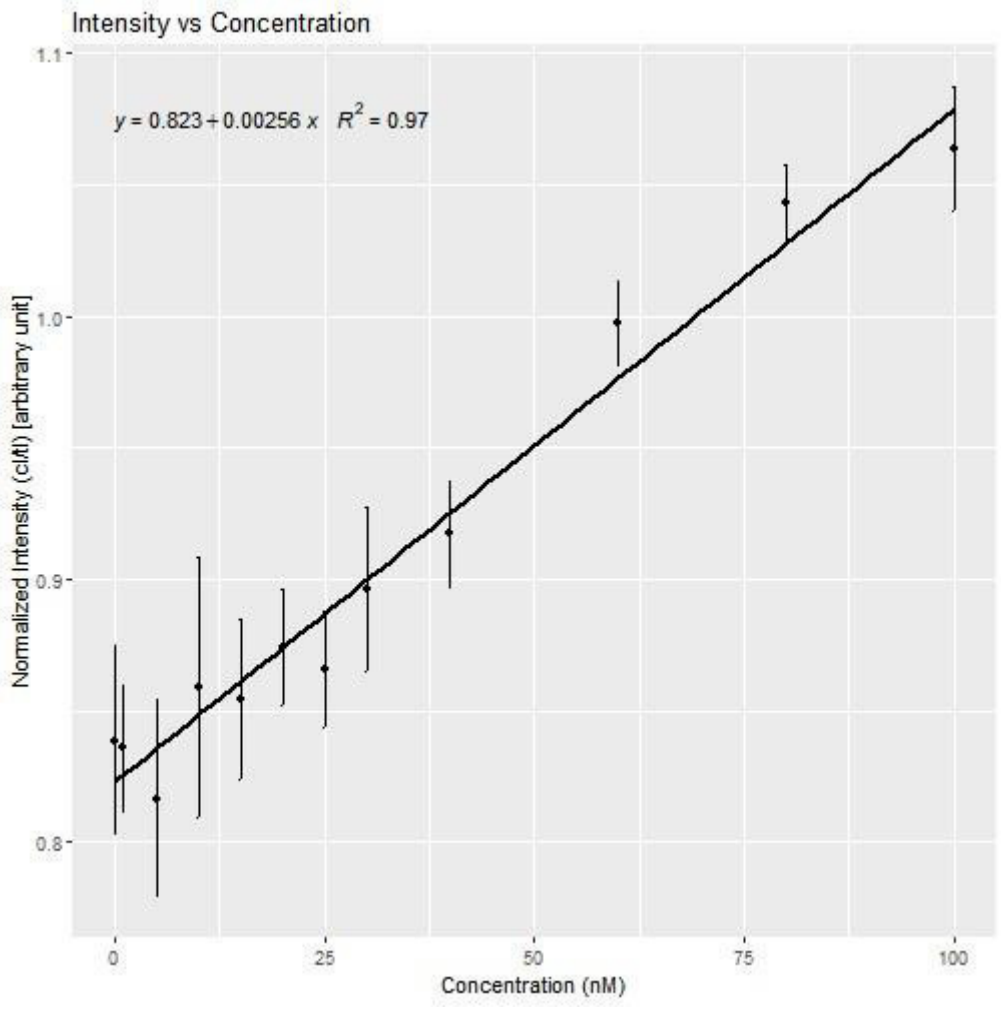

Standardized Intensity Plot (Normalized Intensity vs Concentration):

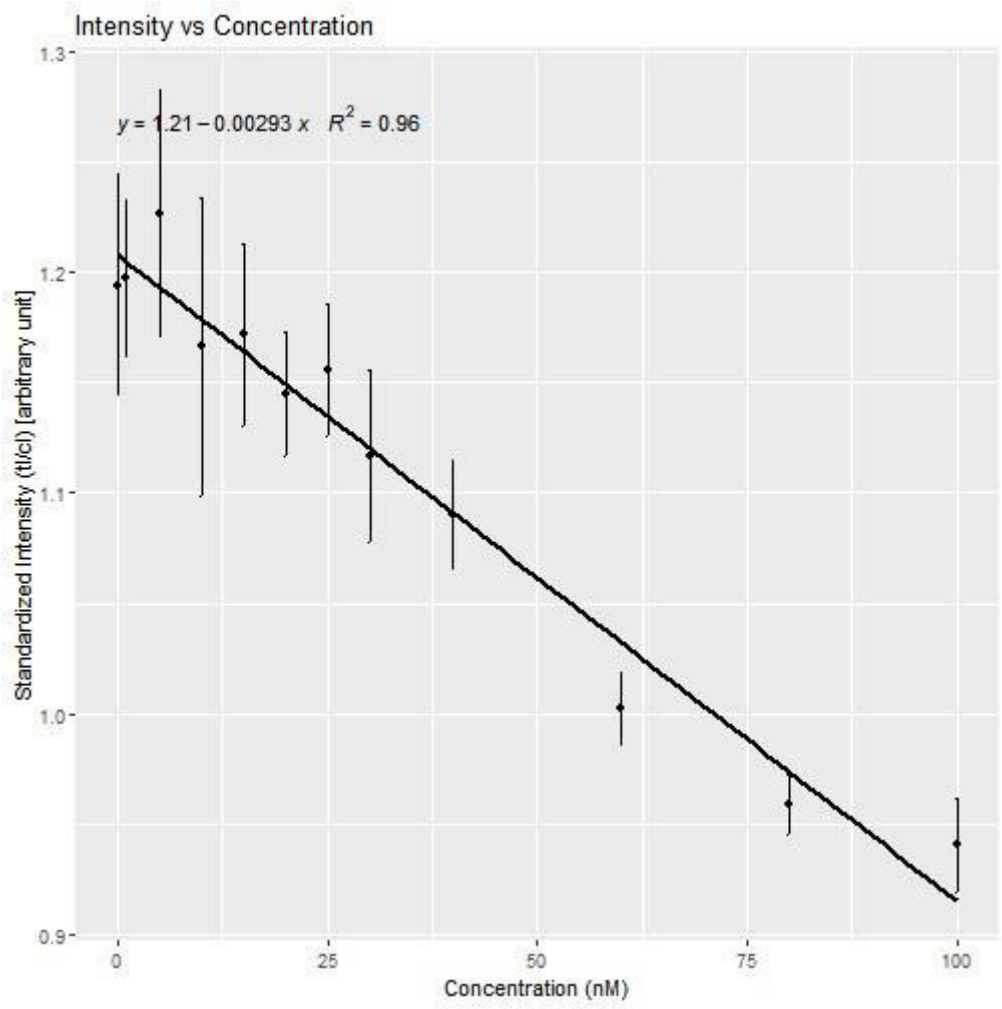

95% Confidence Interval:

Min.Value	Max.Value
0.8567509	0.953511
1.0582215	1.169336

95% Confidence Interval:

Min.Value	Max.Value
0.8567509	0.953511
1.0582215	1.169336

Correlation:

NI_cor	SI_cor
0.9849184	0.9813538

LOD_First Method:

lod_ni	loq_ni	lod_si	loq_si
0.9465362	1.198678	1.003255	1.149937

LOD_Second Method:

lob_ni	lod_ni	loq_ni	lob_si	lod_si	loq_si
0.8977287	0.937441	1.198678	0.9748613	0.9974594	1.149937

Settings used during implementation

Select the type of file: .txt

Intensity value: 1

Slope value: 1

Intercept value: 1

Session Information:

R version 3.5.1 (2018-07-02) Platform: x86_64-w64-mingw32/x64 (64-bit) Running under: Windows >= 8 x64 (build 9200)

Matrix products: default

locale: [1] LC_COLLATE=English_Germany.1252 LC_CTYPE=English_Germany.1252
[3] LC_MONETARY=English_Germany.1252 LC_NUMERIC=C
[5] LC_TIME=English_Germany.1252

attached base packages: character(0)

other attached packages: [1] GNSplex_0.1.0

loaded via a namespace (and not attached): [1] tidyselect_0.2.4 locfit_1.5-9.1 purrr_0.2.5
[4] lattice_0.20-35 colorspace_1.3-2 htmltools_0.3.6
[7] yaml_2.2.0 grDevices_3.5.1 rlang_0.2.2
[10] pillar_1.3.0 later_0.7.5 glue_1.3.0
[13] withr_2.1.2 EBImage_4.22.1 BiocGenerics_0.26.0 [16] RColorBrewer_1.1-2
bindrcpp_0.2.2 jpeg_0.1-8
[19] bindr_0.1.1 plyr_1.8.4 stringr_1.3.1
[22] munsell_0.5.0 gtable_0.2.0 htmlwidgets_1.2
[25] evaluate_0.11 labeling_0.3 Biobase_2.40.0
[28] knitr_1.20 httpuv_1.4.5 parallel_3.5.1
[31] markdown_0.8 highr_0.7 methods_3.5.1
[34] Rcpp_0.12.18 xtable_1.8-3 polynom_1.3-9
[37] ggpmisc_0.3.0 scales_1.0.0 promises_1.0.1
[40] jsonlite_1.5 abind_1.4-5 mime_0.5
[43] ggplot2_3.0.0 stats_3.5.1 datasets_3.5.1

[46] graphics_3.5.1 png_0.1-7 digest_0.6.17
[49] stringi_1.1.7 tiff_0.1-5 dplyr_0.7.6
[52] shiny_1.1.0 grid_3.5.1 tools_3.5.1
[55] bitops_1.0-6 magrittr_1.5 lazyeval_0.2.1
[58] RCurl_1.95-4.11 tibble_1.4.2 crayon_1.3.4
[61] pkgconfig_2.0.2 utils_3.5.1 assertthat_0.2.0
[64] base_3.5.1 rstudioapi_0.7 R6_2.2.2
[67] fftwtools_0.9-8 compiler_3.5.1

S8-Shiny app report: iPhone_GNSplex_Serum

Analysis of the data of lateral flow assay

Initial Data:

Replicate	Test	Control	Conc
R1	1.837941	1.577473	0
R1	1.793863	1.568570	1
R1	1.682933	1.493914	5
R2	1.861876	1.602384	10
R2	1.861303	1.575607	15
R2	1.728782	1.518210	20
R3	1.809022	1.545565	25
R3	1.854788	1.593291	30
R3	1.722505	1.520507	40
R4	1.817732	1.589319	60
R4	1.859975	1.632199	80
R4	1.706194	1.546557	100
R5	1.848091	1.591065	NA
R5	1.827858	1.603789	NA
R5	1.798744	1.587384	NA
R6	1.884875	1.659491	NA
R6	1.765509	1.560062	NA
R6	1.759566	1.589622	NA
R7	1.870799	1.661517	NA
R7	1.870799	1.613687	NA
R7	1.870799	1.553918	NA
R8	1.824395	1.666160	NA
R8	1.846595	1.618664	NA
R8	1.314806	1.229788	NA
R9	1.797113	1.599594	NA
R9	1.602848	1.483151	NA
R9	1.701811	1.597991	NA
R10	1.797271	1.759095	NA
R10	1.735427	1.712039	NA
R10	1.683108	1.644959	NA
R11	1.695619	1.739275	NA
R11	1.728256	1.737603	NA
R11	1.694817	1.690270	NA
R12	1.665508	1.726351	NA
R12	1.746596	1.775527	NA
R12	1.688535	1.727570	NA

Combined replicates:

	NI.crep	SI.crep	NI.sdns	SI.sdns	NI.sd	SI.sd	Concn
R1	0.8734588	1.1450909	0.0147240	0.0193371	0.0798705	0.0458892	0
R2	0.8617775	1.1606544	0.0158756	0.0213425	0.0766770	0.0430052	1
R3	0.8653701	1.1558110	0.0152130	0.0201363	0.0671795	0.0369756	5
R4	0.8861056	1.1288300	0.0176797	0.0222757	0.0794500	0.0428210	10
R5	0.8736112	1.1448018	0.0112778	0.0148652	0.0248063	0.0086079	15
R6	0.8891583	1.1248050	0.0124522	0.0156355	0.0706941	0.0510581	20
R7	0.8604384	1.1630714	0.0288164	0.0391170	0.0000000	0.0539098	25
R8	0.9083907	1.1016388	0.0296875	0.0363034	0.3008248	0.2394093	30
R9	0.9181359	1.0897181	0.0252313	0.0302793	0.0971382	0.0667705	40
R10	0.9808721	1.0195181	0.0049456	0.0051269	0.0571477	0.0573600	60
R11	1.0094906	0.9907369	0.0146477	0.0142964	0.0190787	0.0278229	80
R12	1.0254044	0.9752889	0.0101780	0.0096502	0.0417863	0.0280465	100

Normalized Intensity Plot (Standardized Intensity vs Concentration):

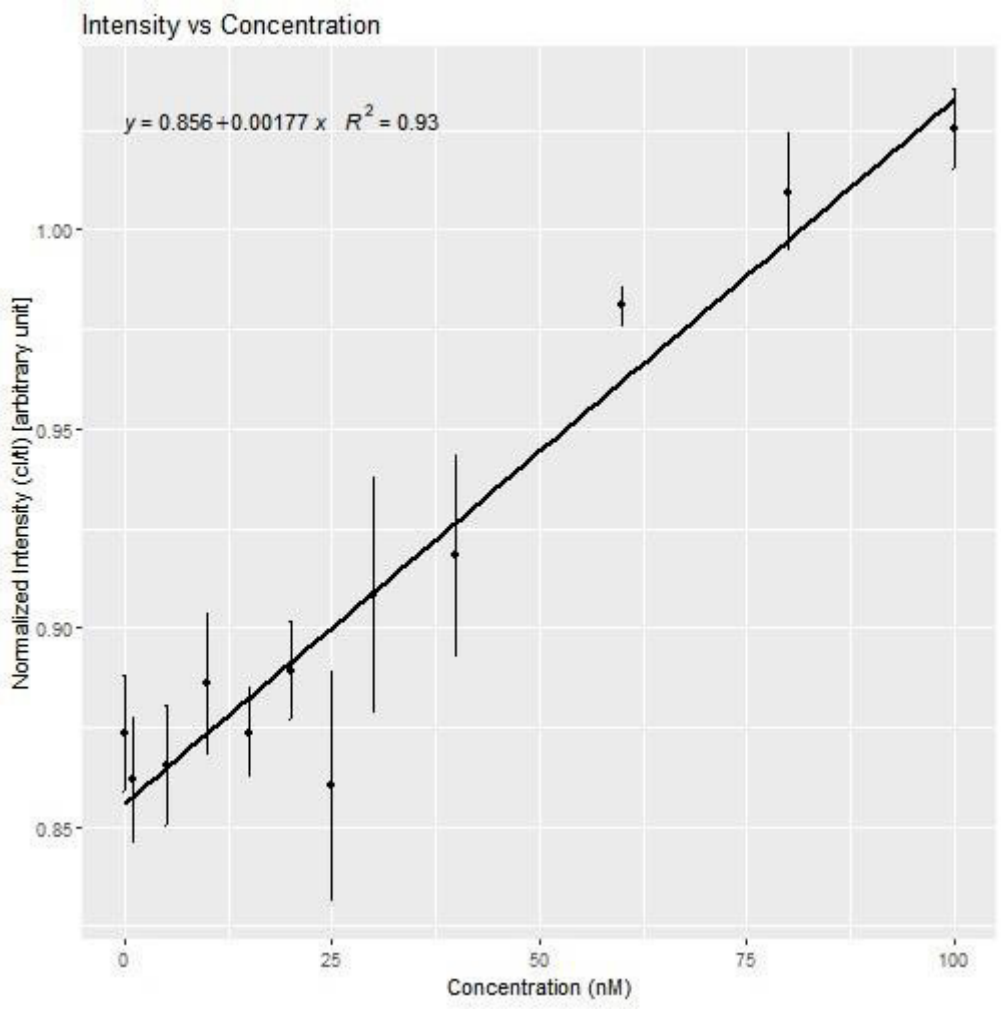

Standardized Intensity Plot (Normalized Intensity vs Concentration):

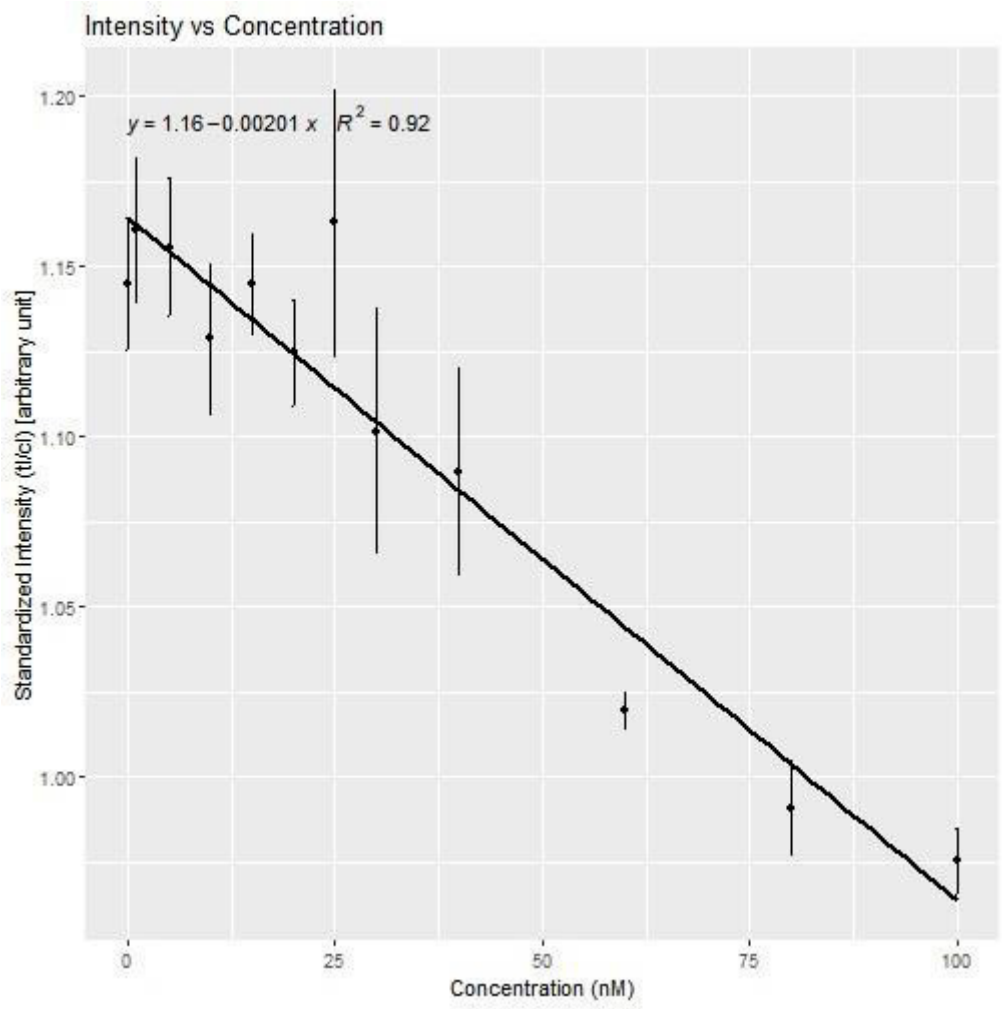

95% Confidence Interval:

Min.Value	Max.Value
0.8784571	0.9469119
1.0609417	1.1390525

95% Confidence Interval:

Min.Value	Max.Value
0.8784571	0.9469119
1.0609417	1.1390525

Correlation:

NI_cor	SI_cor
0.963543	0.9588569

LOD_First Method:

lod_ni	loq_ni	lod_si	loq_si
0.917631	1.020699	1.00424	1.071791

LOD_Second Method:

lob_ni	lod_ni	loq_ni	lob_si	lod_si	loq_si
0.8976799	0.9237953	1.020699	0.9911635	1.014681	1.071791

Settings used during implementation:

Select the type of file: .txt

Intensity value: 1

Slope value: 1

Intercept value: 1

Session Information:

R version 3.5.1 (2018-07-02) Platform: x86_64-w64-mingw32/x64 (64-bit) Running under: Windows >= 8 x64 (build 9200)

Matrix products: default

locale: [1] LC_COLLATE=English_Germany.1252 LC_CTYPE=English_Germany.1252
[3] LC_MONETARY=English_Germany.1252 LC_NUMERIC=C
[5] LC_TIME=English_Germany.1252

attached base packages: character(0)

other attached packages: [1] GNSplex_0.1.0

loaded via a namespace (and not attached): [1] tidyselect_0.2.4 locfit_1.5-9.1 purrr_0.2.5
[4] lattice_0.20-35 colorspace_1.3-2 htmltools_0.3.6
[7] yaml_2.2.0 grDevices_3.5.1 rlang_0.2.2
[10] pillar_1.3.0 later_0.7.5 glue_1.3.0
[13] withr_2.1.2 EBImage_4.22.1 BiocGenerics_0.26.0 [16] RColorBrewer_1.1-2
bindrcpp_0.2.2 jpeg_0.1-8
[19] bindr_0.1.1 plyr_1.8.4 stringr_1.3.1
[22] munsell_0.5.0 gtable_0.2.0 htmlwidgets_1.2
[25] evaluate_0.11 labeling_0.3 Biobase_2.40.0
[28] knitr_1.20 httpuv_1.4.5 parallel_3.5.1
[31] highr_0.7 methods_3.5.1 Rcpp_0.12.18
[34] xtable_1.8-3 polynom_1.3-9 ggpmisc_0.3.0
[37] scales_1.0.0 promises_1.0.1 jsonlite_1.5
[40] abind_1.4-5 mime_0.5 ggplot2_3.0.0
[43] stats_3.5.1 datasets_3.5.1 graphics_3.5.1

[46] png_0.1-7 digest_0.6.17 stringi_1.1.7
[49] tiff_0.1-5 dplyr_0.7.6 shiny_1.1.0
[52] grid_3.5.1 tools_3.5.1 bitops_1.0-6
[55] magrittr_1.5 lazyeval_0.2.1 RCurl_1.95-4.11
[58] tibble_1.4.2 crayon_1.3.4 pkgconfig_2.0.2
[61] utils_3.5.1 assertthat_0.2.0 base_3.5.1
[64] rstudioapi_0.7 R6_2.2.2 fftwtools_0.9-8
[67] compiler_3.5.1

6.2 Supplementary material publication 2

Ruppert C, Kaiser L, Jacob LJ, Laufer S, Kohl M and Deigner HP. Duplex Shiny app quantification of the sepsis biomarkers C-reactive protein and interleukin-6 in a fast quantum dot labeled lateral low assay. J Nanobiotechnol 18, 130 (2020) https://doi.org/10.1186/s12951-020-00688-1

Status: published ***Manuscript pages:*** ***103-107***

Additional Material on the Journal of Nanobiotechnology publication entitled:

Duplex Shiny app quantification of the sepsis biomarkers C-reactive protein and interleukin-6 in a fast quantum dot labeled lateral flow assay

Authors: Christoph Ruppert, Lars Kaiser, Lisa Johanna Jacob, Stefan Laufer, Matthias Kohl and Hans-Peter Deigner

S1 Materials and methods:

S1.1. Material characterization

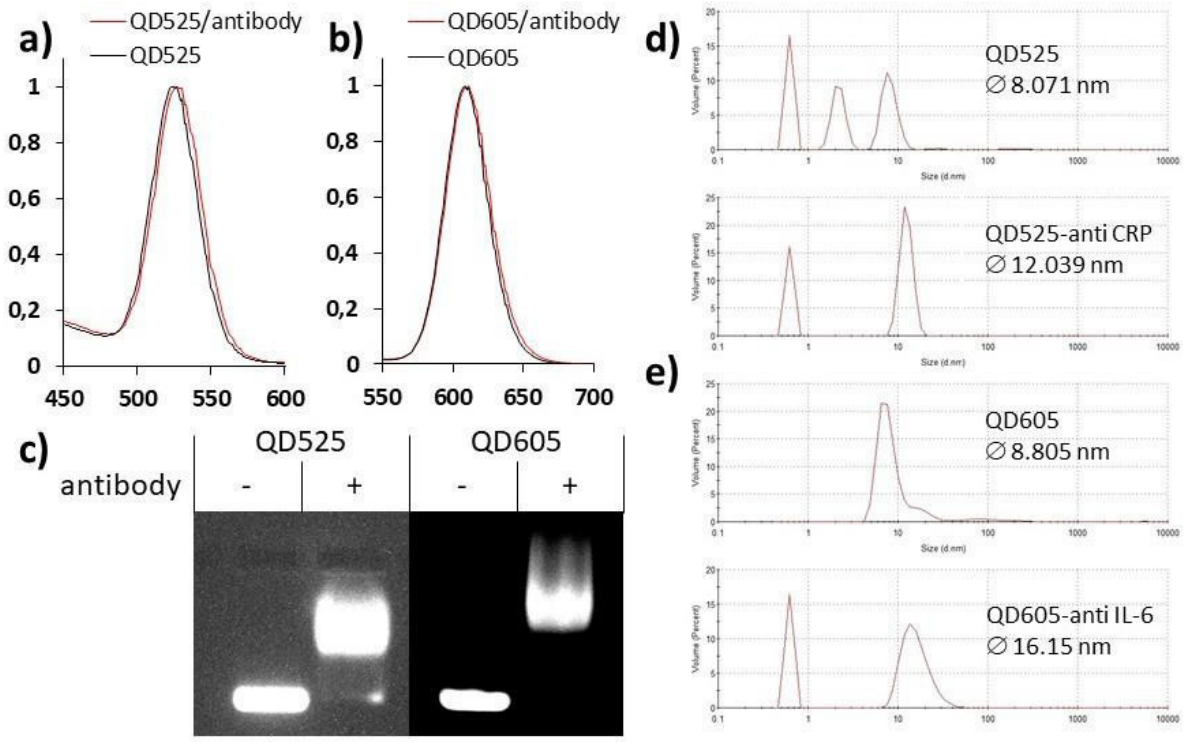

Figure S1.1: Characterization of prepared Quantum Dot – antibody conjugates. (a,b) Fluorescence emission spectra of QD525 (a) and QD605 (b), prior (black curve) and after (red curve) antibody conjugation.(c) Agarose gel electrophoresis of Quantum Dots prior (-) and after (+) conjugation to antibodies against CRP (QD525) or IL-6 (QD605). (d,e) DLS plots of QD525 (d) and QD602 (e) prior (upper chart) and after (lower chart) conjugation with antibody.

S1.2. Imaging Hardware-Settings

For image acquisition a *ChemStudio Plus* BioImager (Analytic Jena) equipped with a 16 Megapixel CCD-camera was used. For all quantum dot dyes the inbuild UV toplight source at λ=365nm center wavelength was used.

Green Channel:	For readout of CANdot-530-anti-CRP / Qdot-525-anti-CRP		
Emission filter:	513-557 bandpass filter (Omega Optical nr. 535AF45)		
Illumination time:	Streptavidin Assay/Sandwich Assay:	20 s	16MP resolution
	Clinical Range Assay:	4s	2x2 binning

Green Channel:	For readout of CANdot-610-anti-IL-6 / Qdot-605-anti-IL-6		
Emission filter:	565-625 bandpass filter (Omega Optical nr. 595BP60/50SQ)		
Illumination time:	Streptavidin Assay/Sandwich Assay:	4 s	16MP resolution
	Clinical Range Assay:	1s	2x2 binning

Images were exported as *.tiff* file and further processed either through *ImageJ* (V. 1.50i) or *the Multiflow-Shiny app*

S2 Results of data processing

S2.1 Streptavidin assay

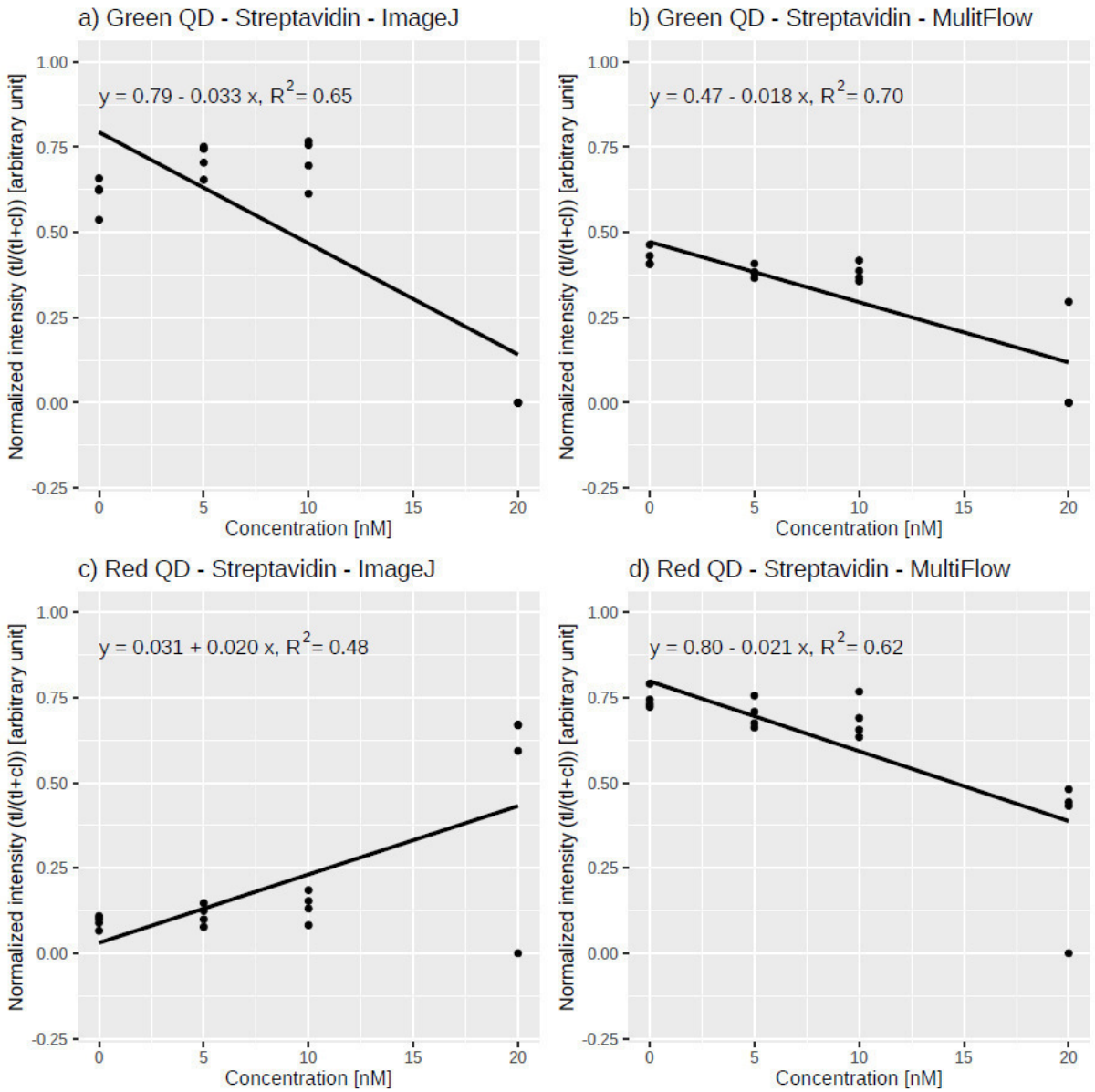

Fig. S2.1: Calibration curves of the Streptavidin, range 0-20nmol/L

S2.2 Clinical range assay

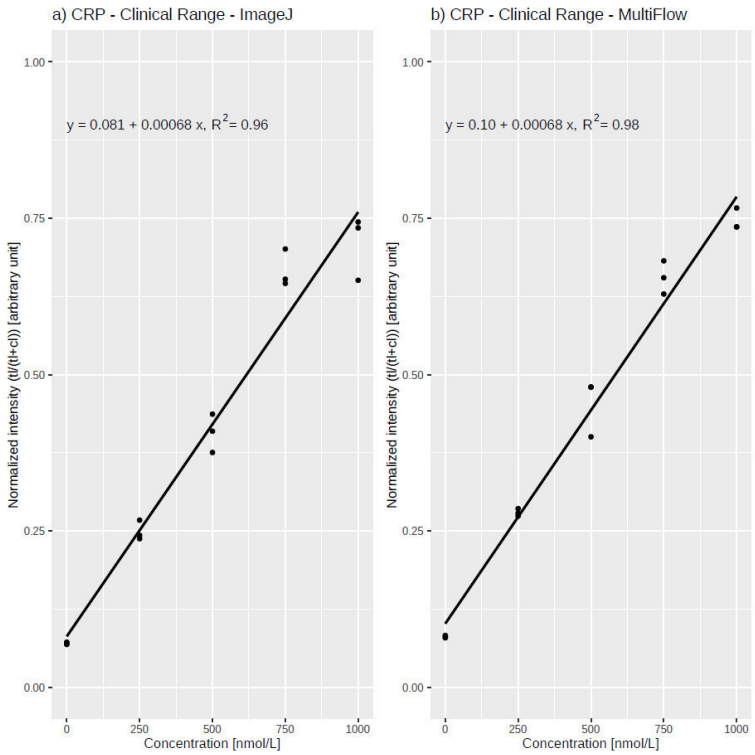

Fig. S2.2: Calibration curves of clinical range assay for CRP singleplex

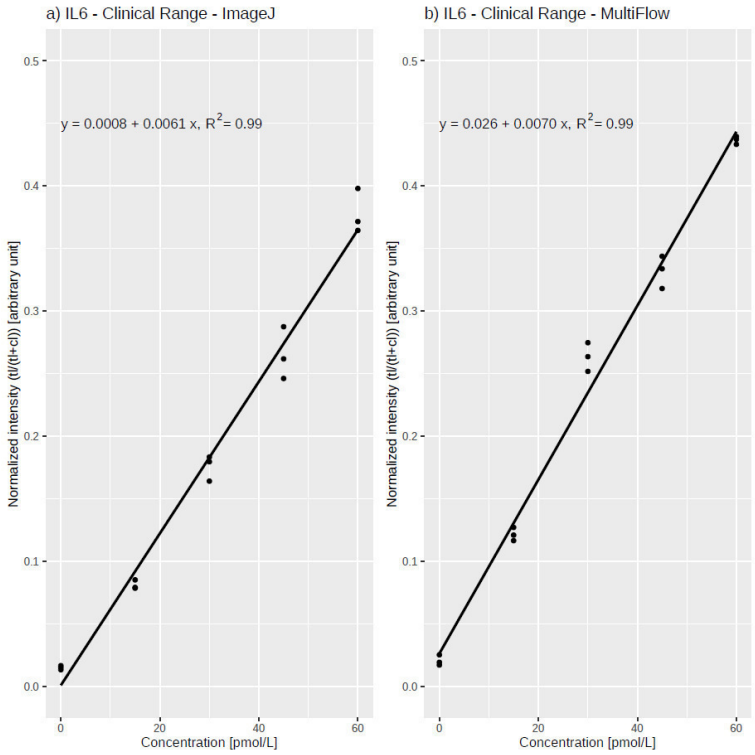

Fig. S2.3: Calibration curves of clinical range assay for IL-6singleplex

6.3 Supplementary material publication 3

Mahmoud M, Ruppert C, Rentschler S, Laufer S and Deigner HP. Combining aptamers and antibodies: lateral flow quantification for thrombin and interleukin-6 with smartphone readout. Sensors and Actuators B: Chemical 333, 129246 (2020) https://doi.org/10.1016/j.snb.2020.129246

Status: published ***Manuscript pages:*** ***109-120***

Electronic Supporting Material

Combining aptamers and antibodies: lateral flow quantification for thrombin and interleukin-6 with smartphone readout

Authors: Mostafa Mahmoud[1,2,3], Christoph Ruppert[1,2,3], Simone Rentschler[1,2,3], Stefan Laufer[3] and Hans-Peter Deigner[1,2,4,5*]

*Correspondence: dei@hs-furtwangen.de

3D-models: all 3D-printed parts where produced with an Ultimaker 3, 3D-printer at 0.2mm layer height resolution in black and red PLA.

3D-models are available in the ESM

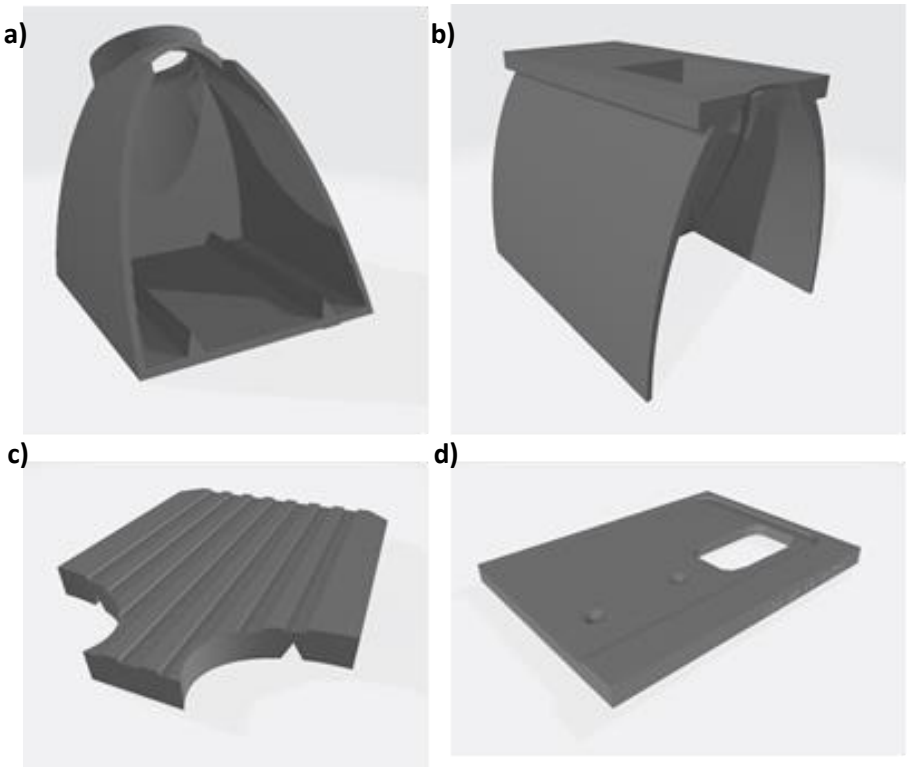

Figure S1: 3D-printed parts for smartphone reader a) bottom part (105 x 133 x 117 mm), holder for UV-LED and electronics, b) Lid (110 x 140 x 112 mm), c) sample plate for up to 7 LFA-strips (90 x 110 x 10 mm), d) Adapter for Huawei P30 Pro (97 x 133 x 8 mm)

Electronic components (LED light source):

UV-LED: model: NCSU276A UV SMD-LED on 10x10mm circuit board (Nichia, Japan)
P=780mW, λ=365nm center wavelength

Power supply: model: SLP033SS (Eaglerise Electric, China)
Input: 100-240V AC (50/60 Hz, 0.08A)
Output: I=350mA, 0.5-10V DC

Heatsink: model: ICK S R 50 x 20 (Fischer Elektronik, Germany)

∅=50mm, h=20mm

All components where purchased from LUMITRONIX LED-Technik (www.leds.de, Germany). The LED-module was attached to the center of the heatsink with double sided heat conducting adhesive tape attached to the darkbox with heat resistant glue and wired according to manufacturer´s recommendation.

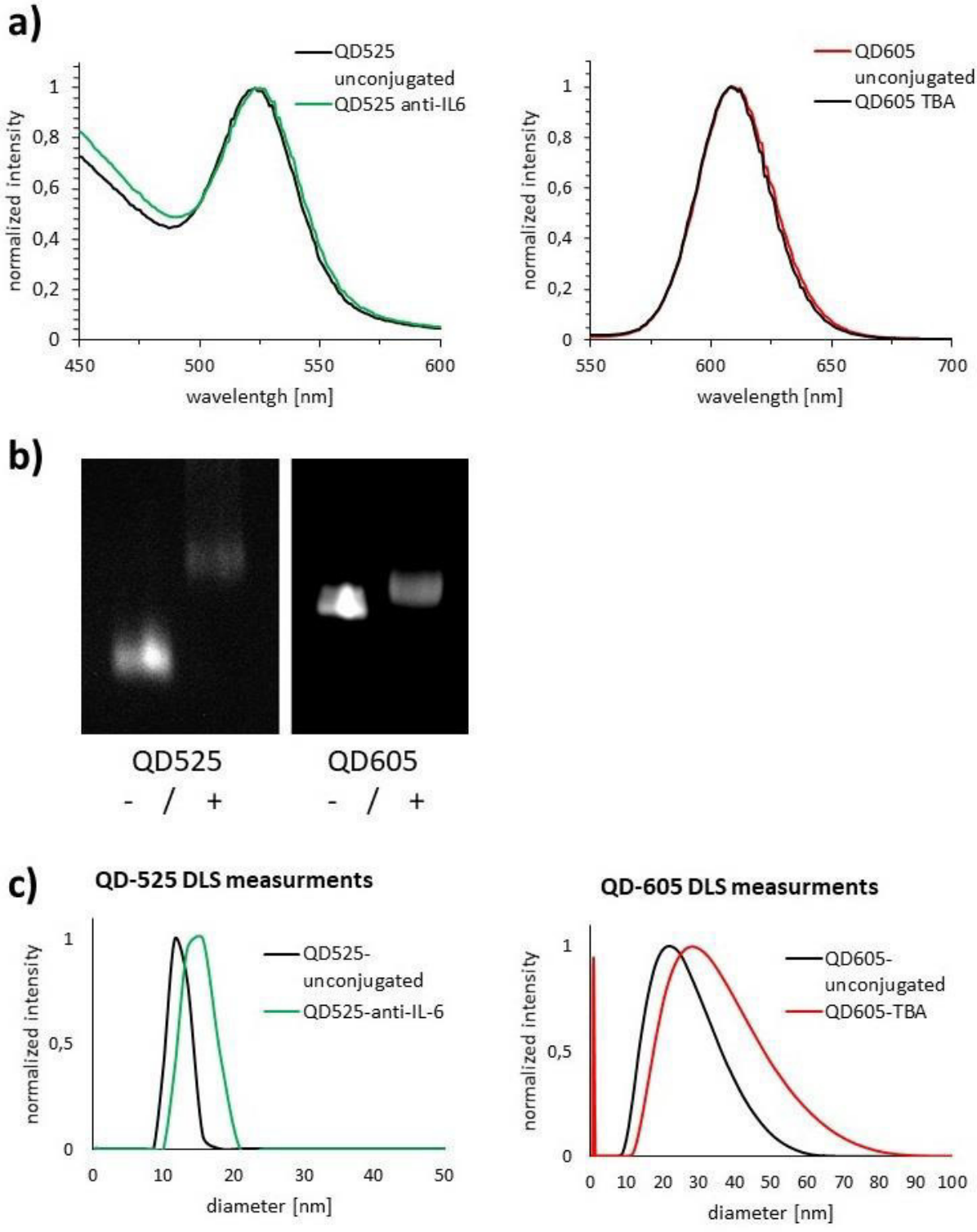

Figure S2 Characterization of the prepared Quantum Dot conjugates. (a) Fluorescence emission spectra of QD525 and QD605 (b) Agarose gel electrophoresis of Quantum Dots prior (-) and after (+) conjugation to antibodies IL-6 (QD525) or thrombin binding aptamer (TBA) (QD605). (c) Dynamic light scattering of Quantum Dots and corresponding antibody and aptamer conjugates. Diameters; QD525- unconjugated: 11.7 nm, QD525-anti IL-6: 15.7 nm, QD605-unconjugated: 21.0 nm, QD605-TBA: 28.2 nm (DLS-spectra acquired with Zetasizer Nano ZS; Malvern Worcestershire UK)

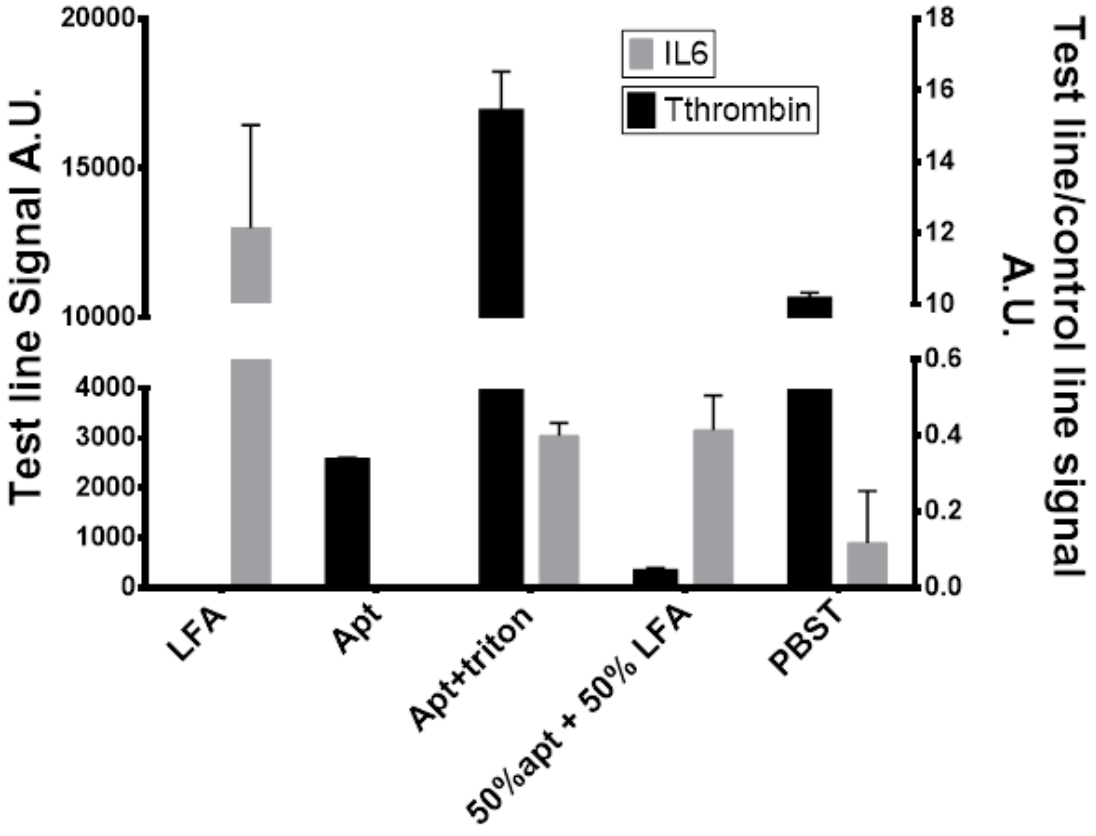

Figure S3 Plot comparing test line signal intensity (A.U.) of thrombin QDs (left y-axis), normalized signal intensity (test line / control line) of IL-6 QDs in different buffers. The intensity of the lines was measured using ImageJ software (gel analyzer tool). The points show the mean value and the error bars represent the standard deviation n=5.

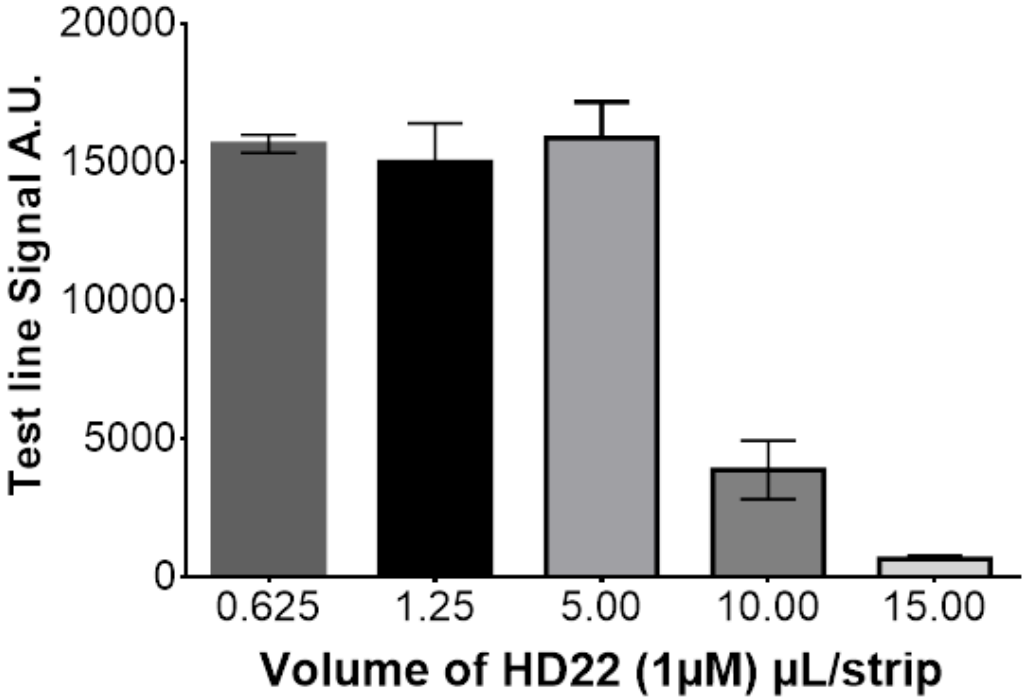

Figure S4 Plot of test line signal intensity (A.U.) for different amounts of HD22 detection aptamer (volume in µL from a 1 µM stock solution). The test line intensity was measured using ImageJ software (gel analyzer tool). The points show the mean value and the error bars represent the standard deviation n=2.

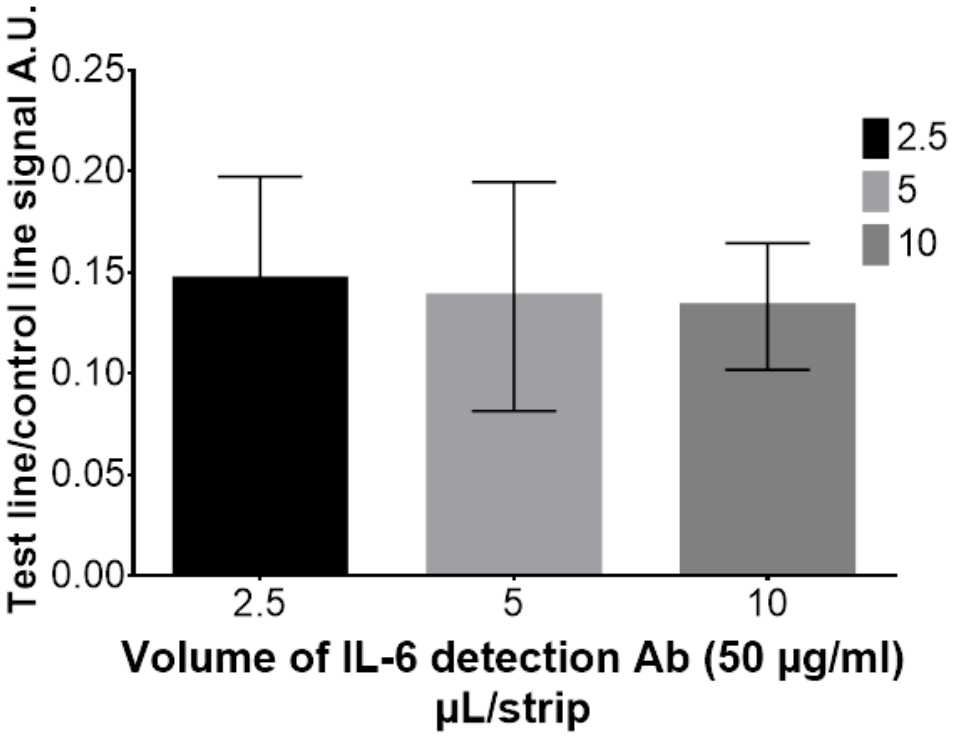

Figure S5 Plot of normalized signal intensity (A.U.) for different amounts of IL-6 detection antibody (volume in µL from a 50 µg/ml stock solution). The signal intensity was measured using ImageJ software (gel analyzer tool) then normalized to the control line signal. The points show the mean value and the error bars represent the standard deviation n=2.

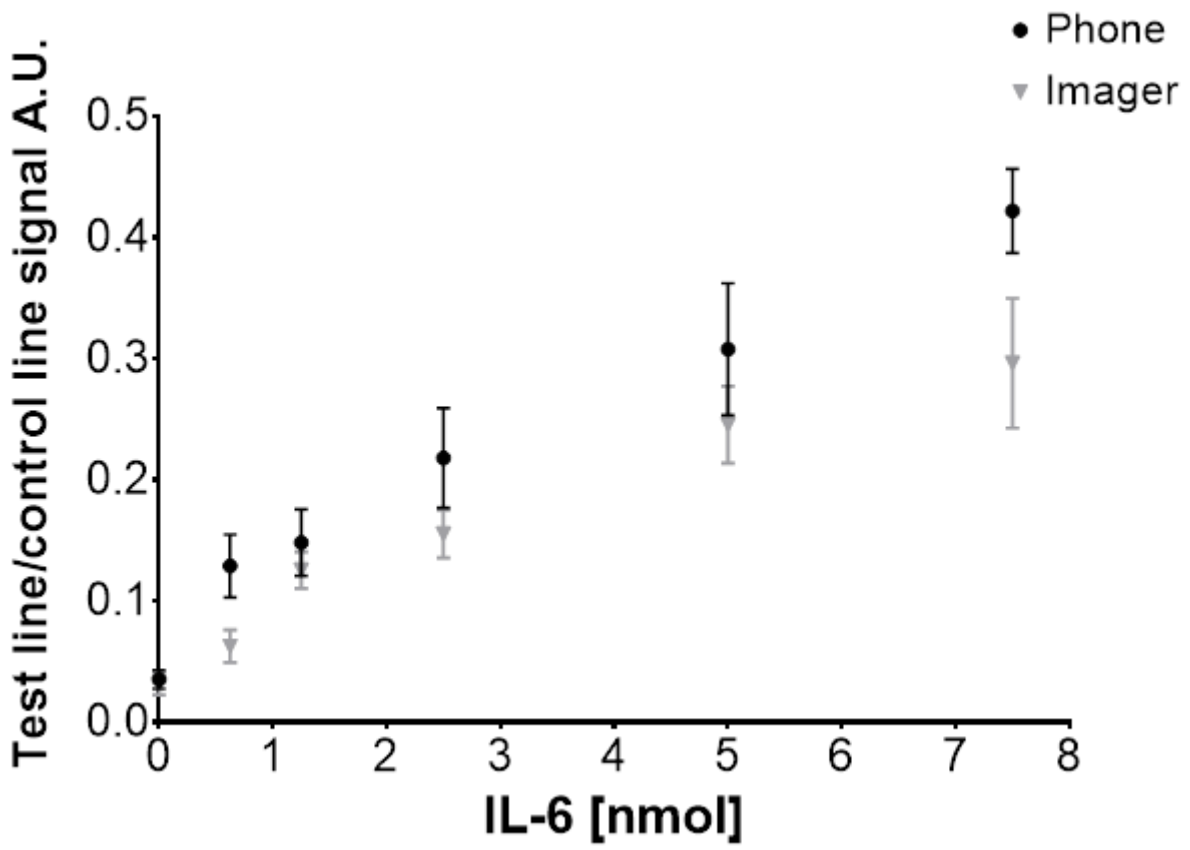

Figure S6 Plot comparing normalized signal intensity (test line/control line A.U.) of images captured using the BioImager and the smartphone setup for the green QDs conjugates. The test line intensity was measured using ImageJ software (gel analyzer tool). The points show the mean value and the error bars represent the standard deviation n=5.

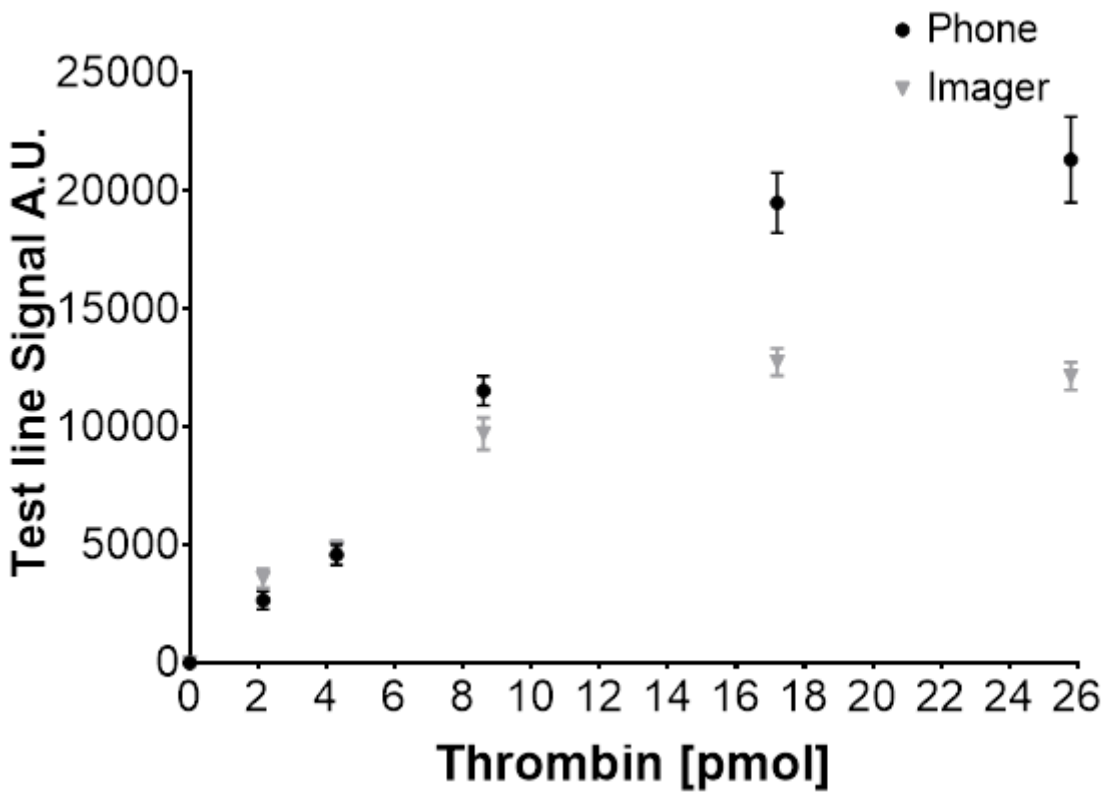

Figure S7 Plot comparing test line signal intensity (A.U.) of images captured using the BioImager and the smartphone setup for the red QDs conjugates. The test line intensity was measured using ImageJ software (gel analyzer tool). The points show the mean value and the error bars represent the standard deviation n=5.

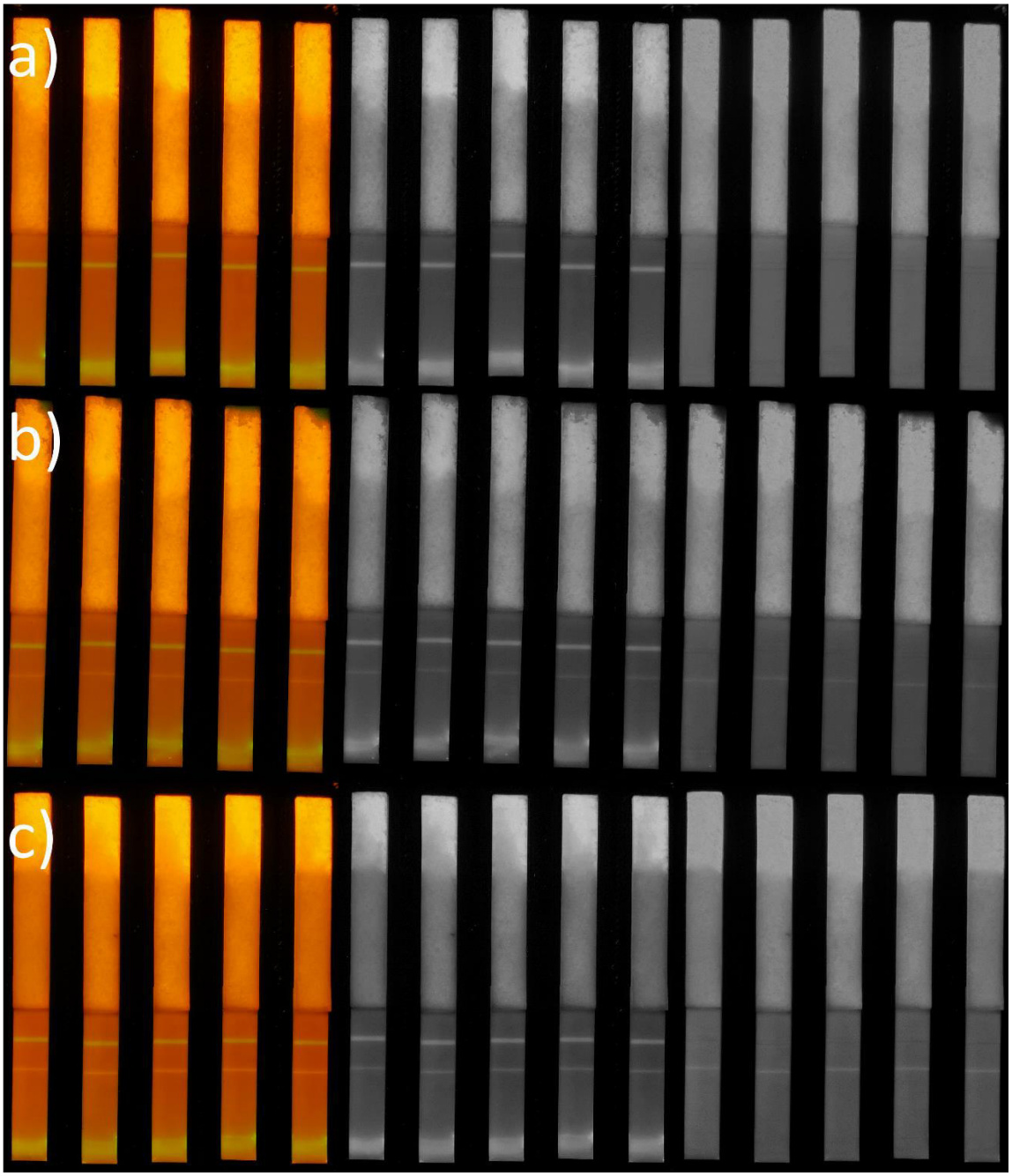

Figure S8 a representative image of the lateral flow strips captured using the smartphone setup (colour image with blue channel subtracted) and after splitting of the channels using imagej to green and red respectively a) negative control (no analyte), b) 2.15 pmol thrombin and 0.625 pmol IL-6, and c) 17.2 pmol thrombin and 5 pmol IL-6.

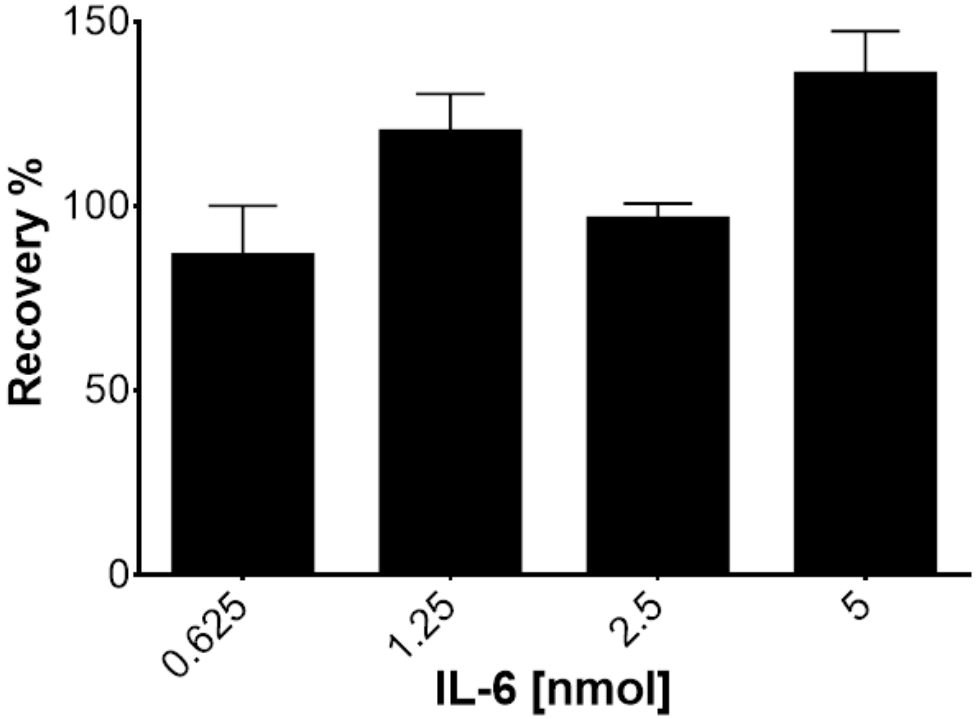

Figure S9 Recovery for 10% serum samples spiked with IL-6 (nmol). The points show the mean value and the error bars represent the standard deviation n=5.

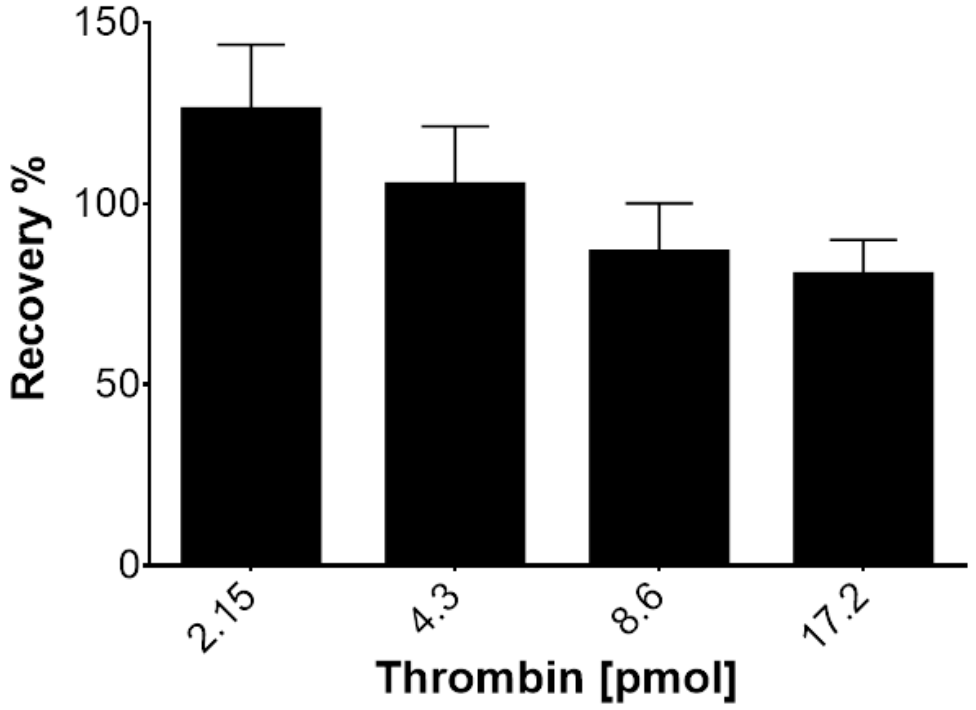

Figure S10 Recovery % for 10% serum samples spiked with thrombin (pmol). The points show the mean value and the error bars represent the standard deviation n=5.

Figure S11 a representative image of the lateral flow strips captured using the smartphone setup (colour image with blue channel subtracted) from left to right, prothrombin thrombin/antithrombin III and prothrombin/antithrombin III. No test line signal could be detected.

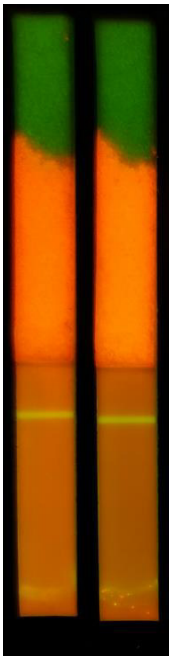

Figure S12 a representative image of the lateral flow strips captured using the smartphone setup (colour image with blue channel subtracted) from left to right, prothrombin thrombin/antithrombin III and prothrombin/antithrombin III. No test line signal could be detected.

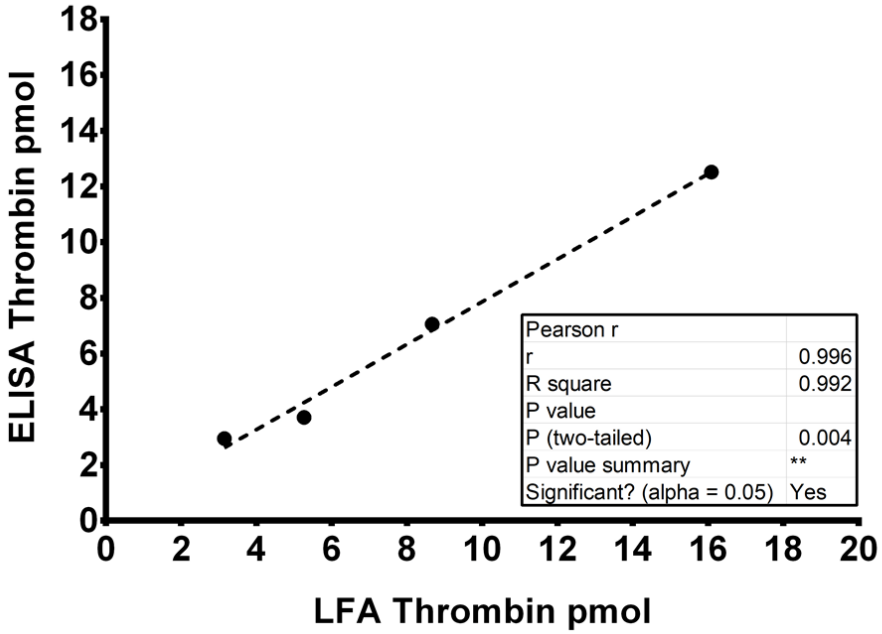

Figure S13 Comparison of thrombin in 10% serum measured with the LFA method and the ELISA kit.

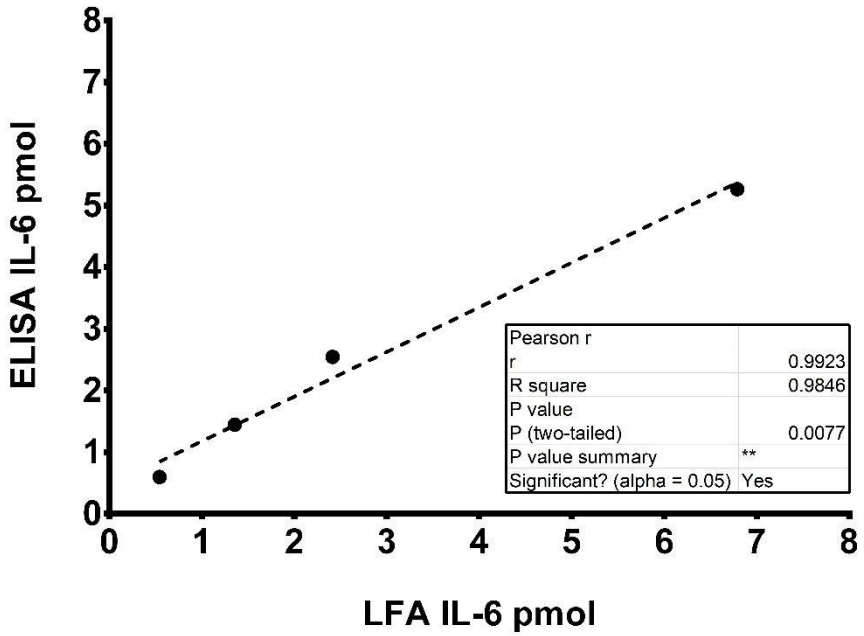

Figure S14 Comparison of IL-6 in 10% serum measured with the LFA method and the ELISA kit.